Synthesis and Application Development of Oxygen (O_2) and Carbon Dioxide (CO_2) Switchable Polymers

Synthesis and Application Development of Oxygen (O_2) and Carbon Dioxide (CO_2) Switchable Polymers

By Lei Lei, B.Eng, M.A.Sc.

A Thesis Submitted to the School of Graduate Studies

in Partial Fulfilment of the Requirements for

the Degree Doctor of Philosophy

DOCTOR OF PHILOSOPHY (2017) McMaster University

(Chemical Engineering) Hamilton, Ontario

TITLE: Synthesis and Application Development of Oxygen (O_2) and Carbon Dioxide (CO_2) Switchable Polymers

AUTHOR: Lei Lei

B.Eng. (Shaanxi University of Science & Technology, China)

M.A.Sc (Beijing University of Chemical Technology, China)

SUPERVISOR: Dr. Shiping Zhu

NUMBER OF PAGES: XXIV, 220

Lay Abstract

Polymer materials are used in every aspect of our daily life, from clothing, furniture to construction. This thesis work is to develop functional polymers that can feel variations in environment (e.g. pH, thermo, light, magnetic, etc) and give out changes in properties. Such materials are smart for stimuli-responsive applications. The first report of carbon dioxide (CO_2)-switchable polymers in 2006 was marked as the start of gas-responsive polymers. Gas triggers interact with specific functionalities in polymer chains and change their physicochemical properties such as chain structure, architecture, hydrophilicity and polarity. Oxygen (O_2) and CO_2 are explored in this work to reversibly trigger changes in volume, shell permeability and surface wettability, of different polymer systems. Potential applications include drug control-release, smart oil/water separation, and so on. This work presents a systematic study on the development of O_2 and/or CO_2-switchable polymers from monomer design, polymer preparation, and advanced application of polymer systems. It represents a significant progress and a solid step forward in the study of gas-switchable polymers.

Abstract

Stimuli-responsive polymers have attracted great attention due to their unique responses in physicochemical properties to changes in external environment and stimuli variations (e.g. pH, thermo, light, electric and magnetic field, etc.). Introduction of gas triggers has greatly expanded the family of stimuli-responsive polymers since the first work on a CO_2-switchable polymer was reported in 2006. Although significant progresses have been achieved over the past decade, studies on gas-switchable polymers are still at an early stage, with many challenges in both fundamental and application areas remaining to be tackled.

This thesis focuses on synthesis and application development of O_2 and CO_2 switchable polymers. The thesis starts from investigating O_2-switchable thermo-responsive fluorinated monomers and their linear random copolymers, which undergo LCST shifting induced by O_2 treatment. It provides good insight and general guidance for design and screening of monomer candidates for the synthesis of O_2-switchable polymers. The second part of the thesis presents development of the first O_2 and CO_2 dual gas-switchable microgel system and building of the microgel-colloidosomes with O_2 and CO_2 tailored shell permeability. The latter is evaluated as microcapsules for hierarchical control-release of water-soluble cargo molecules upon respective O_2 and CO_2 treatment. The last part of the thesis explores preparation of various porous polymer systems from high internal phase emulsion (HIPE) templates.

In particular, a highly porous polyHIPE membrane with "open-cell" structure exhibiting CO_2-switchable surface wettability is promising for smart separation applications. This thesis represents a significant progress and a solid step forward in the development of gas-switchable polymers from monomer design, polymer preparation, and advanced application of polymer systems.

Acknowledgements

I am deeply indebted to my supervisor, Dr. Shiping Zhu, who provides countless support and tireless supervision for the completion of this thesis. Like an old Chinese proverb, “a teacher for a day, a father for a lifetime”, Dr. Zhu always treat us as if we are his own children. With his vast knowledge and experience in science and life, he teaches and guides us beyond our development, provides countless advices and supports for our research and future career. His theory of science on life and happiness immensely inspire and motivate me to go through the ups and downs in research and life. I learned a great deal from his work strategy, to efficiently abstract the “big picture”, pick up the critical points, and solve the key challenges. I truly appreciate his dedication, encouragement, and constructive criticisms, which constantly motivate me to keep going forward and shape me to be a better researcher. I am truly fortunate and proud to be one of his students. Thank you, Dr. Zhu!

I would also like to thank my supervisory committee members, Dr. Emily Cranston and Dr. Alex Adronov. They are both very kind and knowledgeable scientists with great passion for chemistry and chemical engineering research. I am thankful for their time, patience, thought-provoking questions, and valuable suggestions, which deepens my understanding of my own research, broadens my research horizons, and also teaches me to think and solve questions from different angles.

I would like to extend my gratitude to Dr. Qi Zhang, a postdoctoral fellow in our group, for the valuable discussions and for sharing his knowledge and experience on research. I am grateful that we could continue this precious communication until now, and I hope we can keep our fruitful collaborations and friendship strong in the years to come. I would also like to express my gratitude to Dr. Shuxian Shi, who is my master's degree supervisor. She provides me with scientific and emotional supports during my PhD study with incomparable kindness and patience. Dr. Shi opened the door to the wondrous world of polymer science for me, and still providing opportunities and lending a hand whenever I need it. My utmost appreciation to you for being a great teacher and an amazing friend.

I would like to thank the former and current members of PolyMAC Zhu research group, who provide a committed, positive, enjoyable, and challenging environment to live and study. Their dedication and diligence continue to inspire me, while their help and support are truly essential in promoting the completion of this study. To all the friends I have made in McMaster and Hamilton, I thank you all for your time and enthusiasm on potluck, hiking, and coffee, which make my life in Canada more enjoyable and entertaining.

Last but not least, my deepest gratitude goes to my parents and little brother, who are always there for me to rely on, to get support, courage, and hope. Especially for my 25 years of study and 12 years of uprooted living. No words I can say is sufficient to

express my love for you, as you to me; our interactions flow in blood and beat in heart. I am also truly fortunate to meet my goddess Xu Yu (Jenny) during this study, who is now my dear wife. Our love and mutual attraction conform the “Relativity” to overcome time and space. Thanks for your continuous support and encouragement throughout my study. You are definitely the top two people who pushes me to publish scientific papers! Thank you for the amazing time we have shared together so far and I look forward to experience the future of our beautiful life together with you.

Table of contents

List of figures

List of tables

Declaration of academic achievement

This "sandwich" thesis consists of 6 published journal articles (5 original papers and 1 review paper), as well as 1 prepared manuscript. The contributions of the authors in each work are summarized below:

- Lei Lei is the primary author for the 5 original papers and 1 prepared manuscript reproduced in this thesis. (Chapter 3-7 and Appendix)
- Lei Lei is a coauthor of the review paper, reproduced in Chapter 1. He did the literature review and prepared the manuscript together Dr. Qi Zhang.
- Dr. Qi Zhang (a postdoctoral fellow in Zhu's group) is a coauthor for the 5 original works, 1 prepared manuscript (Chapter 3-7 and Appendix), and the first author of the review paper (Chapter 2). He provided good input through brainstorming and discussions.
- Dr. Shiping Zhu is the advisor for all the works, providing ideas, valuable discussions, revisions and quality control for all the manuscripts.
- Dr. Shuxian Shi from Beijing University of Chemical Technology (BUCT) is a coauthor for all the 5 original papers and 1 prepared manuscript (Chapter 3-7 and Appendix), who provided valuable discussion and revision of the manuscript.

List of Publications

Journal papers

[8] **Lei Lei**, Qi Zhang, Shuxian Shi, Shiping Zhu*. Highly porous poly(high internal phase emulsion) membranes with "open-cell" structure and CO_2-switchable wettability used for controlled oil/water separation. (Submitted to Langmuir).

[7] **Lei Lei**, Qi Zhang, Shuxian Shi, Shiping Zhu*. Breathable microgel-colloidosome: Gas-switchable microcapsules with O_2 and CO_2 tunable shell permeability for hierarchical size-exclusive control-relesase. *Langmuir*, 2017, 33 (24), 6108–6115.

[6] Qi Zhang, **Lei Lei**, Shiping Zhu. Gas-responsive polymers. *ACS Macro Lett*. 2017, 6, 515–522. (Cover)

[5] **Lei Lei**, Qi Zhang, Shuxian Shi, Shiping Zhu*. Oxygen-switchable thermo-responsive random copolymers, *Polym. Chem.,* 2016, 7, 5456-5462.

[4] Meng Li, **Lei Lei**, Qi Zhang, Shiping Zhu*. CO_2-breathing induced reversible activation of mechanophore within microgels, *Macromol. Rapid Commun*. 2016, 37, 957–962.

[3] **Lei Lei**, Qi Zhang, Shuxian Shi, Shiping Zhu*. Oxygen and carbon dioxide dual gas-switchable thermoresponsive homopolymers, *ACS Macro Lett*., 2016, 5(7), 828–832.

[2] **Lei Lei**, Qi Zhang, Shuxian Shi, Shiping Zhu*. High internal phase double emulsions and their templated porous polymer systems - A combination of high internal phase emulsion and double emulsion, *Journal of Colloid Interface Sci.,* 2016, 483, 232-240.

[1] **Lei Lei**, Qi Zhang, Shuxian Shi, Shiping Zhu*. Oxygen and carbon dioxide dual gas-responsive and switchable microgels prepared from emulsion copolymerization of fluoro- and amino-containing monomers. *Langmuir*, 2015, 31(7), 2196-2201.

Book chapter

[1] He Zhu[§], **Lei Lei**[§], Shiping Zhu*. Development of novel materials from polymerization of Pickering emulsion templates. Springer, AG 2017, *Advances in Polymer Sciences*. DOI: 10.1007/12_2017_15 ("§": Equally contribute)

1 INTRODUCTION

This chapter introduces the organization of this thesis, and the research objectives for each chapter.

§ 1.1 Thesis organization

This thesis is organized in "sandwich" style, which includes five published research articles in peer-reviewed journals, one viewpoint paper, and one newly prepared manuscript. Throughout the thesis, the bibliographic formats have been modified, with all the figures and tables re-numbered, for consistence. This thesis starts with a literature review of gas-switchable polymers (Chapter 2) and focuses on the synthesis and application development of O_2 and CO_2 switchable polymers. The research contents of this thesis are grouped into two main parts for clarity. Part I focuses on the synthesis and gas-switchability investigation of various O_2 and CO_2 switchable polymers systems including random copolymers, homopolymers and microgels.

(Chapter 3, 4 and 5). Part II reports the preparation the gas-switchable microgel-colloidsome and porous poly(high internal phase emulsion) (polyHIPE) membranes, and explores their potential applications for O_2 and CO_2 tunable multi-stage control-release and CO_2 controlled oil/water separation respectively (Chapter 6 and 7). Chapter 8 summarises all the works and provides a perspective view of this area. Included in Appendix is a published paper on preparation of various porous polymer devices from emulsion templates, which do not involve gas-switchable polymers.

Chapter 2 presents a literature review and perspective on the development of gas-responsive polymers. Based on different gas triggers, this review provides a comprehensive introduction of their interactions with specific functionalities and their state-of-art of applications. This review is published in *ACS Macro Lett.*, **2017**, 6 (5), 515–522 (DOI: 10.1021/acsmacrolett.7b00245). It is evident from this review that the study on gas-switchable polymers is still in infancy and full of opportunities and challenges. The following chapters report studies on various O_2 and/or CO_2-switchable polymers.

Part I: Synthesis of O_2 and CO_2 –switchable polymers

This part starts with the investigation of the hydrophilicity and O_2-switchability of various O_2-switchable fluorinated monomers (Chapter 3). Based on the specific O_2 and CO_2 switchable functionalities, the O_2 and CO_2 dual gas-switchable monomer was chemically designed, which facilitates the preparation of the first CO_2 and O_2 dual gas-

switchable homopolymer (Chapter 4). Furthermore, the first O_2 and CO_2 dual gas-switchable microgel system was prepared from the emulsion copolymerization (Chapter 5).

Chapter 3 reports a systematic investigation of O_2-switchability of various fluorinated monomers. The O_2-switchable properties of commercial fluorinated monomers FMA and FS, and newly synthesized F1EA, F2EA and F3EA are compared and analysed by LCST shifting of their thermo-responsive random copolymers in aqueous solution upon O_2 treatment. This work was published in *Polymer Chemistry*, **2016**, 7, 5456-5462 (DOI: 10.1039/C6PY01145D). It provides a general methodology for development and screening of the O_2-switchable monomers.

Chapter 4 reports a new monomer design that combines both O_2 and CO_2 switchable thermo-responsive functionalities into a single monomer. The gas-switchable properties of its homopolymers are investigated through LCST shifting of their aqueous solutions upon O_2 and CO_2 treatment. This work was published in *ACS Macro Lett.*, **2016**, 5 (7), 828–832 (DOI: 10.1021/acsmacrolett.6b00426). It provides an effective method to prepare multi-responsive homopolymers. The monomer design approach is transformative and it could be expanded to other areas.

Chapter 5 reports preparation of the first type of O_2 and CO_2 dual gas-switchable microgels. Their responsiveness upon O_2 and CO_2 treatment as a function of monomer

composition is thoroughly investigated. This work was published in *Langmuir*, **2015**, 31 (7), 2196–2201 (DOI: 10.1021/la504829j).

Part II: Applications of O_2 and CO_2 –switchable polymers

This part focuses on exploring the potential applications of O_2 and CO_2 switchable polymer devices. Microgel-colloidosome (MGC) was built up from the O_2 and CO_2 dual gas-switchable microgel particles, which was then used as microcapsule for O_2 and CO_2 tunable multi-stage control-release application (Chapter 6). Highly porous polyHIPE membranes with "open-cell" structure and CO_2-switchable surface wettability was also prepared and evaluated for CO_2 controlled oil/water separation (Chapter 7).

Chapter 6 reports fabrication and application of microgel-colloidosomes (MGC) based on the O_2 and CO_2 dual gas-switchable microgels prepared in chapter 5. Oil-in-water (O/W) Pickering emulsions stabilized by the microgel particles are used as the templates to generated MGCs, which are then used as microcapsules with tunable shell permeability for hierarchical releasing of cargo molecules upon respective O_2 and CO_2 treatment. This work was published in *Langmuir,* **2017**, 33 (24), 6108–6115 (DOI: 10.1021/acs.langmuir.7b01092). The MGCs prepared in this work are promising for applications in controllable release, separation, and reaction of multiple ingredients.

Chapter 7 reports synthesis of highly porous polyHIPE membranes with CO_2-tunable surface wettability through incorporation of CO_2-switchable monomer in HIPE template preparation. The membranes with "open-cell" porous structure are used as CO_2 switch in controlled oil/water separation. The manuscript of this work has been prepared for publication. This work represents a combination of stimuli-responsive functionality and novel macrostructure, which has promising applications in the areas of control-release, smart separation, tissue engineering and so on.

Chapter 8 highlights the major contributions of this thesis study and offers some perspectives and recommendations for the future research.

Appendix reports preparation of porous spheres and porous matrixes from microgel-stabilized high HIPE with double emulsion morphology, through curing of either dispersed or continuous phase. Since this work does not involve O_2 and/or CO_2 switchable properties, it is included as an appendix of the thesis. This work was published in *Journal of Colloid and Interface Science*, **2016**, 483 (1), 232–240. It represents a facile method for the preparation of advanced porous polymer products.

§ 1.2 Research objectives

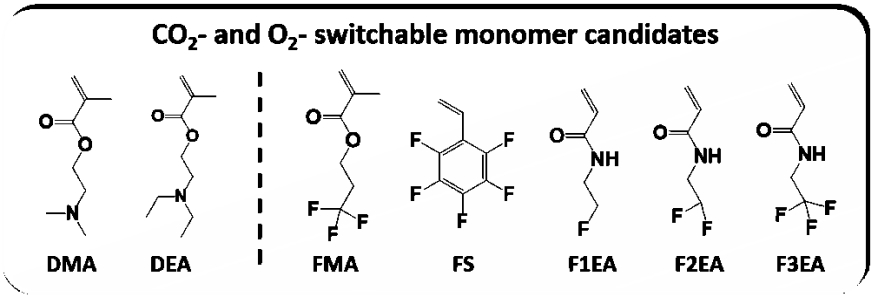

Figure 1-1. Molecular structure of CO_2 and O_2 gas-switchable monomer candidates

The overall objective of this thesis is to study the preparation and application of O_2- and/or CO_2- switchable polymers, derived from the monomer candidates listed in Figure 1-1. N, N-dimethylaminoethyl methacrylate (DMAEMA) and N, N-diethylaminoethyl methacrylate (DEAEMA) are well reported CO_2-switchable monomers.[1–3] In addition to CO_2-switchability, PDMAEMA exhibits thermo-responsive properties with a lower critical solution temperature (LCST) at about 40 ^oC.[1] 2,2,2-Trifluoroethyl methacrylate (FMA) and 2,3,4,5,6-pentafluorostyrene (FS) are commercially available monomers candidates, which have been reported in preparation for O_2-switchable polymer materials.[4–6] The newly synthesized fluorinated acrylamide monomers, including N-(2-fluoroethyl) acrylamide (F1EA), N-(2,2-difluoroethyl)acrylamide (F2EA), and N-(2,2,2-trifluoroethyl)acrylamide (F3EA), are hypothesized to be promising O_2-switcable monomers due to their relatively hydrophilic structure and variable number of fluorine atoms compared to FMA and FS. [7,8] It is important to note that CO_2 and O_2 switchabilities are based on

different mechanisms. CO_2 molecules dissolved in an aqueous solution could protonate the tertiary amine groups in DMA/DEA and significantly increase hydrophilicity.[1,3] Van der Waals intermolecular interactions between dissolved O_2 molecules and the fluorine atoms decrease hydrophobicity of the fluorinated segments and enable O_2-switchability of the polymers. [4–6]

Based on these gas-switchable monomer candidates, the specific research objectives of each chapter are summarized below, with a detailed description of contributions provided:

- To investigate O_2-switchable properties of commercially available fluorinated monomers FMA and FS, and newly synthesized F1EA, F2EA and F3EA, to provide a general methodology for development and selection of O_2-switchable monomers and polymers (Chapter 3).
- To provide a chemistry method for a combination of both O_2 and CO_2 switchable functionalities into a single monomer, and to investigate gas-switchability of the homopolymers (Chapter 4).
- To develop the first O_2 and CO_2 dual gas-switchable microgel system and to investigate changes in their properties in response to trigger gas treatment (Chapter 5).

- To fabricate dual gas-switchable microgel-colloidosomes based on the microgels prepared in chapter 5, and to investigate their loading and control releasing profiles of cargo molecules upon O_2 and CO_2 treatment (Chapter 6).
- To prepare porous membranes with CO_2-switchable surface wettability from high internal phase emulsion (HIPE) templates, and to investigate their application for CO_2 controlled oil/water separation (Chapter 7).
- To develop various advanced porous polymer materials from microgel-stabilized high internal phase Pickering emulsion, which include porous spheres and porous matrixes, through curing of dispersed or continuous phase of the emulsions (Appendix).

§ 1.3 References

[1] Han, D.; Tong, X.; Boissiere, O.; Zhao, Y. ACS Macro Lett. 2012, 1, 57–61.

[2] Lin, S.; Theato, P. Macromol. Rapid Commun. 2013, 34, 1118–1133.

[3] Yan, Q.; Zhao, Y. Chem. Commun. 2014, 50 (79), 11631–11641.

[4] Choi, J. Y.; Kim, J. Y.; Moon, H. J.; Park, M. H.; Jeong, B. Macromol. Rapid Commun. 2014, 35 (1), 66–70.

[5] Zhang, Q.; Zhu, S. ACS Macro Lett. 2014, 3 (8), 743–746.

[6] Zhang, Q.; Zhu, S. Macromol. Rapid Commun. 2014, 35 (19), 1692–1696.

[7] Lei, L.; Zhang, Q.; Shi, S.; Zhu, S. Polym. Chem. 2016, 7 (34), 5456–5462.

[8] Bak, J. M.; Kim, K.-B.; Lee, J.-E.; Park, Y.; Yoon, S. S.; Jeong, H. M.; Lee, H. Polym. Chem. 2012, 1, 2219–2223.

2 GAS-RESPONSIVE POLYMERS

This chapter is a literature review on the development of gas-responsive polymers. This review offers a comprehensive introduction of various gases triggers and their specific corresponding functionalities, and their state-of-art of applications. This review is a reproduce of the published Viewpoint Paper in Qi Zhang, Lei Lei, Shiping Zhu, "Gas-responsive Polymers" *ACS Macro Letter*, **2017**, 6 (5), 515–522 (DOI: 10.1021/acsmacrolett.7b00245) with the permission from ACS publisher. The review represents a profound understanding and perspective on the development of gas-switchable polymers.

Author contributions

The idea of this timely review was initiated by Dr. Shiping Zhu. Dr. Qi Zhang (a postdoctoral fellow in Zhu's group) and I (as a PhD candidate) did the literature

review together and prepared the first manuscript. Dr. Zhu did final revision and provided quality control of the manuscript.

§ 2.1 Abstract

Gas-responsive polymers have inspired much interest over the past ten years. Gas triggers can interact with functionalities on polymer chains and thus modulate their chain structures, architectures and aggregation states. This review summarizes the latest research progresses in the theme of developing different gas triggers for fine control over some critical properties of polymers, as well as their potential applications in various areas. We focus on the interactions/reactions between gases and gas-responsive functionalities of polymers, and highlight some state-of-art developments, which provided good insight and understanding of each particular gas-responsive polymer. We also offer a perspective point of view on future research directions on gas-responsive polymers, both in fundamental studies and in potential application developments.

§ 2.1 Introduction

Over the past decades, stimuli-responsive polymers have been developing rapidly, and receiving growing interest from both academia and industry.[1-4] External stimuli cause changes in the physical/chemical properties of polymers, and lead to their rearrangement or changes in dimensions, structures, and interactions, as well as

aggregation states.[2] Such "smart" polymers have found diverse applications in various areas, including functional materials,[5-7] nanomedicine and nanotechnology,[8-11] bio-imaging,[12] sensing,[13, 14] and so on. The stimulus (also called trigger) can be either physical or chemical. The most well-studied and understood stimulus are pH,[15, 16] light,[17, 18] and temperature.[19] However, each type of the stimuli has drawbacks, which can limit their applicability. For pH, it has the salt accumulation issue, which may weaken the switchability of pH-responsive polymers.[20] Ultraviolet light would cause damage to biological tissues. Thermosensitive polymers acquire high costs in energy consumption, if operated in a large volume. The recent advent of gas stimuli has provided great opportunity for the development of smart materials and systems. Compared to the other stimuli, most gases are easy to add and easy to remove in large volume operations. Therefore, gas triggers are of great interest in industrial applications.

Several gaseous triggers have been reported so far, including carbon dioxide (CO_2),[21-23] oxygen (O_2),[24, 25] nitric oxide (NO),[26-28] hydrogen sulfide (H_2S),[29] sulfur oxide (SO_2),[30] and so on. As an abundant, nontoxic, and environmentally benign gas, CO_2 has been widely used in chemical engineering processes (e.g., supercritical CO_2 extraction), polycarbonate synthesis,[31] as well as an inert gas in welding and fire extinguisher. O_2 is as important as CO_2 in photosynthesis and respiration, while it is also a very useful gaseous oxidant in chemical engineering industry.[32] H_2S, NO and CO, though quite toxic, are found to be the key signaling molecules in living creatures

involved in various biological pathways.[33] Having a pungent, irritating smell, SO_2 is also a toxic gas, but useful as a good reductant, good candidate material for refrigerants, as well as an important compound in winemaking. All the gases of COx, NOx and SOx are important in environment protection. Previous studies and industrial practices have already proven the usefulness and importance of these gases, and now they have been given a new mission in the emerging research field of stimuli-responsive polymers. While CO_2 is the most studied gas trigger, researches on other gas-responsive polymers are at their infancy stages.

Herein, we summarize the latest research progresses on the theme of employing various gas triggers for fine control over some critical properties of polymers and their nanoaggregates, as well as their potential applications in different areas. For each specific gas-responsive polymer system, we focus on the interactions or reactions between gases and gas-responsive functionalities of polymers, and highlight some state-of-art developments to give a better understanding of each particular gas-responsive polymer or application. Finally, we will give a perspective point of view on future research directions on gas-responsive polymers, both in fundamental research and potential application studies.

§ 2.2 CO_2-responsive Polymers

As a non-toxic, inexpensive, benign, and abundant gas, CO_2 became the most studied gas trigger in the past ten years. It can selectively react with specific functionalities

(such as tertiary amine and amidine groups) to make a dramatic change on their hydrophilicities and polarities. Moreover, due to the reversible nature of those reactions, CO_2 could be completely removed by washing with inert gases (argon or nitrogen or air) under a mild condition, thus free of contamination by accumulated chemical agents. Therefore, CO_2 is a truly mild and "green" trigger to the target polymers. Several review papers on CO_2-responsive polymers have recently been published.[23, 34-37] To assist readers have a comprehensive view on gas-responsive polymers, we briefly highlight some of the key research progresses in a time order.

The reaction of carbon dioxide with primary amines is a well-known chemical reaction, which has been widely used for the absorption of greenhouse gases in industry. However, the inverse process usually requires more hash conditions, such as high temperature or vacuum. In 2006, Jessop et al. first reported the amidine-CO_2 reversible chemistry.[22] The amidine group in its neutral state reacted with carbonic acid to form amidinium bicarbonate, and reverted back to its neutral state upon the removal of CO_2 under milder conditions, as compared to primary amines.[22] The big difference in polarity and solubility between these two states has provided plenty of opportunities in making CO_2-switchable surfactants and polymers. Several different approaches have been successfully developed since then, to make CO_2-redispersible polymer latexes, including switchable surfactant, switchable initiator, switchable comonomer, switchable reactive surfactant, and so on.[38-42]

However, the amidine groups have limited stability in water due to partial hydrolysis, not to mention that the synthesis of amidine groups is complex and costly.[43, 44] Thanks to Zhao's discovery of CO_2 reversible chemistry based on tertiary amines, research on CO_2-responsive polymers has entered into a new era with blowout growth.[45] It was found that the neutral tertiary amine groups of commercially available monomers such as diethylaminoethyl methacrylate (DEAEMA) could be effectively protonated by carbonic acid, and it was reversible upon the removal of CO_2.[45] Moreover, this group of amines was found to have improved stability over hydrolysis, which are advantageous over amidines. Over the past several years, lots of well-defined CO_2-responsive polymers have been prepared via controlled living radical polymerization (CLRP), and their changes in solubility, size and morphology of aggregates towards CO_2 have been thoroughly investigated.[46-58] For example, Yan et al. recently showed that CO_2 could act as a physiological trigger to biomimic shape transformations of the organelles.[52] They designed and synthesized a series of ABC-type triblock copolymers, which was composed of a hydrophilic PEO stabilizer, middle hydrophobic polystyrene (PS), and CO_2-responsive PDEAEMA block (A). The copolymers could self-assemble into three different initial nanostructures: spherical particles, worm-like micelles, and giant vesicles, while varying the middle PS block. After treated with CO_2, the morphology of the nanoaggregates turned into swollen spheres, straight and rigid nanowires, and compartmentalized large-compound sacs, respectively.[52] It was proved that these morphological transformations were caused by the synergy effect of corona–chain repulsion and core–chain restricted

hydration.[52] Later on, more and more CO_2-regulated morphology deformations of block copolymer assemblies were reported.

In the meanwhile, CO_2-responsive microgels (cross-linked polymers) have also gained much interest, and they were found to be very useful in diverse application areas, such as CO_2 capture, efficient emulsion separation (e.g. emulsification and demulsification for Pickering emulsions), and so on.[59, 60]

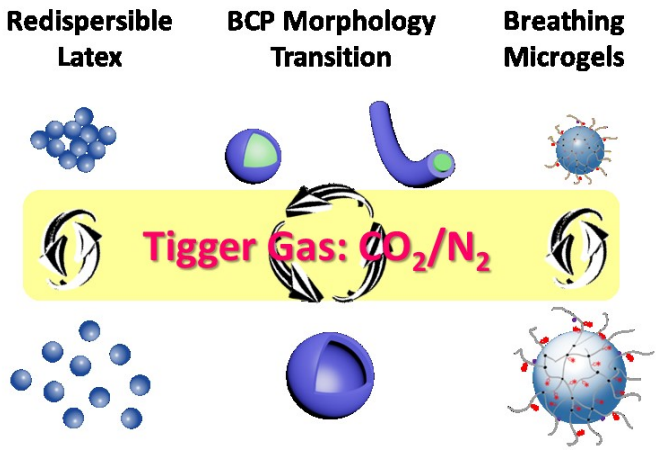

Figure 2-1. Schematic presentation of representative CO_2-responsive polymers: reversibly coagulatable and redispersible polymeric latexes; morphology transformation of self-assembles of block copolymers; swelling and deswelling of microgels.

Except for the different types of CO_2-responsive polymers mentioned above, a diversity of examples utilizing CO_2-responsive polymers have been reported during the past a few years, including gas-switchable surfaces,[61] redispersion of carbon nanotubes (CNT),[62] in-situ recovery of gold nanoparticle (AuNP) catalyst,[63] recyclable draw solute for forward osmosis desalination,[64] and so on.

§ 2.3 O_2-responsive Polymers

Accounting for 20.8 vol.% of air, O_2 is the most important gas for all lives on earth. It is also a very useful gaseous oxidant in chemical industries.[65, 66] However, it has not been used as a trigger for stimuli-responsive polymers, until very recently. Jung et al. reported pentafluorophenyl end-capped poly(ethylene glycol) (PF-PEG-PF) as the first example of O_2-sensitve polymers.[24] The polymer in water showed a LCST of 24.5 °C, which increased by only 1.5 °C to 26 °C upon O_2 aeration. They also proved that this LCST shift was caused by the intermolecular interactions between O_2 molecules and the carbon-fluorine bonds, since the ortho-fluorine of PF-PEG-PF downfield shifted in the ^{19}F NMR spectra in D_2O, whereas the chemical shift of the protons of PEG did not change in the ^{1}H NMR spectra in D_2O.[24]

On the basis of this discovery, Zhu's group reported a new design of fluorinated polymers, targeting for a more general and efficient strategy for O_2-responsive polymers.[25] The strategy was based on commercially available fluorinated monomers. They synthesized a random copolymer of 2,2,2-trifluoroethyl methacrylate (FMA) and N,N-dimethylaminoethyl methacrylate (DMA) via atom transfer radical polymerization (ATRP). The copolymer poly(DMA-co-FMA) (PNF) displayed a LCST around room temperature in aqueous solution. Alternative treatment of O_2 and N_2 towards the PNF solution at room temperature would make it undergo a reversible

transparent-turbid transition. The LCST increased dramatically from 24.5 to 55 °C, as determined from the turbidity change. Moreover, purging with N_2 for 1 h could remove O_2 and LCST went back to the initial value.[25] The switchability of PNF was attributed to the intermolecular interaction between O_2 and fluorinated moieties. Following this, the same group continued to conduct a systematic study on O_2-switchable thermo-responsive random copolymers based on different fluorinated monomers, including acrylamide homologues: N-(2-fluoroethyl)acrylamide (F1EA), N-(2,2-difluoroethyl)acrylamide (F2EA), and N-(2,2,2-trifluoroethyl)acrylamide (F3EA), as well as 2,3,4,5,6-pentafluorostyrene (FS).[67] LCSTs of these copolymers could be precisely designed in a wide range of temperatures by varying their chemical compositions. More importantly, LCSTs could be further switched to different levels by treating O_2 or CO_2, and be recovered to the initial states by washing off the trigger gas.[67] Later on, they reported the first O_2 and CO_2 dual gas-switchable thermo-responsive homopolymer based on a newly synthesized monomer N-(2-fluoroethyl amide)-N-(2-(diethylamino)ethyl) acrylamide, (AM(F1EA-DEAE)), which possessed both O_2-switchable fluorinated ethyl amide and CO_2-switchable N,N-diethylamino ethyl moieties on the polymer side chain.[68] Poly(AM(F1EA-DEAE)) prepared via reversible addition-fragmentation chain transfer polymerization (RAFT) exhibited good temperature-responsive properties in water, and the LCST could be reversibly tuned to different levels by respectively purging O_2 or CO_2 into its aqueous solution. The O_2-treatment shifted LCST to a higher temperature, while the CO_2-treatment made the polymer fully water soluble. The polymer could be readily recovered to its

initial state by washing off the trigger gas with an inert gas such as nitrogen. This work provided an effective monomer design approach for the preparation of O_2 and CO_2 dual gas-responsive polymers.

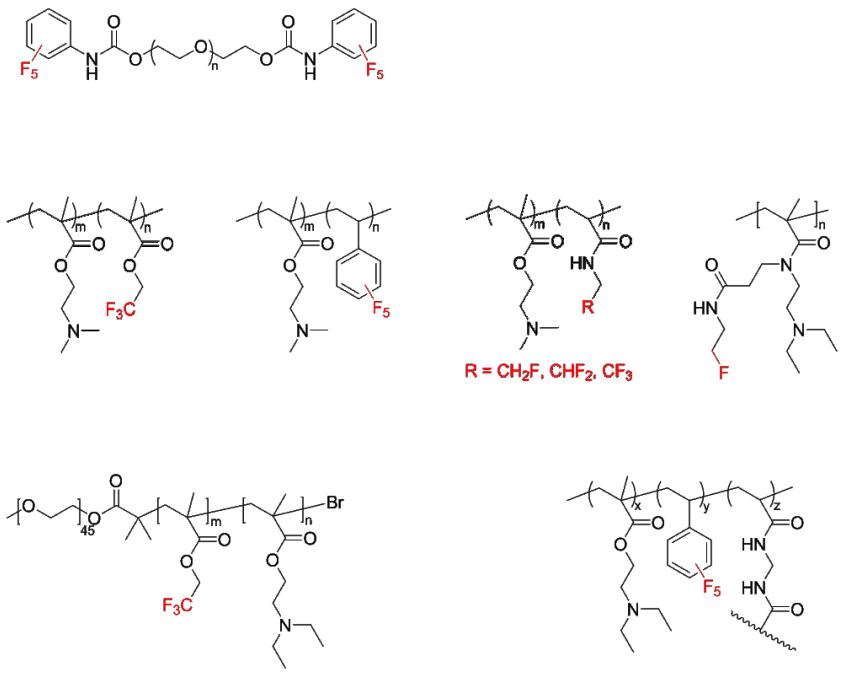

Figure 2-2. Summary of chemical structures of the reported O_2-responsive polymers.

O_2 is also capable for making vivid changes in polymeric nanoparticles. Zhu et al. reported a novel approach for preparing CO_2- and O_2-responsive polymeric self-assemblies.[69] As shown in Figure 2-3, the amphiphilic copolymer, PEO-b-(DEAEMA-co-FMA), bearing both CO_2-responsive amine moieties and O_2-responsive fluorinated moieties, could self-assemble into vesicles in water. It underwent various shape transformations upon O_2 and CO_2 treatments. With O_2 bubbling, the vesicles

expanded 8 times in volume, while CO_2 bubbling collapsed the vesicular morphology and transformed it into small spherical micelles.[69]

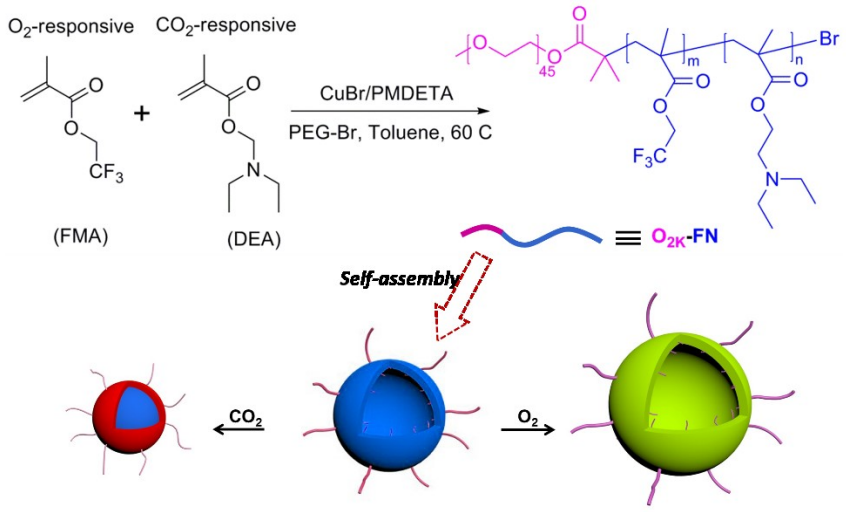

Figure 2-3. Synthesis routes of CO_2- and O_2-sensitive diblock copolymer PEO-b-(DEAEMA-co-FMA), and schematic representation of CO_2- and O_2-driven self-assembly and shape transformation behavior of the vesicles. Reprinted with permission from ref [69]. Copyright 2014 American Chemical Society.

Later, Lei et al. reported O_2 and CO_2 dual-gas-responsive microgels.[70] Incorporation of fluorinated monomer 2,3,4,5,6-pentafluorostyrene (FS) rendered the microgels good responsivity towards O_2, as evident from the increased swelling. Moreover, microgels having different levels of responsivity could be designed and prepared by varying FS content in the copolymer. The microgels were more responsive to CO_2 than O_2, and multicycles of $O_2/CO_2/N_2$ aerations showed no loss in the dual gas responsivity and switchability.[70]

§ 2.4 NO-responsive Polymers

Known as an atmospheric pollutant, NO is a practically important intermediate in the chemical industry, and it also plays an important role in many physiological and pathological processes in mammals including humans.[71-74] Compared to the quite abundant research on small molecules for NO-releasing[75, 76] and detection,[77, 78] NO-responsive polymers has rarely been studied.

Very recently, Hu et al. reported the first example of NO-responsive polymers, which was prepared through the copolymerization of N-isopropylacrylamide (NIPAM) with two types of NO-responsive monomers, N-(2-aminophenyl) methacrylamide hydrochloride (NAPMA) and 2-(3-(2-aminophenyl)ureido)ethyl methacrylate hydrochloride (APUEMA), both bearing NO-responsive o-phenylenediamine functional groups.[26] Upon exposure to NO, NAPMA monomer reacted effectively with NO to generate amide-substituted benzotriazole intermediates, which spontaneously hydrolyzed into carboxyl moieties with the liberation of a benzotriazole motif (Figure 2-4a), resulting in an increased hydrophilicity of the copolymer. On the other hand, the urea-functionalized benzotriazole derivatives resulted from APUEMA monomer had an increased hydrophobicity (Fig. 2-4b). The copolymer thus exhibited obvious change in solubility, leading to the drop of LCST from 28 to 7.5 °C. This in turn induced nanoparticle formation through self-assembly. Moreover, with the help of environmentally sensitive fluorescence dyes, this NO-triggered self-assembly process could be employed to detect and image endogenous NO.[26]

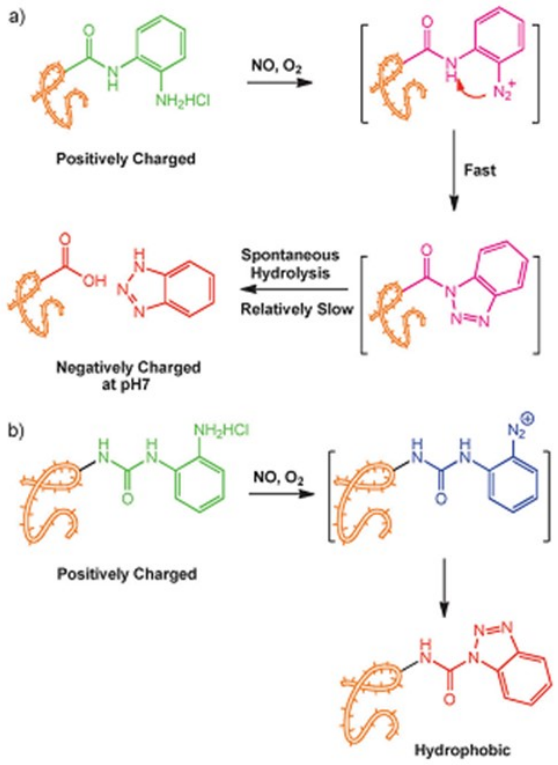

Figure 2-4. Schematic illustration of the respective NO-triggered mechanism of the copolymers bearing NAPMA and APUEMA moieties. Reproduced with permission from ref [26]. Copyright 2014 John Wiley and Sons.

Later, the same group reported the use of endogenous gaseous molecules (NO and CO_2) to regulate the self-assembly of a dual-responsive triblock copolymer.[27] The amphiphilic copolymer, consisting of a hydrophilic poly(oligo(ethylene glycol) methyl ether methacrylate) (POEGMA) corona, and two blocks possessing individual CO_2-responsiveness and NO-sensitivity, were designed and synthesized via sequential RAFT polymerization. Initially, the self-assemblies of block copolymers (BCP) had a particulate nanostructure, which was swelled upon CO_2 treatment. Subsequent NO addition selectively transformed the interior block to more hydrophobic benzotriazole moieties, leading to the

morphological transition from swollen micelles to nanorods.[27]

It should be mentioned that although not reversible, the reaction between o-phenylenediamine functional groups and NO are very efficient even under low concentration (NO detection limits were around several μM).

§ 2.5 H_2S-responsive Polymers

Similar as NO, hydrogen sulfide (H_2S) is well known not only as a toxic gas in the atmosphere, but also as an important neuromodulator and cell signaling molecule in human bodies. Very recently, Yan et al. developed a new class of oazidomethylbenzoate (AzMB)-containing BCP (Figure 2-5).[29] The polymer could spontaneously form a vesicular architecture in aqueous media on the basis of their amphiphilicity. The particular functionality in the polymer endowed these vesicles with unique sensitivity towards H_2S. H_2S activated a controlled disassembly of the polymersomes by site-specific cleavage of the AzMB groups. These H_2S-responsive vesicles could potentially be used as nanovectors for drug delivery. Such H_2S-responsive polymers would open up a new avenue to construct bioresponsive nanocapsules for more biological applications.

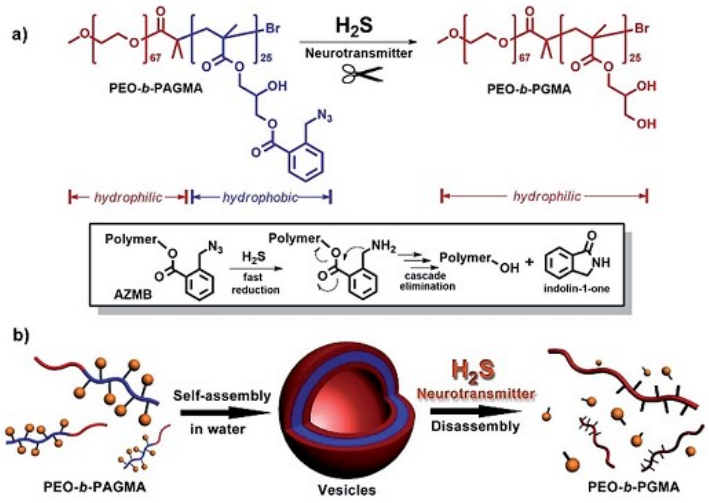

Figure 2-5. (a) H_2S-responsive cleavage of o-azidomethylbenzoate (AzMB)-containing diblock copolymer (PEO-*b*-PAGMA) and H_2S induced cascade reaction mechanism. (b) Schematic illustration of their polymer self-assembly into vesicles and H_2S-responsive controlled disassembly process. [29] - Published by The Royal Society of Chemistry.

§ 2.6 SO_2-responsive Polymers

SO_2 is a toxic gas with a pungent and irritating smell. It is a very useful in winemaking, while also a good reductant, a good candidate material for refrigerants. Tang et al. developed a new class of SO_2-responsive polymers based on the interactions between SO_2 and triazole groups.[30] Water-soluble, α-helical random copolypeptides bearing pyridinium tetrafluoroborate (PyBF4) and oligo-ethylene glycol (OEG) pendants (PPLG-PyBF4-r-OEG) were prepared through sequential postpolymerizations, including nucleophilic substitutions, copper-mediated [2+3] alkyne−azide 1,3-dipolar cycloaddition, and ion-exchange reaction. The aqueous solution of the resultant polymer was found to undergo a reversible solution phase transition by sequentially bubbling SO_2 and N_2, as revealed from

UV−vis spectroscopy and dynamic light scattering (DLS) results. ^{1}H NMR analysis confirmed that the interaction between SO_2 and triazole groups was essential for solution phase transition.[30] This discovery sheds some light on the molecular design of SO_2-responsive polymers and broadens the application of gas-responsive polymers.

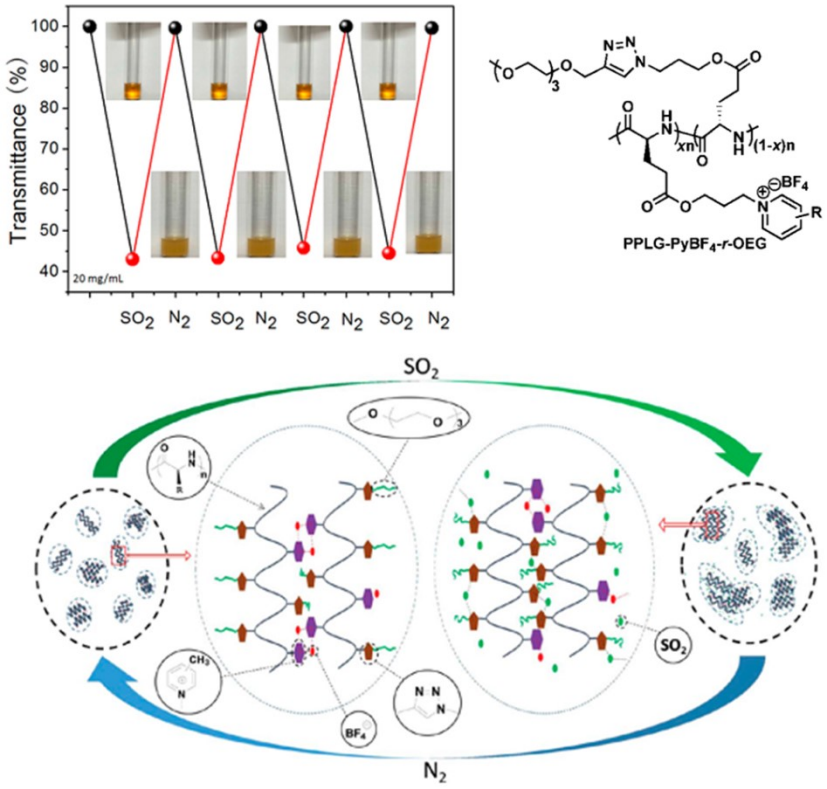

Figure 2-6. Plot of transmittance at λ = 500 nm versus gases for the aqueous solution (20 mg mL^{-1}) of PPLG-PyBF4-*r*-OEG at 25 °C and the optical images of PPLG-PyBF4-*r*-OEG solution at different conditions. Proposed mechanism of SO_2-induced reversible solution phase transition. Reprinted with permission from ref [30]. Copyright 2016 American Chemical Society.

§ 2.7 Conclusion and Outlook

Stimuli-responsive polymers have received growing attention due to their unique properties.

Introducing gas molecules into the big family of triggers has been emerging, undergoing a rapid development over the past decade. Since gases could be easily added and easily removed in large volume operations, compared with other traditional chemical or physical stimuli, they are of great interest in both industrial applications and academic research. In this feature article, we highlight the latest research progresses on the theme of employing various gas triggers for fine control over some critical properties of polymers, as well as their potential applications in different areas. Despite the rapid progresses that have been achieved in the past a few years, it is noteworthy that this field is still at the start. Oxygen (O_2), nitrogen (N_2), carbon oxides (COx), nitrogen oxides (NOx), sulfur oxides (SOx), and hydrogen sulfide (H_2S) have been and will continue to be the key gases for studies, because of their high relevance to environment and health issues, as well as potential applications in material processing and medicine. However, there are still plenty of remaining challenges for gas-responsive polymers in the future, both in fundamental research and potential application studies.

Among all the trigger gases, CO_2 has been best studied. It has clear advantages in supply abundance, non-toxicity and low cost, making it particularly suitable for the development of large-scale green processes in chemical industries. Bubbles, drops and particles are a century long subject of R&D in reaction and separation industries, with numerous matured unit operation technologies available, which are readily employed in applications of the gases. Reversibly coagulatable and re-dispersable latex is a good example. Millions of tons of polymer latexes are produced annually by emulsion polymerization. The unique properties of latex products offer a variety of applications in rubber, plastic, coating, paper,

textile, leather, and construction industries, as well as biomedicine and pharmaceuticals.[79, 80] Most emulsion products contain about 45 to 60 vol% water. In solid form, latexes are coagulated by large amount of salts or acids, washed and dried. Wasteful water and intensive energy are big problems. In liquid form, half of the costs spent in storage and transportation are for water. Reversible coagulation and redispersion of latexes have been demonstrated with CO_2/N_2.[38-42]

Another example is the use of CO_2-responsive polymers for chemical separation. Reaction and separation are the two foundations in chemical industries. In general, separation costs twice as much as reaction. Developing more cost effective and environmentally benign separation technologies represents a major direction in the chemical engineering innovations. Recently, an innovative approach by employing CO_2-responsive polyethylenimine (PEI) as extractants in liquid-liquid extraction of alpha-tocopherol from the tocopherol homologues has been reported.[81] Polymer chains dissolve in one phase and interact with targeted homologue molecules. Upon switching, the chains bring the homologue molecules into another phase and thus facilitate the separation. The polymer can readily be switched back and release the extracted homologue. This innovative approach saves back extraction steps, thus significantly reducing the use of energy and organic solvent.

There are many opportunities for innovation in our daily practices, which we have taken for granted and seldom thought about existence of the opportunities. Current research on CO_2-responsive polymers is mainly in academic laboratories and has not yet been evaluated

under industrial conditions. Consequently, future efforts in this area should be made to explore more powerful gas-responsive polymer systems, and to adapt them to the well-developed unit operations with bubbles, drops and particles in reaction and separation industrial processes.

Some of the studied trigger gases, such as NO, CO, and H_2S, are also intracellular signaling molecules. There are opportunities in biomedical areas. To advance practical applications of their relative responsive polymers, the key challenge is to improve the response specificity, sensitivity and reversibility. Since their equilibrium concentrations in living organisms are relatively low, usually at several μM, or even nM level. As such, it would be highly desirable to design polymers precisely with well-defined hierarchical structures, so as to give accurate response towards the specific trigger. On the other hand, biocompatibility, biodegradability and biotoxicity must also be considered in the polymer design. These gas-responsive polymers could thus expand their scope of potential applications to smart nanocarriers for drug delivery, magnetic resonance imaging (MRI) agents for signals reporting and visualizing.

It is no doubt that there will be more and more innovative approaches proposed and creative strategies developed in this emerging area, which brings a bright future for the gas-responsive polymers.

§ 2.8 References

[1] Liu, F.; Urban, M. W., *Prog Polym Sci* **2010,** *35*, 3-23.

[2] Stuart, M. A. C.; Huck, W. T. S.; Genzer, J.; Muller, M.; Ober, C.; Stamm, M.; Sukhorukov, G. B.; Szleifer, I.; Tsukruk, V. V.; Urban, M.; Winnik, F.; Zauscher, S.; Luzinov, I.; Minko, S., *Nat Mater* **2010,** *9*, 101-113.

[3] Feng, A. C.; Yuan, J. Y., *Macromol Rapid Comm* **2014,** *35*, 767-779.

[4] Ray, J. G.; Naik, S. S.; Hoff, E. A.; Johnson, A. J.; Ly, J. T.; Easterling, C. P.; Patton, D. L.; Savin, D. A., *Macromol Rapid Comm* **2012,** *33*, 819-826.

[5] Zhang, J. L.; Zhang, M. X.; Tang, K. J.; Verpoort, F.; Sun, T. L., *Small* **2014**, *10*, 32-46.

[6] Katsuno, C.; Konda, A.; Urayama, K.; Takigawa, T.; Kidowaki, M.; Ito, K., *Adv. Mater.* **2013**, *25*, 4636-4640.

[7] Zhai, L., *Chem. Soc. Rev.*, **2013**, *42*, 7148-7160.

[8] Mura, S.; Nicolas, J.; Couvreur, P., *Nat. Mater.* **2013**, *12*, 991-1003.

[9] Hong, B. J.; Chiper, A. J.; Nguyen, S. T., *J. Am. Chem. Soc.* **2013**, *135*, 17655-17658.

[10] Ge, Z. S.; Liu, S. Y., *Chem. Soc. Rev.* **2013**, *42*, 7289-7325.

[11] Williams, R. J.; Smith, A. M.; Collins, R.; Hodson, N.; Das, A. K.; Ulijin, R. V., *Nat. Nanotechnol.* **2009**, *4*, 19-24.

[12] Shim, M. S.; Kwon, Y. J., *Adv. Drug Delivery Rev.* **2012**, *64*, 1046-1058.

[13] Yan, Q.; Yuan, J. Y.; Kang, Y.; Cai, Z. N.; Zhou, L. L.; Yin, Y. W., *Chem. Commun.* **2010**, *46*, 2781-2783.

[14] Liu, L. X.; Li, W.; Liu, K.; Yan, J. T.; Hu, G. X.; Zhang, A. F., *Macromolecules* **2011**, *44*, 8614-8621.

[15] Dai, S.; Ravi, P.; Tam, K. C., *Soft Matter* **2008,** *4*, 435-449.

[16] Du, J. Z.; O'Reilly, R. K, *Macromol. Chem. Phys*. **2010**, *211*, 1530-1537.

[17] Zhao, Y., *Macromolecules* **2012,** *45*, 3647-3657.

[18] Yan, Q.; Xin, Y.; Zhou, R.; Yin, Y. W.; Yuan, J. Y., *Chem. Commun.* **2011,** *47*, 9594-9596.

[19] Lutz, J. F.; Akdemir, O.; Hoth, A., *J. Am. Chem. Soc.* **2006,** *128*, 13046-13047.

[20] Fielding, L. A.; Edmondson, S.; Armes, S. P., *J. Mater. Chem.* **2011**, *21*, 11773-11780.

[21] Endo, T.; Nagai, D.; Monma, T.; Yamaguchi, H.; Ochiai, B., *Macromolecules* **2004**, *37*, 2007-2009.

[22] Liu, Y. X.; Jessop, P. G.; Cunningham, M.; Eckert, C. A.; Liotta, C. L., *Science* **2006**, *313*, 958-960.

[23] Lin, S. J.; Theato, P., *Macromol. Rapid Comm.* **2013**, *34*, 1118-1133.

[24] Choi, J. Y.; Kim, J. Y.; Moon, H. J.; Park, M. H.; Jeong, B., *Macromol. Rapid Comm.* **2014,** *35*, 66-70.

[25] Zhang, Q.; Zhu, S. P., *Macromol. Rapid Comm.* **2014,** *35*, 1692-1696.

[26] Hu, J. M.; Whittaker, M. R.; Duong, H.; Li, Y.; Boyer, C.; Davis, T. P., *Angew. Chem. Int. Edit.* **2014,** *53*, 7779-7784.

[27] Hu, J. M.; Whittaker, M. R.; Li, Y.; Quinn, J. F.; Davis, T. P., *Polym. Chem.* **2015,** *6*, 2407-2415.

[28] Hu, J. M.; Whittaker, M. R.; Yu, S. H.; Quinn, J. F.; Davis, T. P., *Macromolecules* **2015,** *48*, 3817-3824.

[29] Yan, Q.; Sang, W., *Chem. Sci.*, **2016**, *7*, 2100-2105.

[30] Zhu, M.; Wu, Y.; Ge, C.; Ling, Y.; Tang, H., *Macromolecules* **2016**, *49*, 3542–3549.

[31] Qin, Z.; Thomas, C. M.; Lee, S.; Coates, G. W., *Angew. Chem. Int. Ed.* **2003**, *42*, 5484 -5487.

[32] Choudhary, V. R.; Dhar, A.; Jana, P.; Jha, R.; Uphade, B. S., *Green Chem.*, **2005**, *7*, 768-770.

[33] Wang, R., Springer Science & Business Media: New York, 2004.

[34] Quek, J. Y.; Davis, T. P.; Lowe, A. B., *Chem. Soc. Rev.*, **2013**, *42*, 7326-7334.

[35] Yan, Q.; Zhao, Y., *Chem. Commun.*, **2014**, *50*, 11631-11641.

[36] Cunningham, M. F.; Jessop, P. G., *European Polymer Journal* **2016**, *76*, 208-215.

[37] Darabi, A.; Jessop, P. G.; Cunningham, M. F., *Chem. Soc. Rev.* **2016**, *45*, 4391-4436.

[38] Fowler, C. I.; Muchemu, C. M.; Miller, R. E.; Phan, L.; O'Neill, C.; Jessop, P. G.; Cunningham, M. F., *Macromolecules* **2011,** *44*, 2501-2509.

[39] Su, X.; Jessop, P. G.; Cunningham, M. F., *Macromolecules* **2012,** *45*, 666-670.

[40] Mihara, M.; Jessop, P.; Cunningham, M., *Macromolecules* **2011,** *44*, 3688-3693.

[41] Zhang, Q.; Wang, W. J.; Lu, Y. Y.; Li, B. G.; Zhu, S. P., *Macromolecules* **2011,** *44*, 6539-6545.

[42] Zhang, Q.; Yu, G. Q.; Wang, W. J.; Yuan, H. M.; Li, B. G.; Zhu, S. P., *Langmuir* **2012,** *28*, 5940-5946.

[43] Vincent, S.; Mioskowski, C.; Lebeau, L., *J. Org. Chem.* **1999,** *64*, 991-997.

[44] Papandreou, G.; Tong, M. K.; Ganem, B., *J. Am. Chem. Soc.* **1993,** *115*, 11682-11690.

[45] Han, D; Tong, X.; Boissière, O.; Zhao, Y., *ACS Macro Lett.*, **2012**, *1*, 57–61.

[46] Zhang, Q.; Yu, G. Q.; Wang, W. J.; Li, B. G.; Zhu, S. P., *Macromol. Rapid Comm.* **2012,** *33*, 916-921.

[47] Zhang, Q.; Yu, G. Q.; Wang, W. J.; Yuan, H. M.; Li, B. G.; Zhu, S. P., *Macromolecules* **2013,** *46*, 1261-1267.

[48] Yan, Q.; Zhou, R.; Fu, C. K.; Zhang, H. J.; Yin, Y. W.; Yuan, J. Y., *Angew. Chem. Int. Edit.* **2011,** *50*, 4923-4927.

[49] Yan, Q.; Wang, J. B.; Yin, Y. W.; Yuan, J. Y., *Angew. Chem. Int. Edit.* **2013,** *52*, 5070-5073.

[50] Yan, Q.; Zhao, Y., *Angew. Chem. Int. Edit.* **2013,** *52*, 9948-9951.

[51] Yan, B.; Han, D. H.; Boissiere, O.; Ayotte, P.; Zhao, Y., *Soft Matter* **2013,** *9*, 2011-2016.

[52] Yan, Q.; Zhao, Y., *J. Am. Chem. Soc.* **2013,** *135*, 16300-16303.

[53] Liu, H. B.; Guo, Z. R.; He, S.; Yin, H. Y.; Fei, C. H.; Feng, Y. J., *Polym. Chem.* **2014,** *5*, 4756-4763.

[54] Liu, H. B.; Zhao, Y.; Dreiss, C. A.; Feng, Y. J., *Soft Matter* **2014,** *10*, 6387-6391.

[55] Feng, A. C.; Zhan, C. B.; Yan, Q.; Liu, B. W.; Yuan, J. Y., *Chem. Commun.* **2014,** *50*, 8958-8961.

[56] Liu, B. W.; Zhou, H.; Zhou, S. T.; Zhang, H. J.; Feng, A. C.; Jian, C. M.; Hu, J.; Gao, W. P.; Yuan, J. Y., *Macromolecules* **2014,** *47*, 2938-2946.

[57] Yan, Q.; Zhang, H.; Zhao, Y., *ACS Macro Lett.* **2014,** *3*, 472−476.

[58] Liu, H.; Guo, Z.; He, S.; Yin, H.; Fei, C.; Feng, Y., *Polym. Chem.*, **2014**, *5*, 4756-4763.

[59] Morse, A. J.; Armes, S. P.; Thompson, K. L.; Dupin, D.; Fielding, L. A.; Mills, P.; Swart, R., *Langmuir* **2013**, *29*, 5466-5475.

[60] Liu, P. W.; Lu, W. Q.; Wang, W. J.; Li, B. G.; Zhu, S., *Langmuir* **2014**, *30*, 10248-10255.

[61] Kumar, S.; Tong, X.; Dory, Y. L.; Lepage, M.; Zhao, Y., *Chem. Commun.* **2013**, *49*, 90–92.

[62] Ding, Y.; Chen, S.; Xu, H.; Wang, Z.; Zhang, X., *Langmuir* **2010**, *26*, 16667-16671.

[63] Zhang, J.; Han, D.; Zhang, H.; Chaker, M.; Zhao. Y.; Ma, D., *Chem. Commun.* **2012**, *48*, 11510–11512.

[64] Cai, Y.; Shen, W.; Wang, R.; Krantz, W. B.; Fane A. G.; Hu, X., *Chem. Commun.* **2013**, *49*, 8377-8379.

[65] Mallat, T.; Baiker, A., *Chem. Rev.* **2004,** *104*, 3037-3058.

[66] Punniyamurthy, T.; Velusamy, S.; Iqbal, J., *Chem. Rev.* **2005,** *105*, 2329-2363.

[67] Lei, L.; Zhang, Q.; Shi, S. X.; Zhu, S., *Polymer Chemistry*, **2016,** *7*, 5456-5462.

[68] Lei, L.; Zhang, Q.; Shi, S. X.; Zhu, S., *ACS Macro Lett. ACS Macro Lett.* **2016**, 5, 828–832.

[69] Zhang, Q.; Zhu, S. P., *ACS Macro Lett.* **2014,** *3*, 743-746.

[70] Lei, L.; Zhang, Q.; Shi, S. X.; Zhu, S. P., *Langmuir* **2015,** *31*, 2196-2201.

[71] Ignarro, L. J.; Cirino, G.; Casini, A.; Napoli, C., *J. Cardiovasc Pharm.* **1999,** *34*, 879-886.

[72] Ignarro, L. J., *Bioscience Rep.* **1999,** *19*, 51-71.

[73] Ignarro, L. J., *Angew. Chem. Int. Edit.* **1999,** *38*, 1882-1892.

[74] Riccio, D. A.; Schoenfisch, M. H., *Chem. Soc. Rev.* **2012,** *41*, 3731-3741.

[75] Smith, D. J.; Chakravarthy, D.; Pulfer, S.; Simmons, M. L.; Hrabie, J. A.; Citro, M. L.; Saavedra, J. E.; Davies, K. M.; Hutsell, T. C.; Mooradian, D. L.; Hanson, S. R.; Keefer, L. K., *J. Med. Chem.* **1996,** *39*, 1148-1156.

[76] Malinski, T.; Taha, Z., *Nature* **1992,** *358*, 676-678.

[77] Kojima, H.; Nakatsubo, N.; Kikuchi, K.; Kawahara, S.; Kirino, Y.; Nagoshi, H.; Hirata, Y.; Nagano, T., *Anal. Chem.* **1998,** *70*, 2446-2453.

[78] Lim, M. H.; Wong, B. A.; Pitcock, W. H.; Mokshagundam, D.; Baik, M. H.; Lippard, S. J., *J. Am. Chem. Soc.* **2006,** *128*, 14364-14373.

[79] El-Aasser, M. S.; Miller, C. M. In *Polymeric dispersions, Principles and applications*; Asua, J. M., Ed.; Kluwer Academic Publishers: Dordrecht, The Netherlands, and Boston, MA, 1997.

[80] Cunningham, M. F., *Prog. Polym. Sci.* **2008**, *33*, 365-398.

[81] Yu, G.; Lu, Y.; Liu, X.; Wang, W. J.; Yang, Q.; Xing, H.; Ren, Q.; Li, B. G.; Zhu, S., *Ind. Eng. Chem. Res.* **2014**, *53*, 16025-16032

3 O_2 AND CO_2- SWITCHABLE THERMO-RESPONSIVE RANDOM COPOLYMERS

In this chapter, a serious of fluorinated acrylamide monomers with optimized water solubility and variable number (1, 2 and 3) of fluorine atoms, were introduced to the family of O_2-swichable monomers. The O_2-switchable properties of both the commercialized fluorinated monomers FMA and FS, and the newly discovered F1EA, F2EA and F3EA was investigated based on the LCST shift of their thermo-responsive random copolymers. This chapter is a reproduction of the published paper in Lei Lei, Qi Zhang, Susan Shi, Shiping Zhu "Oxygen-switchable thermo-responsive random copolymers" *Polymer Chemistry*, **2016**, 7, 5456-5462 (DOI: 10.1039/C6PY01145D) with the permission from John Wiley and Sons. This work provides a general methodology for design and screening of monomer candidates for the O_2-switchable polymer

preparation. The supporting information referred in the text is attached at the end of this chapter.

Author contributions

The initial idea of this work is generated through the discussions with Dr. Shiping Zhu and Dr. Qi Zhang. I did all the experiments and prepared the first manuscript under Dr. Zhu's supervision. Dr. Qi Zhang and Dr. Shuxian Shi provided valuable discussion and the first revision. Dr. Zhu did final revision and provided quality control of the manuscript.

§ 3.1 Abstract

Herein, we report the synthesis of oxygen (O_2)-switchable thermo-responsive random copolymers based on fluorinated acrylamide monomer homologues: N-(2-fluoroethyl)acrylamide (F1EA), N-(2,2-difluoroethyl)acrylamide (F2EA), and N-(2,2,2-trifluoroethyl)acrylamide (F3EA). Copolymerizing these monomers with N,N-dimethylaminoethyl methacrylate (DMA) via reversible addition-fragmentation chain transfer (RAFT) polymerization yield thermo-responsive random copolymers, which have dual switchability towards O_2 and carbon dioxide (CO_2). The inherent low critical solution temperature (LCST) of these copolymers can be precisely designed in a wide range of temperatures by varying their chemical compositions. Importantly, this LCST can be reversibly switched to different levels by respectively purging O_2 or CO_2 into

the aqueous solution, and be recovered to its initial state by washing off the trigger gas. This work provides a versatile and effective approach for the preparation of O_2-responsive polymers, with a big operation window of temperature.

§ 3.2 Introduction

Stimuli-responsive polymers have attracted huge interest in polymer science over the past decades. Upon applying external stimuli, such as pH,[1] light,[2, 3] thermo,[4] ionic strength,[5] magnetic and electro field,[6, 7] these "smart" polymers respond with changes in their physicochemical properties and give output signals, such as shrinking and expansion of volume,[8, 9] transformation of shape and morphology,[10, 11] optical change, and self-assembled architecture modulation.[12] Stimuli-responsive polymers have many high potential applications for functional materials,[13] sensors,[14] and nanotechnologies.[15] The thermo-responsivity is the most fundamental and best-studied system among various types of stimuli. The lower critical solution temperature (LCST) is the key property, which is extensively exploited in developing thermo-responsive polymers. These polymers undergo phase separation at LCST.[16] The LCST can be pre-designed by varying chemical composition of copolymers. Increasing hydrophobic component usually decreases the LCST, while hydrophilic composition makes polymers more water soluble and thus increases the LCST.[17, 18]

An effective approach to regulate LCST is to introduce polymer an additional functionality, which can vary its hydrophilicity or polarity by an external trigger such as pH, and thus induce LCST shift to a certain degree. Zhao et al.[19] discovered that

poly(N, N-dimethylaminoethyl methacrylate) (PDMAEMA) in water can react with carbon dioxide (CO_2) and have its LCST reversibly tuned by purging and removing CO_2 gas from the system. Copolymerization of the CO_2-responsive monomers with thermo-responsive monomers like N-isopropylacrylamide (NIPAM) and 2-(2-methoxyethoxy)ethyl methacrylate (MEO_2MA) provides a general strategy for the development of CO_2-switchable polymers with tunable LCST. Huang et al.[20] synthesized an acrylamide monomer bearing both isopropyl amide (thermo-responsive moiety) and N, N-diethylamino ethyl (CO_2/pH-responsive moiety) groups, which represents another type of thermo-responsive polymers with their LCST tunable by pH and CO_2. Lei et al.[21] synthesized a new monomer N-(2-fluoroethyl amide)-N-(2-(diethylamino)ethyl) acrylamide, i.e. AM-(F1EA-DEAE), bearing both O_2- and CO_2-switchable moieties, and prepared the first O_2-switchable thermo-responsive homopolymer system with its LCST tunable by CO_2 and O_2 treatment.

Compared to other stimuli, gas triggers have advantages in application where a large volume operation is required (compared to thermo-responsive systems that require heat transfer, which is limited by large volume) or where little contamination is allowed (compared to pH-responsive systems that use strong base and acid, which result in buffer contamination and salt accumulation). CO_2 has been well reported as a green and abundant gas-trigger.[22, 23] CO_2-responsivity has been applied to various functional material systems, such as redispersible latexes,[24-30] vesicle/microgel "breathing",[9, 31] and block copolymer self-assemblies with their morphology

transition between "micelle", "worm" and "vesicle".[11, 32] CO_2 can reversibly react with amine, amidine, and carboxyl moieties in aqueous solution,[12] and dramatically change their hydrophobicity/polarity properties. Moreover, these changes can be recovered upon purging CO_2 by an inert gas like N_2, without any salt accumulation and contamination to the system.

Beside CO_2, oxygen (O_2) was thought to be another promising gas trigger candidate. It is well known that perfluorocarbons (PFCs) are useful in enhancing O_2 dissolution (with solubility increased 20 times in water),[33] O_2 carrier and delivery,[34] and O_2 molecular separation. However, it is until very recently that O_2-switchable polymers have been reported. Jeong et al.[32] prepared pentafluorophenyl end-capped poly(ethylene glycol) (PF-PEG-PF) and showed that intermolecular interactions of pentafluorophenyl moieties with O_2 slightly increased the polymer solubility in aqueous solution, thus increasing the solution LCST from 24.5 to 26 ^oC. Zhang et al.[8] prepared fluorinated random copolymers from commercially available monomers 2,2,2-trifluoroethyl methacrylate (FMA) and N,N-dimethylaminoethyl methacrylate (DMA) and found that aqueous solutions of the copolymers treated by O_2 dramatically increased the LCST from 24.5 to 50 °C, which provided a big operation window for the development of O_2-switchable materials. Later on, Zhang et al.[31] also developed O_2 and CO_2 dual-responsive nanoaggregates of the fluoro- and amino-containing copolymers. The vesicles self-assembled from these copolymers in aqueous solution underwent different volume/shape transformations upon O_2 and CO_2 treatments. CO_2

and O_2 dual gas-switchable microgel systems were also developed based on poly(2-(diethylamino)ethyl methacrylate-*co*-2,3,4,5,6-pentafluorostyrene), i.e. P(DEA-*co*-FS).[9] The microgel volume could be reversibly expanded to various levels triggered by either CO_2 or O_2 aeration and the volume could be recovered to its initial state by "washing off" the trigger gases with an inert gas like nitrogen (N_2). This volume expansion upon CO_2 and O_2 treatment of the microgels provide a mimetic model for hemoglobin "breathing".

An examination of the literatures revealed that only pentafluorophenyl (PF),[32] 2,2,2-trifluoroethyl methacrylate (FMA),[8, 31] and 2,3,4,5,6-pentafluorostyrene (FS)[9] have been explored as the monomer candidates for developing O_2-switchable polymer systems. Among these candidates, the PF-capped polymers have very limited O_2-switchability with a narrow LCST shift of only 1.5 ^oC upon O_2 treatment.[32] The FMA and FS polymers also suffer from limited solubility in water due to their inherent hydrophobicity. For example, as reported in the previous work,[9] copolymerizing FS with 2-(diethylamino)ethyl methacrylate (DEA) enabled both O_2- and CO_2-responsivity of P(DEA-*co*-FS) microgels. Based on intuition, the O_2-responsivity could be improved by increasing the FS content. Unfortunately, it was proven to be impossible. This is because further increase in the FS content would make the microgels dramatically insoluble in water. To broaden the operation window of O_2-responsivity, a new type of relatively more hydrophilic fluorine-containing monomers are highly desirable. Developing such hydrophilic fluorinated vinyl

monomers serves as the objective of this work. A comprehensive examination of the literatures reveals that fluorinated acrylamide monomers having one, two and three fluorine atoms substituted in N-ethyl group (F1EA, F2EA and F3EA) have been synthesized by Lee et al.[17, 18] The water solubility, thermo-responsivity and biocompatibility of their copolymers were investigated. However, their O_2-switchable properties have not been explored.

In this work, these relatively hydrophilic fluorinated acrylamide monomers (F1EA, F2EA, and F3EA compared with FS and FMA) were synthesized and evaluated as potential O_2-switchable monomer candidates. The monomers were random copolymerized with N,N-dimethylaminoethyl methacrylate (DMA, CO_2-switchable monomer) through reversible addition-fragmentation chain transfer (RAFT) free radical polymerization. A series of CO_2 and O_2 dual gas-switchable thermo-responsive random copolymers were thus prepared. The precise LCST tailoring was achieved by varying the copolymer composition, which were also regulated by switching of the copolymers with the gas treatment of O_2 and CO_2. The work significantly expanded the operation window of temperature in gas switching systems.

§ 3.3 Experiments and Characterization

3.3.1 Materials

2,2,2-Trifluoroethyl methacrylate (FMA, 99%, Aldrich), 2,3,4,5,6-pentafluorostyrene (FS, 99%, Aldrich) and N,N-dimethylaminoethyl methacrylate (DMA, 99%, Aldrich) were passed through an inhibitor remover column before use. 2,2'-Azobis (2-methylpropionitrile) (AIBN, 98%, Aldrich) was recrystallized from methanol twice and stored in refrigeration prior to use. 2-Fluoroethylamine hydrochloride (90%, Aldrich), 2,2-difluoroethylamine (97%, Oakwood), 2,2,2-trifluoroethylamine hydrochloride (99.5%, Aldrich), 4-(dimethylamino)pyridine (DMAP, 99%, Aldrich), triethylamin (TEA, 99%, Aldrich), acryloyl chloride (97%, Aldrich), dichloromethane (DCM, 98%, Aldrich), hexane (99.5%, Aldrich), ethyl acetate (98%, Aldrich), 2-(dodecylthiocarbonothioylthio)-2-methylpropionic acid (DMP, 98%, Aldrich), 1,4-dioxane (99.8%, Fluka), tetrahydrofuran (THF, 99.5%, Aldrich) and toluene (99.8%, Aldrich) were all used as received, if not described otherwise. Milli-Q grade water prepared from Barnstead Nanopure Diamond system was used in all aqueous solution preparation. CO_2, O_2, and N_2 gases were controlled by FMA-A2100 flow meters (Omega) to maintain a constant gas flow of 10 mL/min.

3.3.2 Experiments

3.3.2.1 Preparation of fluorinated acrylamide monomers

N-fluoroethyl acrylamide monomers bear one (F1EA), two (F2EA) and tree (F3EA) fluorine atoms were synthesized following the method reported by Lee et al.[17, 18] The synthesis route was shown in Figure 2-S1 and described as following for reader's

convenience. Take N-(2,2-difluoroethyl)acrylamide (F2EA) preparation for an example. 2,2-Difluoroethylamine (10 g, 123.4 mmol), TEA (27.63 g, 185.1 mmol), DMAP (1.21 g, 9.87 mmoL, 8 mol%) and CH_2Cl_2 (130 mL) were added into a 250 mL round-bottom flask and cooled in ice water. Acryloyl chloride (13.96 g, 154.3 mmol) diluted with 20 mL dichloromethane was added drop-wise into the mixture under stirring within 20 min. The mixture was then allowed to react at room temperature for 24 hours. The product mixture was then washed with brine three times and the organic layer was dried with Na_2SO_4 and evaporated under reduced pressure. The residual product was purified by column chromatography with hexane and ethyl acetate mixture (V:V=1:2, with 1 vol. % TEA) as eluent, giving a white crystal solid product (7.83g, yield 47%). F1EA and F3EA were synthesised following the same procedure, giving a transparent oily liquid product of 23% yield and a white solid product of 50% yield, respectively.

3.3.2.2 Preparation of fluorinated random copolymers

A series of fluorinated random copolymers were prepared through reversible addition-fragmentation chain transfer (RAFT) copolymerization of N,N-dimethylaminoethyl methacrylate (DMA) with 5 mol% of the different fluorinated monomers (FS, FMA, F1EA, F2EA, F3EA). DMA was also random copolymerized with F2EA under different molar fractions (5, 10, 20, 40 and 50 mol%). In all the polymerization runs, the recipe was fixed to [Monomer]:[DMP]:[AIBN] = 100:1:0.4 with dioxane as the solvent. 2-Dodecylsulfanylthiocarbonylsulfanyl-2-

methylpropionic acid (DMP) was used as the chain transfer agent and azobisisobutyronitrile (AIBN) as the initiator. Take poly(N,N-dimethylaminoethyl methacrylate-*co*-N-2-fluoroethyl acrylamide), i.e. P(DMA-*co*-F2EA), with 10 mol% F2EA as an example. All the chemicals including DMA (2.83 g, 18 mmol), F2EA (0.27 g, 2 mmol), DMP (72.9 mg, 0.2 mmol), AIBN (13.1 mg, 0.08 mmol) and 6 ml dioxane were charged into a 25 mL round-bottom flask and sealed with rubber stopper. The solution was degassed with N_2 for 30 min under stirring. After that, the flask was placed into an oil bath set to 70 ^{o}C. The polymerization was carried out for 24 hours. The product was diluted with THF and precipitated in cold hexane upon vigorous agitation. This process was repeated three cycles for polymer product purification. At the end, the polymer was vacuum dried at room temperature until a constant weight.

3.3.2.3 O_2 and CO_2-switchable LCST tests

The LCST of the fluorinated random copolymers in aqueous solution was reflected by their temperature-based turbidity change, which was characterized by Cary 300 UV-vis spectrophotometer at 500 nm wavelength. The LCST was defined as the temperature at which 50% decrease in transmittance occurred. For O_2 and CO_2-switchable LCST characterization, the polymer aqueous solution (10 mg/mL) was firstly treated with a specific gas (O_2, CO_2 or N_2) at 10 mL/min for 1 hour and it was finely sealed with parafilm. Specifically, the polymer aqueous solution was charged into 20 ml flask and enfolded into crushed ice during gas treatment.

3.3.3 Characterization

^{1}H NMR spectra collected in $CDCl_3$ and DMSO-d_6 on Bruke AV200/600 MHz NMR spectrometer were used to determine the monomer structures and polymer compositions, respectively. The molecular weight and the polydispersity index of the polymers were collected from PL-GPC 50 (A Varian, Inc. Company) by using DMF as effluent. The LCST of polymer aqueous solution (10 mg/mL) was characterized by Cary 300 UV-vis spectrophotometer at 500 nm wavelength. The heating process was set from 5 to 85 °C at 1 °C/min acceleration. Each sample was treated with a specific gas (O_2, CO_2 and N_2) for 1 hour and finely sealed in a closed vial during the measurements.

§ 3.4 Results and Discussion

3.4.1 Synthesis and characterization of the fluorinated random copolymers

Firstly, the fluorinated acrylamide monomers bearing one (F1EA) two (F2EA) and three (F3EA) fluorine atoms (FEAs) were prepared following the procedure descried by Lee et al.[17, 18] Since O_2-switchability of the fluorinated polymers is determined by their water solubility and the number of fluorine atoms,[9, 31] the fluorinated acrylamide monomers were hypothesized to possess improved hydrophilicity and water solubility, compared to the commercially available 2,2,2-trifluoroethyl methacrylate (FMA) monomer. The reasons were three-fold: 1) the "methacrylic (CH_2=C(CH_3)-R)" moiety in FMA was changed to "acrylic (CH_2=CH-R)" in FEAs; 2) the "ester group (-

COO-)" in FMA was varied to "amide group (-CONH-)" in FEAs; 3) the number of fluorine atoms in N-ethyl group of FEAs was varied from one (F1EA) to two (F2EA) and three (F3EA), which could regulate both water solubility and O_2-switchable properties. The differences in structure between FMA and FEAs were shown in Figure 3-1 a). ^1H NMR spectra in Figure 3-S2 confirmed successful synthesis of the fluorinated acrylamide monomers.

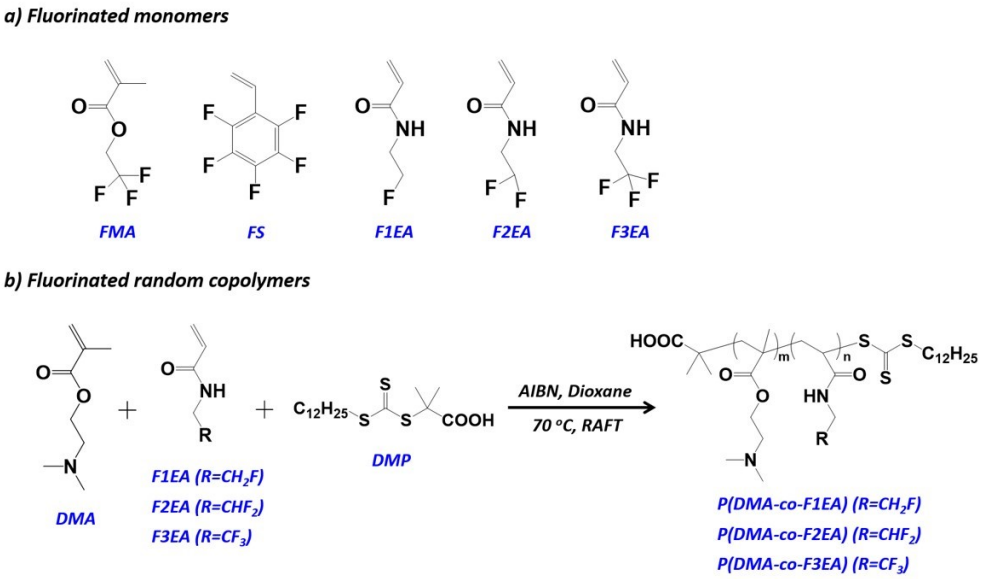

Figure 3-1. a) Molecular structures of FMA, FS and the fluorinated acrylamide monomers: F1EA, F2EA and F3EA. b) Synthesis route of random copolymers based on the fluorinated acrylamide monomers through RAFT polymerization.

Based on all the fluorinated monomers (FMs) shown in Figure 3-1 a) and N,N-dimethylaminoethyl methacrylate (DMA), P(DMA-*co*-FMs) random copolymers were prepared by reversible addition fragmentation chain transfer (RAFT) polymerization with 2-dodecylsulfanylthiocarbonylsulfanyl-2-methylpropionic acid (DMP) as the

chain transfer agent and azobisisobutyronitrile (AIBN) as the initiator. The procedure is schematically illustrated in Figure 3-1 b). Table 3-1 summarizes all the random copolymers prepared and used in this work. The chemical compositions of the copolymers were estimated from the ^{1}H NMR spectra in Figure 3-S3 to Figure 3-S8. For example, the F2EA molar fractions in P(DMA-*co*-F2EA) copolymers (Run 4-9) were calculated from "$A_j/(A_c + A_j/2)$ X 100%", where "A" refers to the integration area for specific hydrogen atoms in the NMR spectra. "A_c" is attributed to $-CHF_2$ of F2EA and "A_j" is for $-CH_2CH_2N(CH_3)_2$ of DMA, in Figure 3-S8. The molecular weight and the polydispersity of all the polymers used in this work were measured by GPC, as listed in Table 3-1.

Table 3-1. Random copolymers prepared based on the fluorinated monomers and the characterization results of their gas-switchable thermo-responsive properties.

Run	*Sample* [a]	*DMA/FM (mol:mol)* [b]	*"FM" content (mol%)* [c]	M_w *(g/mol)* [d]	*PDI* [d]	*LCST (°C)* [e]		
						N_2	O_2	$\Delta(O_2 - N_2)$
1	PNFS-5	95:5	4.6	8900	1.21	36	65	29
2	PNFMA-5	95:5	5.1	8700	1.31	38	73	35
3	PNF1-5	95:5	3.7	8200	1.30	78	85	7
4	PNF2-5	95:5	5.4	8300	1.27	65	>85	>20
5	PNF3-5	95:5	4.1	8400	1.32	52	>85	>33
4	PNF2-5	95:5	5.4	8300	1.27	65	>85	>20
6	PNF2-10	90:10	8.6	8100	1.18	50	75	25
7	PNF2-20	80:20	19.0	7900	1.21	45	65	20
8	PNF2-40	60:40	39.4	7500	1.22	25	43	18
9	PNF2-50	50:50	46.3	7400	1.33	20	36	16

Note: a: Random copolymers (run 1-5) prepared based on fluorinated monomers (FMs); "N" represents "DMA"; F1, F2, F3 represent F1EA, F2EA and F3EA respectively. b: Targeted DMA/FM molar ratio in the copolymer. c: Molar fraction of the fluorinated monomer in

P(DMA-co-FM) random copolymers calculated based on ^{1}H NMR spectra. d: Molecular weight and polydispersity index measured from GPC. e: LCST of the polymer aqueous solution (10 mg/mL) under N_2 and O_2 treatment.

2.4.2 Thermo-responsive properties of the fluorinated random copolymers

Different fluorinated monomers (FMA, FS, F1EA, F2EA and F3EA) of 5 mol% were randomly copolymerized with a thermo-responsive and CO_2-switachable monomer DMA to prepare P(DMA-*co*-FM) random copolymers, as shown in the Run 1-5 of Table 3-1. All these random copolymers with close molecular weight could be easily dissolved in water at room temperature. PDMA is known to have a LCST around 50 ^{o}C.[19] The LCST of P(DMA-*co*-FM) random copolymers is defined as the temperature, at which 50% of the change in polymer aqueous solution transmittance occurs.[17] Figure 3-2 shows the LCST of the copolymer aqueous solution (10 mg/mL) investigated by Cary 300 UV-vis spectrophotometer. It was found that FS- and FMA-based copolymers (PNFS-5 and PNFMA-5) had their LCSTs at 36 ^{o}C and 38 ^{o}C, respectively. Compared to PNFMA-5, PNF3-5 had a dramatically increased LCST from 38 ^{o}C to 52 ^{o}C, suggesting increased monomer hydrophilicity (note: both contain 3 fluorine atoms). This was resulted from the difference in molecular structure between FMA and F3EA ("methacrylic" in FMA versus "acrylic" in F3EA; "ester" in FMA versus "amide" in F3EA). When the number of fluorine atoms in F3EA progressively decreased to two (F2EA) and one (F1EA), the LCST of the copolymers PNF2-5 and PNF1-5 further increased to 65 ^{o}C and 78 ^{o}C, because of improved monomer hydrophilicity (through reducing the number of fluorine atoms). It becomes clear that

the hydrophilicity of fluorinated monomers could be increased either by introducing hydrophilic functional group or decreasing the number of substituted fluorine atoms.

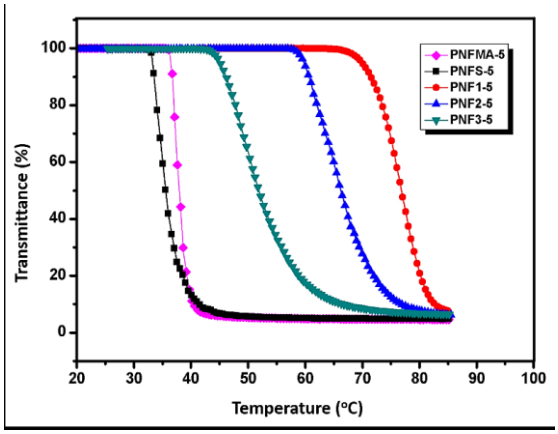

Figure 3-2. Temperature based transmittance changes of P(DMA-co-FM)-5 random copolymers aqueous solution (10 mg/mL). "FMs" represents different fluorinated monomers (FMA, FS, F1EA, F2EA, F3EA).

Compared to F1EA and F3EA, F2EA showed a balance between water solubility and number of fluorine atoms for the thermo-responsive properties, which was consistent with Lee et al's work.[17, 18] The LCST of thermo-responsive copolymers strongly depended on the monomer composition. The LCST of PNF2 could be tuned by adjusting the mole fraction of DMA and F2EA in the copolymer chains. A series of PNF2 copolymers having different F2EA molar fractions were synthesized and characterized (Run 4, 6-9 in Table 3-1 and Figure 3-3 a). Their inherent LCST curves were measured based on 10 mg/mL P(DMA-co-F2EA) (i.e. PNF2) aqueous solutions. It was found that, with the increased F2EA component 5, 10, 20, 40, 50 mol%, the LCST of PNF2 decreased from 65, 50, 45, 25 to 20 °C. This was because that F2EA was more hydrophobic than DMA, and that PF2EA had a much lower solubility in water

than PDMA.[17, 18] The increased hydrophobic component decreased the temperature of phase transition. Figure 3-3 b) shows the LCST of P(DMA-*co*-F2EA) copolymer as a function of F2EA molar fraction. The data correlation suggested that in the range of 5-50 mol%, the LCST decreased linearly with the F2EA fraction (f_{F2EA}): "LCST = $-0.93 \bullet f_{F2EA} + 64$".

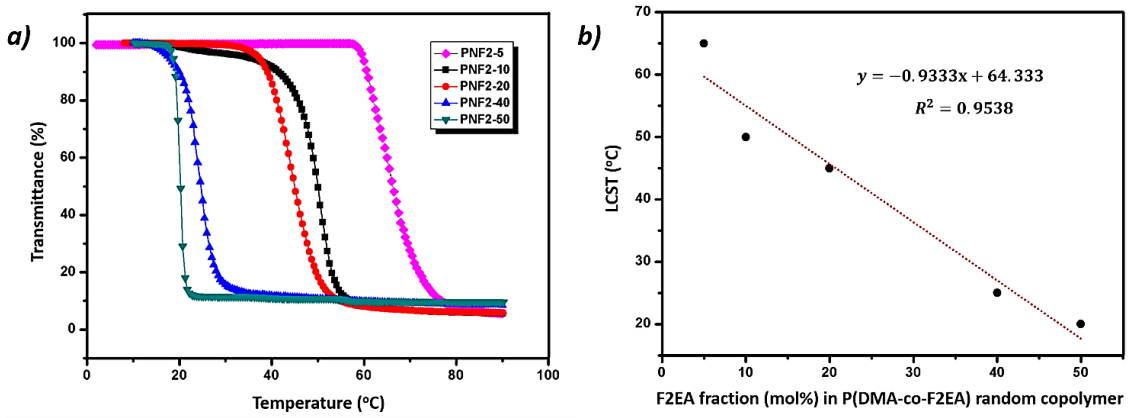

Figure 3-3. a) Temperature-based transmittance changes of P(DMA-*co*-F2EA) (PNF2) random copolymers with different F2EA molar fractions (5, 10, 20, 40 and 50 mol%). b) LCST of P(DMA-*co*-F2EA) random copolymers as a function of F2EA molar fraction.

2.4.3 O_2 and CO_2 switchable thermo-responsive random copolymers: O_2-induced LCST shifting

In addition to the thermo-responsive properties, all the fluorinated acrylamide copolymers of F1EA, F2EA and F3EA showed O_2-switchable properties, which were compared with the previous reported copolymers of commercially available fluorinated monomers (FMA and FS). The O_2-switchable properties were reflected by the shift in LCST of copolymer aqueous solution before (N_2) and after O_2 treatment at 10 mL/min for 60 min.

2.4.3.1 Reversible LCST shifting upon O_2 and CO_2 treatment.

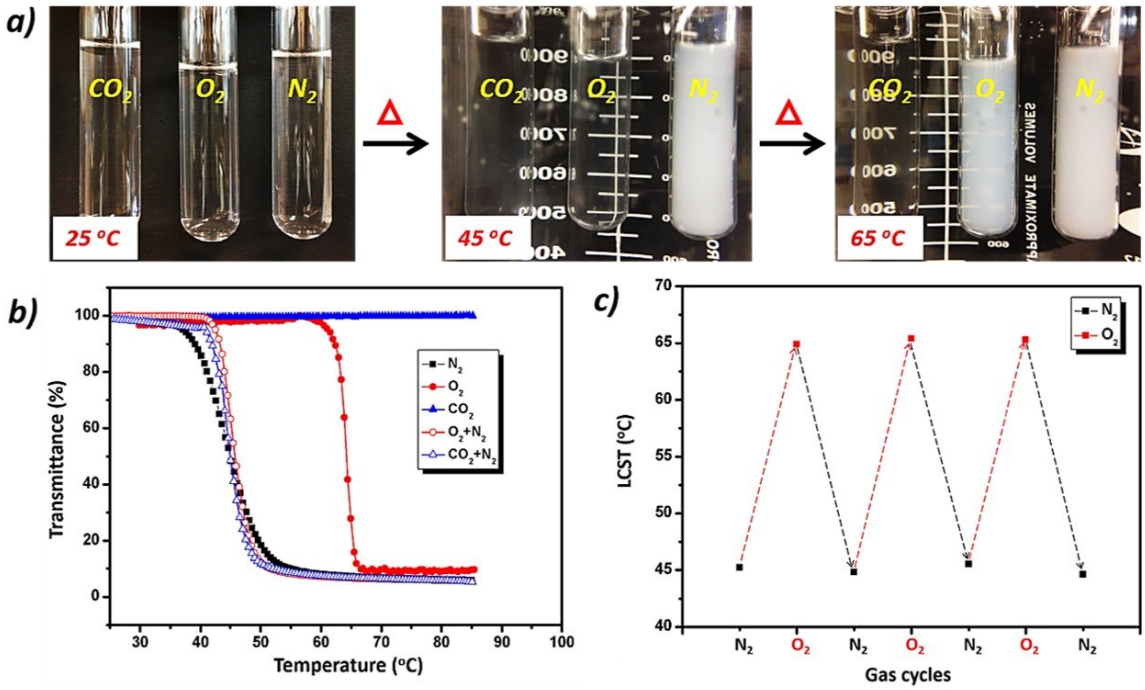

Figure 3-4. a) Photographs of P(DMA-*co*-F2EA)-20 (PNF2-20) aqueous solution (10 mg/mL) at different temperature. The polymer aqueous solution was pretreated with CO_2, O_2 and N_2 respectively. b) LCST curves of PNF2-20 aqueous solution (10 mg/mL) after different gas treatment procedures. c) The reversibility of PNF2-20 aqueous solution upon O_2 and N_2 treatment.

Figure 3-4 a) shows the photograph of gas-treated (CO_2, O_2 and N_2) PNF2-20 aqueous solution (10 mg/mL) at different temperatures, which exhibited very different temperature-dependent turbidity changes. The trigger gas (O_2 and CO_2) treatment clearly increased hydrophilicity of the random copolymer. As seen in Figure 3-4 b), the inherent LCST (under N_2 treatment) of PNF2-20 was determined to be 45 °C, which increased to 65 °C after 1 hour O_2 treatment at 10 mL/min under ice-bath

protection. The van der Waals intermolecular interactions between O_2 molecules and fluorine atoms in F2EA increased the system's hydrophilicity and made the copolymer O_2-switchale.[31, 32] Different from O_2, the copolymer treated with CO_2 for 1 hour became totally water soluble and there was no LCST transition observed up to 85 °C. This was because CO_2 dissolved in aqueous solution protonated the tertiary amine and dramatically increased the system hydrophilicity.[12, 19] It has been reported in literature that CO_2-induced LCST shift could be regulated by the CO_2 treatment time (i.e., partial protonation of the tertiary amine atoms).[19] Both CO_2- and O_2-induced increases in LCST were easily recovered by washing off the trigger gas through N_2 purging for about 30 min or by boiling the aqueous solutions for 2 min. The O_2-induced LCST shift and recovery of PNF2-20 aqueous solution were repeated for many cycles, without any lose of O_2-responsive properties, as seen in Figure 3-4 c).

2.4.3.2 Effect of FM type and content in the copolymer on LCST

Figure 3-5 a) shows the temperature-based transmittance change of the copolymers of DMA with F1EA, F2EA, F3EA, FMA and FS, in 10 mg/mL aqueous solution. All the polymers showed increased LCST with O_2 treatment. Specifically, the LCST of FMA-based copolymer (PNFMA-5) increased from 38 °C to 73 °C, while FS-based copolymer (PNFS-5) increased from 36 °C to 65 °C. Figure 3-5 a, b) show that, treated with O_2, the copolymers based on F1EA, F2EA and F3EA experienced an incomplete change in transmittance due to the temperature limit of 85 °C in the LCST characterization. The hydrophilicity of the copolymers was in the order of PNF2-5, PNF3-5 and PNF1-5.

PNF2-5 had the highest O_2-induced hydrophilicity at 85 ^oC as seem from Figure 3-5 a) and b). It is very encouraging that only 5 mol% F3EA in the copolymer with DMA (PNF3-5), could obtain at least 33 ^oC of O_2-induced LCST increase (from 52 ^oC to 85^oC). This represented a significant improvement from previously reported 10.5 mol% FMA copolymer with DMA, P(DMA-*co*-FMA), which gave an increase from 24.5 to 55^oC after O_2 treatment.[27] Figure 3-5 c, d) show the LCST curves and the LCST increase of P(DMA-*co*-F2EA) copolymers after O_2-treatment. With the increased F2EA fraction in the PNF2 copolymer, the increase in O_2-induced LCST gradually decreased. At the low fluorinated monomer content, the number of fluorine atoms played the major role in interacting with O_2 and in increasing the polymer hydrophilicity. At the high fluorinated monomer content, the hydrophobicity derived from the fluorinated monomers restricted the increase in O_2-induced hydrophilicity. F2EA appeared to be the best O_2-responsive monomer candidate reported so far. It provides adequate O_2-responisve capability, while not severely restricted by hydrophobicity. Moreover, the LCST of P(DMA-*co*-F2EA) could be tailor-made to various different levels for a wide range of applications.

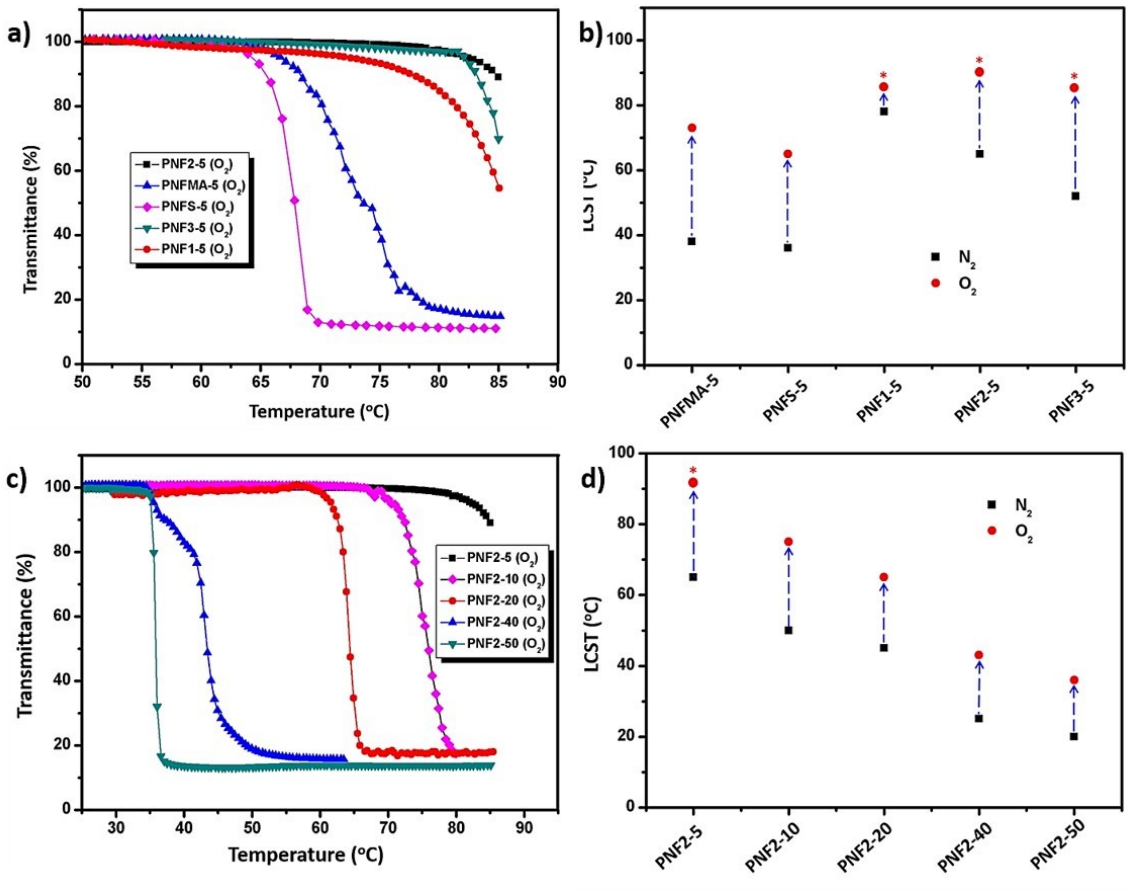

Figure 3-5. a) Temperature based transmittance changes of P(DMA-*co*-FMs) random copolymer with 5 mol% of different fluorinated monomers (FMs). b) LCST shift of P(DMA-*co*-FMs) before and after O_2 treatment. c) Temperature based transmittance changes of P(DMA-*co*-F2EA) random copolymers with 5, 10, 20, 40 and 50 mol% of F2EA content. d) LCST shift of P(DMA-*co*-F2EA) random copolymers before and after O_2 treatment. "*" means that the LCST characterization were restricted due to the high temperature.

It is important to mention that gas-switchable systems are usually limited to the operation temperature.[12] O_2-responsivity is based on van der Waals forces intermolecular interactions, while CO_2-responsivity is on protonation. O_2-responsivity is more easily to be weakened by elevating temperature, which seriously breaks O_2-fluorine interaction, decreases O_2 solubility, and drives O_2 out of the

aqueous solution. Actually, most gas-switchable applications are in the range of 10~60 °C, the O_2-responsive polymers reported in this work are promising as the O_2 responsive polymer systems.

§ 3.5 Conclusion

In conclusion, O_2-switchable thermo-responsive random copolymers have been prepared from RAFT polymerization based on fluorinated acrylamide monomers (F1EA, F2EA and F3EA) and DMA. Improved water solubility and O_2-responsivity of these copolymers have been demonstrated, in comparison to the previously reported commercially available O_2-responsive monomer candidates (FMA and FS). The inherent LCST of these thermo-responsive copolymers can be precisely designed in a wide range of operation temperatures (from 20 to 65 °C) by varying their chemical composition. Furthermore, the shifting of LCST can be reversibly tuned by purging O_2 into their aqueous solutions, and recovered by removing the trigger gas with an inert gas washing or heating. Compared to FMA and FS, these fluorinated acrylamide monomers are more hydrophilic and efficient in introducing O_2-switchability to the gas-responsive system. Their O_2-switchabilities are also more durable in the higher temperature range. They are potentially good O_2-switchable monomer candidates. This work provides a robust and efficient approach for the development of O_2-responsive monomers and their polymers, which significantly expanded the operation window.

§ 3.6 References

[1] J. Morse, S. P. Armes, K. L. Thompson, D. Dupin, L. A. Fielding, P. Mills and R. Swart, *Langmuir*, **2013**, 29, 5466-5475.

[2] Q. Yan, Y. Xin, R. Zhou, Y. Yin and J. Yuan, *Chemical communications*, **2011**, 47, 9594-9596.

[3] Li and S. Liu, *Chemical communications*, **2012**, 48, 3262-3278.

[4] Jean-Franc¸ ois Lutz, O. z. r. Akdemir and A. Hoth, *J. Am. Chem. Soc.*, **2006**, 128, 13046-13047.

[5] Zhao and J. S. Moore, *Langmuir*, **2001**, 17, 4758-4763.

[6] S. Murdan, *Journal of Controlled Release*, **2003**, 92, 1-17.

[7] J. Thevenot, H. Oliveira, O. Sandre and S. Lecommandoux, *Chemical Society reviews*, **2013**, 42, 7099-7116.

[8] Q. Zhang and S. Zhu, *Macromolecular rapid communications*, **2014**, 35, 1692-1696.

[9] L. Lei, Q. Zhang, S. Shi and S. Zhu, *Langmuir*, **2015**, 31, 2196-2201.

[10] Q. Yan and Y. Zhao, *Angewandte Chemie*, **2013**, 52, 9948-9951.

[11] Feng, C. Zhan, Q. Yan, B. Liu and J. Yuan, *Chemical communications*, **2014**, 50, 8958-8961.

[12] Q. Yan and Y. Zhao, *Chemical communications*, **2014**, 50, 11631-11641.

[13] K. Akamatsu, M. Shimada, T. Tsuruoka, H. Nawafune, S. Fujii and Y. Nakamura, *Langmuir*, **2010**, 26, 1254-1259.

[14] K. Paek, H. Yang, J. Lee, J. Park and B. J. Kim, *ACS Nano*, **2014**, 8, 2848-2856.

[15] R. J. Williams, A. M. Smith, R. Collins, N. Hodson, A. K. Das and R. V. Ulijn, *Nature nanotechnology*, **2009**, 4, 19-24.

[16] T. Thavanesan, C. Herbert and F. A. Plamper, *Langmuir*, **2014**, 30, 5609-5619.

[17] S. Sun, P. Wu, W. Zhang, W. Zhang and X. Zhu, *Soft Matter*, **2013**, 9, 1807-1816.

[18] J. M. Bak, K.-B. Kim, J.-E. Lee, Y. Park, S. S. Yoon, H. M. Jeong and H.-i. Lee, *Polym. Chem*., **2013**, 4, 2219-2223.

[19] J. M. Bak and H.-i. Lee, *Journal of Polymer Science Part A: Polymer Chemistry*, **2013**, 51, 1976-1982.

[20] Han, X. Tong, O. Boissière and Y. Zhao, *ACS Macro Letters*, **2012**, 1, 57-61.

[21] X. Jiang, C. Feng, G. Lu and X. Huang, *ACS Macro Letters*, **2014**, 3, 1121-1125.

[22] L. Lei, Q. Zhang, S. Shi and S. Zhu, *ACS Macro Letters*, **2016**, 5 (7), 828–832.

[23] Y. Liu, P. G. Jessop, M. Cunningham, C. A. Eckert and C. L. Liotta, *Science*, **2006**, 313, 958-960.

[24] J. Heldebrant, C. R. Yonker, P. G. Jessop and L. Phan, *Energy & Environmental Science*, **2008**, 1, 487-493.

[25] C. O'Neill, C. Fowler, P. Jessop and M. Cunningham, *Green Materials*, **2013**, 1, 27-35.

[26] X. Su, P. G. Jessop and M. F. Cunningham, *Macromolecules*, **2012**, 45, 666-670.

[27] J. Pinaud, E. Kowal, M. Cunningham and P. Jessop, *ACS Macro Letters*, **2012**, 1, 1103-1107.

[28] M. Mihara, P. Jessop and M. Cunningham, *Macromolecules*, **2011**, 44, 3688-3693.

[29] Q. Zhang, G. Yu, W. J. Wang, H. Yuan, B. G. Li and S. Zhu, *Langmuir*, **2012**, 28, 5940-5946.

[30] Q. Zhang, G. Yu, W. J. Wang, B. G. Li and S. Zhu, *Macromolecular rapid communications*, **2012**, 33, 916-921.

[31] Q. Zhang, W.-J. Wang, Y. Lu, B.-G. Li and S. Zhu, *Macromolecules*, **2011**, 44, 6539-6545.

[32] Q. Zhang and S. Zhu, *ACS Macro Letters*, **2014**, 3, 743-746.

[33] J. Y. Choi, J. Y. Kim, H. J. Moon, M. H. Park and B. Jeong, *Macromolecular rapid communications*, **2014**, 35, 66-70.

[34] K. C. Lowe, M. R. Davey and J. B. Power, *Trends Biotechnol*., **1998**, 16, 272-277.

[35] H. W. Kim and A. G. Greenburg, *Artif. Organs*, **2004**, 28, 813-828.

[36] B. A. Suvorov, Russ. J. *Gen. Chem*. **2003**, 73 (1), 119–122

§ 3.7 Supporting information

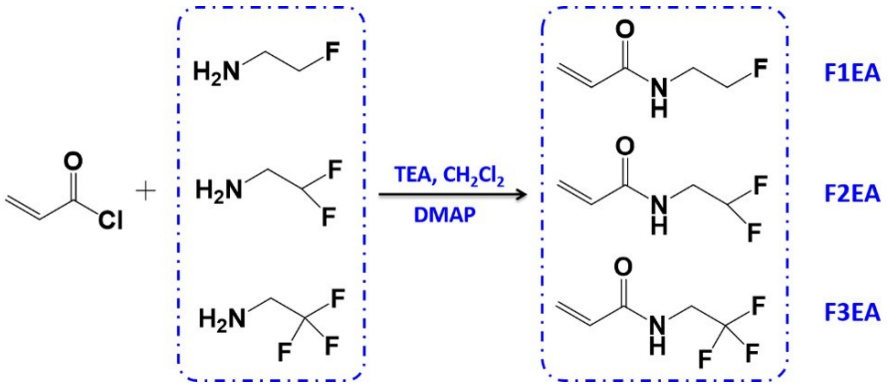

Figure 3-S1. Schematic illustration of fluorinated acrylamide monomers (F1EA, F2EA, F3EA) preparation.

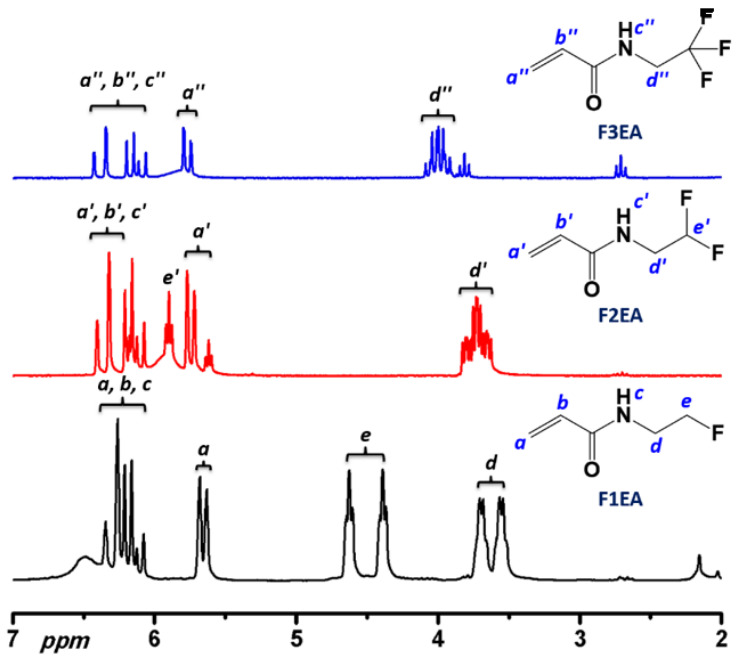

Figure 3-S2. ^{1}H NMR spectra of fluorinated acrylamides (F1EA, F2EA, F3EA) in $CDCl_3$.

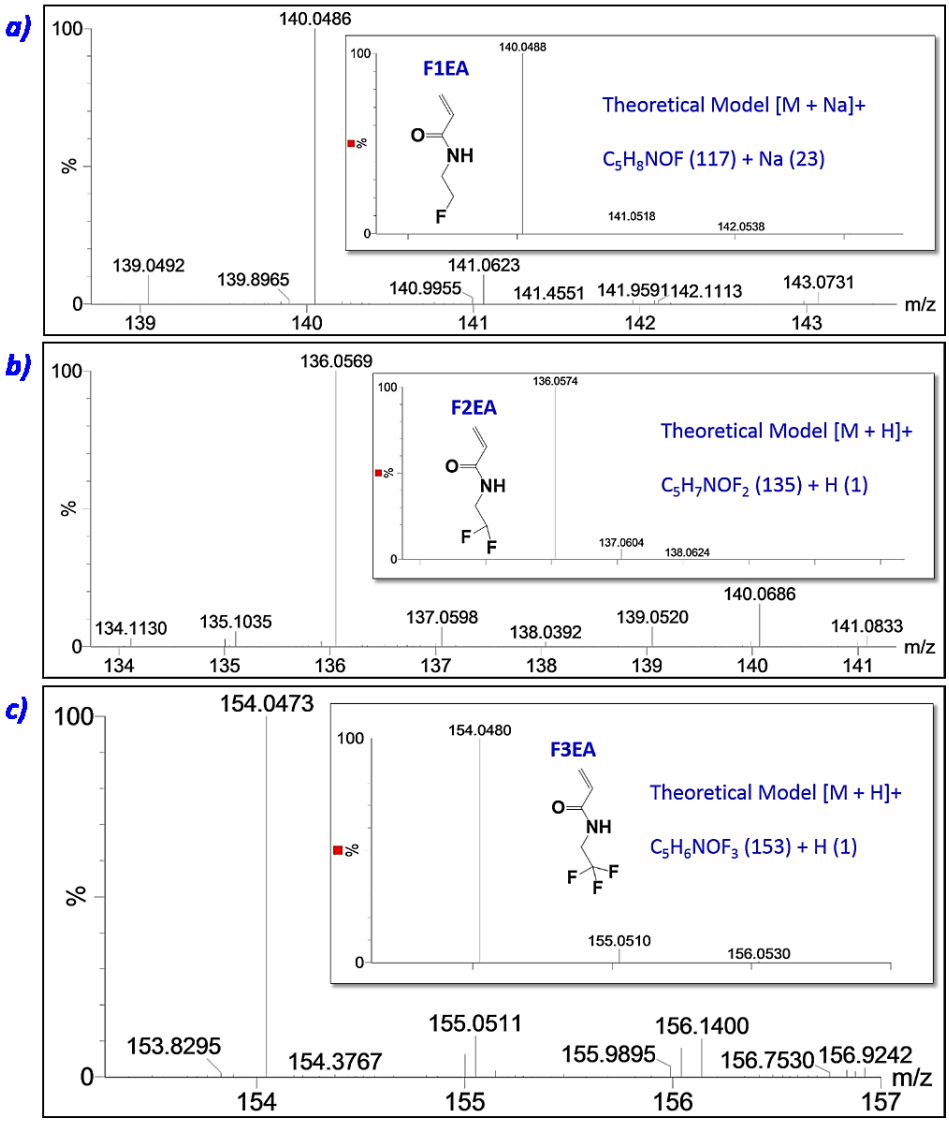

Figure 3-S3. Mass spectrometry (MS) of a) F1EA b) F2EA and c) F3EA. The high-resolution mass spectrometry was performed on Micromass Quattro Ultima (LC-ESI/APCI Triple Quadrupole Mass Spectrometer) with an electrospray ionization (ESI) source. (Polartiy: +ve)

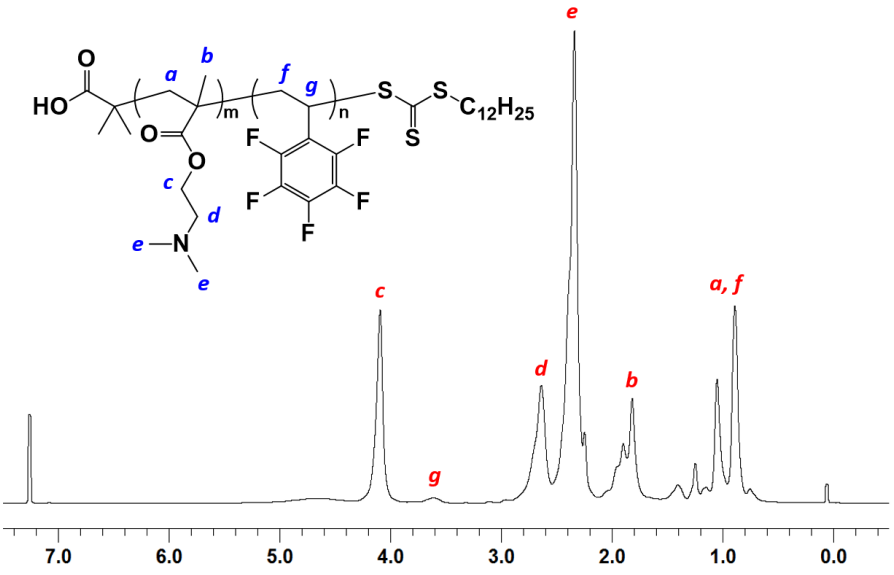

Figure 3-S4. ^{1}H NMR spectra of P(DMA-*co*-FS)-5 in $CDCl_3$.

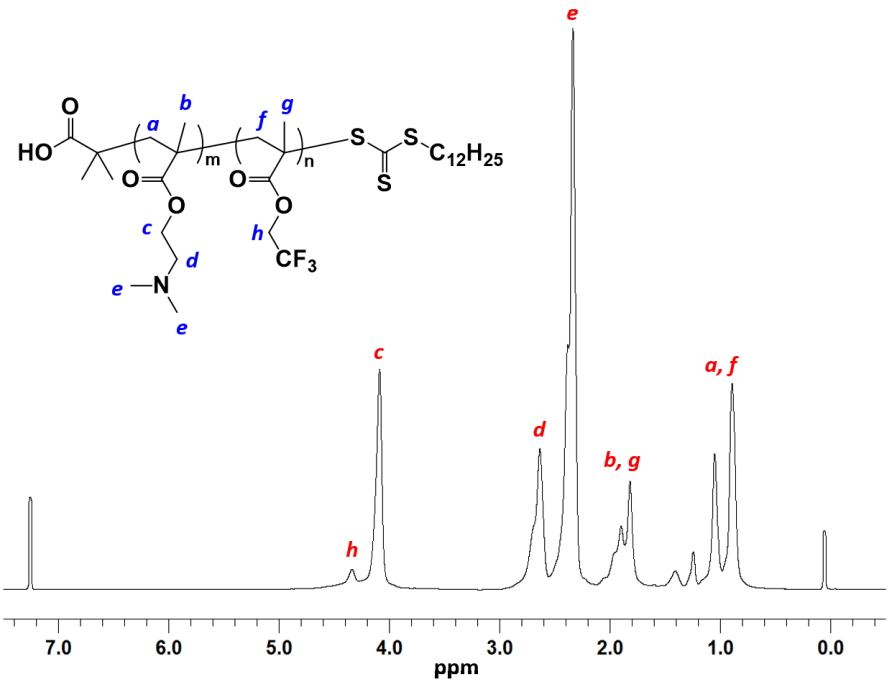

Figure 3-S5. ^{1}H NMR spectra of P(DMA-*co*-FMA)-5 in $CDCl_3$.

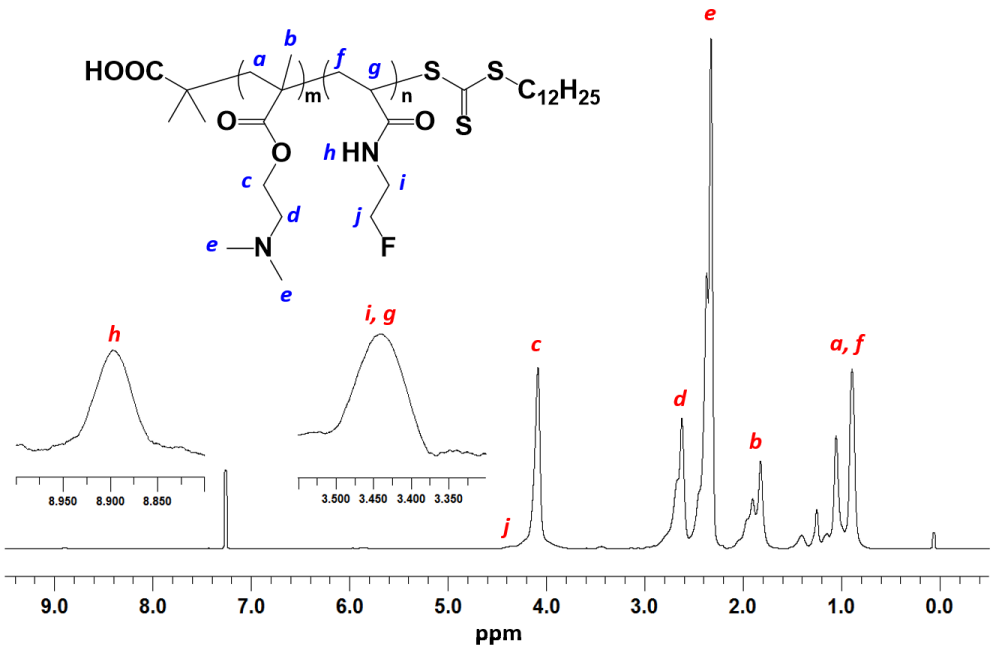

Figure 3-S6. ^{1}H NMR spectra of P(DMA-*co*-F1EA)-5 in $CDCl_3$.

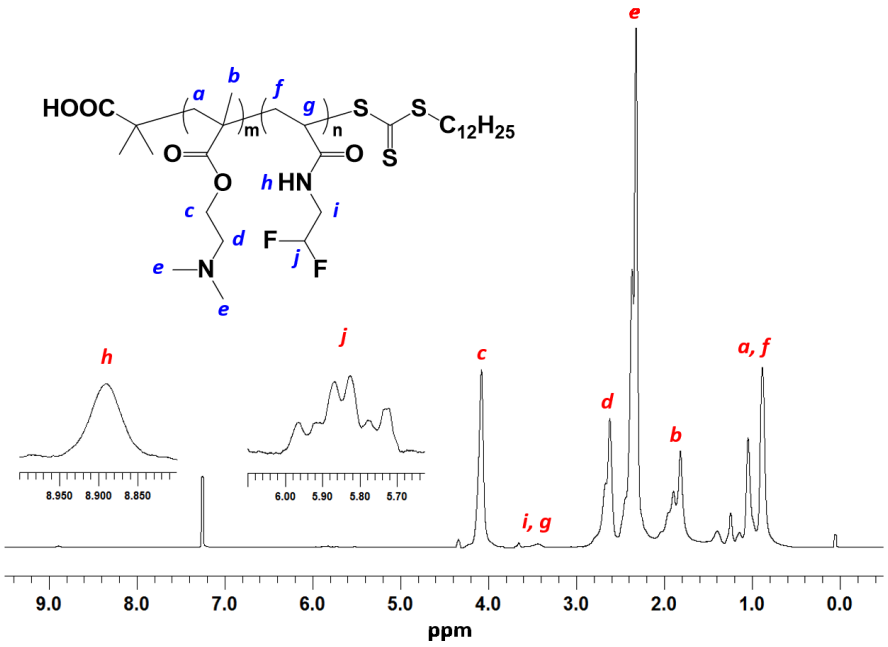

Figure 3-S7. ^{1}H NMR spectra of P(DMA-*co*-F2EA)-5 in $CDCl_3$.

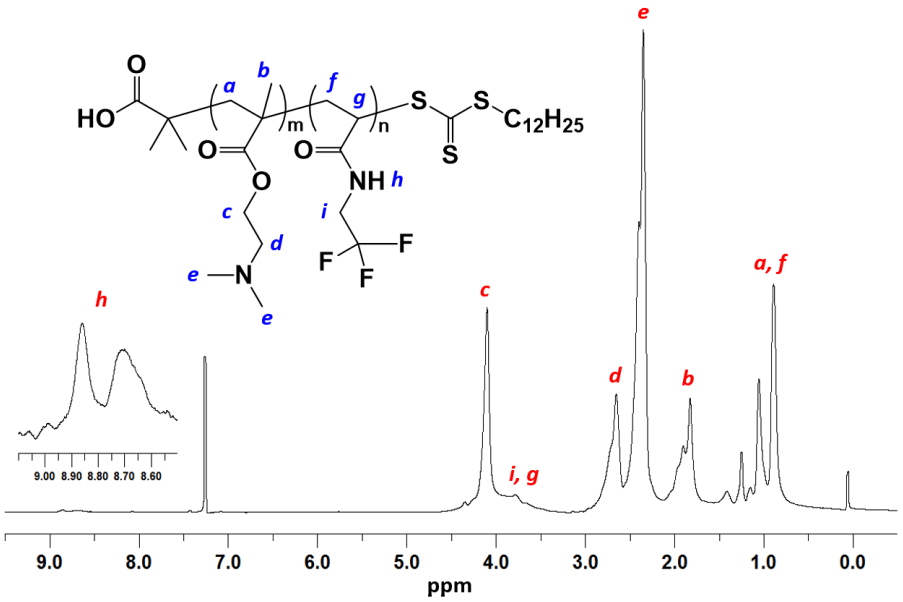

Figure 3-S8. ^{1}H NMR spectra of P(DMA-$_{co}$-F3EA)-5 in $CDCl_3$.

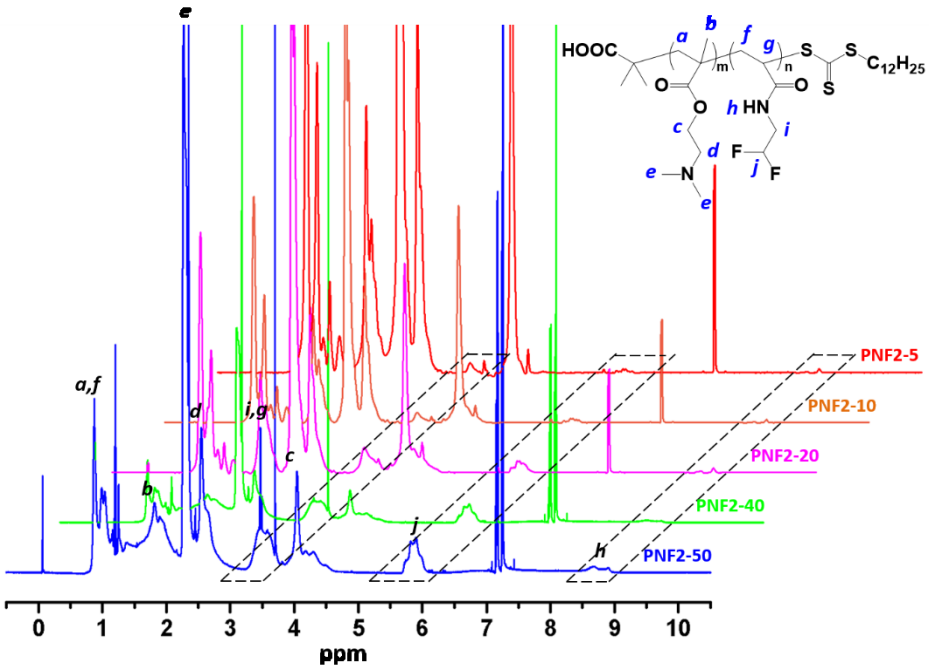

Figure 3-S9. ^{1}H NMR spectra of P(DMA-*co*-F2EA) with 5, 10, 20,40, 50 mol% F2EA content in $CDCl_3$. (PNF2-5, PNF2-10, PNF2-20, PNF2-40, PNF2-50)

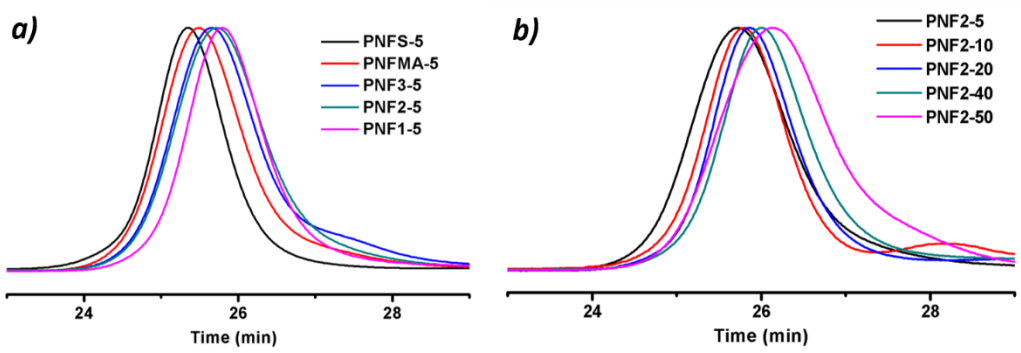

Figure 3-S10. GPC characterization of a) P(DMA-*co*-FMs) with 5 mol% of different fluorinated monomers (FS, FMA, F1EA, F2EA, F3EA) and b) P(DMA-*co*-F2EA) with 5, 10, 20,40, 50 mol% F2EA content in CDCl3. (PNF2-5, PNF2-10, PNF2-20, PNF2-40, PNF2-50), the molecular weight and polydispersity of all the random copolymers were listed in Table 2-1.

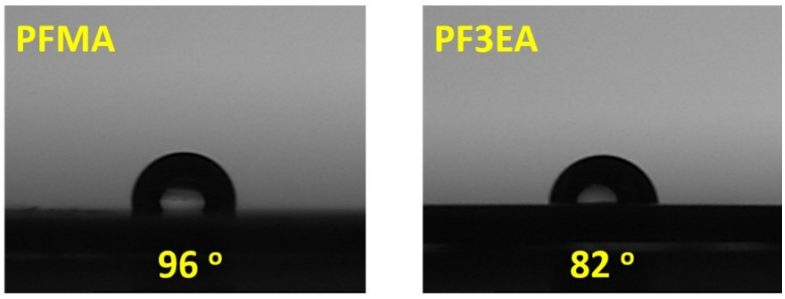

Figure 3-S11. Water contact angle of the PFMA and PF3EA homopolymer films.

4 O_2 AND CO_2-SWITCHABLE THERMO-RESPONSIVE HOMOPOLYMERS

This chapter reports synthesis of the first O_2 and CO_2 dual gas-switchable functional monomer "AM(F1EA-DEAE)" based on the O_2 switchable monomer candidate F1EA prepared in Chapter 3 and CO_2 switchable monomer DEA. The gas-switchable properties of their homopolymers are investigated. This chapter is reproduced from the published paper in Lei Lei, Qi Zhang, Susan Shi, Shiping Zhu "Oxygen and Carbon Dioxide Dual Gas-Switchable Thermoresponsive Homopolymers" *ACS Macro Lett.*, **2016**, 5 (7), pp 828–832 (DOI: 10.1021/acsmacrolett.6b00426) with the permission of ACS publisher. The supporting information referred in the text is attached at the end of this chapter.

Author contributions

This work is inspired from the publication of Jiang, et al. "Thermoresponsive Homopolymer Tunable by pH and CO_2" *ACS Macro Lett.*, **2014**, 3 (11), pp 1121–1125, after the discussion with Dr. Qi Zhang. Lei Lei did all the experiments and prepared the draft supervised by Dr. Shiping Zhu. Dr. Qi Zhang and Dr. Shuxian Shi provided valuable discussion. Dr. Zhu did final revision and provided quality control of the manuscript before submission.

§ 4.1 Abstract

Herein, we report the first oxygen (O_2) and carbon dioxide (CO_2) dual gas-switchable thermo-responsive polymers based on a newly synthesized monomer N-(2-fluoroethyl amide)-N-(2-(diethylamino)ethyl) acrylamide, i.e. AM(F1EA-DEAE), which bears both O_2-switchable fluorinated ethyl amide (F1EA) and CO_2-switchable N,N-diethylamino ethyl (DEAE) moieties on its side chain. PolyAM(F1EA-DEAE) samples prepared from reversible addition-fragmentation chain transfer (RAFT) polymerization exhibited good temperature-responsive properties. Their inherent low critical solution temperature (LCST) could be reversibly tuned to different levels by respectively purging O_2 or CO_2 into its aqueous solution. The O_2-treatment shifted LCST to a higher temperature, while the CO_2-treatment made the polymer fully water soluble. The polymer could be readily recovered to its initial state by washing off the trigger gas with an inert gas such as nitrogen. This work provides an effective

monomer design approach for the preparation of O_2- and CO_2 dual gas-responsive polymers.

§ 4.2 Introduction

Stimuli-responsive polymers able to shift their physicochemical properties in responsive to external input-stimulus like pH,[1] light,[2] thermo,[3] ionic strength,[4] and magnetic/electro field,[5-6] have gained great interest over the past decades. Such appealing stimuli-responsive switching features make the polymers "smart" and promise potential applications in sensors,[7] optoelectronics,[8] and control-release systems.[9] Among various types of stimuli, the thermo-responsivity attracts the most attention. Lower critical solution temperature (LCST) is the key design parameter in developing thermo-responsive polymers.[10] The shift of LCST reflects the change in water solubility or hydrophilicity of polymer induced by an extra stimulus such as pH.[11-12] Gases represent a novel class of stimuli having clear advantages in applications, which require large volume operation (versus varying temperature through heating and cooling) or require little contamination (versus varying pH through adding strong acid and base), in comparison to other type stimuli-responsive systems. CO_2 is the most reported gas trigger since it is green and abundant.[13-14] CO_2-responsive polymers have been used to prepare various functional materials such as redispersible latexes,[15-21] "breathable" vesicles and microgels,[22-23] self-assembled morphology transitions between "micelles", "worms" and "vesicles",[24] and even

mechano-responsive polymers based supersaturated CO_2 solution.[25] Oxygen (O_2) is another outstanding gas trigger, which has been reported very recently. However, almost all O_2-switchable polymers reported so far are from copolymerization of fluorinated O_2-switchable monomers with some other hydrophilic monomers.[22, 26-27] Homo-polymerization of fluorinated monomers would result in very hydrophobic polymers with limited water solubility and thus impair their O_2-switchable properties. Therefore, no O_2-switchable homopolymers have been reported so far.

Recently, multi-stimuli-responsive polymers represents an emerging area in smart polymer research and development.[28-29] Adding two or more stimuli to a single stimuli-responsive system is of particular interest since it broadens the selection of triggers, improves the degree of responsive precision, and enlarge the operation window for switching.[30] Multi-stimuli-responsive polymers (e.g. thermo-light,[31] thermo-pH/CO_2,[11-12] light-pH-thermo[32] and etc.) have been reported by incorporating various types of functional monomers in either block or random copolymers. However, block copolymerization normally involves time-consuming and troublesome intermediate steps for macroinitiator preparation and purification. Random copolymerization inevitably requires additional effort for investigating copolymer composition distribution. Multi-functional monomers are thus highly desirable for preparation of multi-stimuli-responsive polymers. Huang et al.[12] synthesized an acrylamide monomer bearing both themo-responsive isopropyl amide and CO_2/pH-responsive N,N-diethylamino ethyl groups, which can be polymerized into a thermo-responsive poly(N-(2-(diethylamino)ethyl)-N-(3-(isopropylamino)-3-

oxopropyl)-acrylamide) homopolymers with its LCST tunable by both pH and CO_2. It provides an effective alternative approach in preparation of multi-stimuli-responsive polymers through the design and synthesis of multi-stimuli-responsive monomers.

In this work, we design and synthesize a novel monomer N-(2-fluoroethyl amide)-N-(2-(diethylamino)ethyl) acrylamide, i.e. AM(F1EA-DEAE), based the newly reported O_2-switchable monomer candidate N-(2-fluoroethyl) acrylamide (F1EA),[33-34] and the well-studied CO_2-switchable poly((N,N-diethylamino)ethyl methacrylate) (PDEAEMA).[35] This monomer bears a fluorinated ethyl amide (F1EA) moiety and an N,N-diethylamino ethyl (DEAE) moiety. The former is O_2-switchable while the latter is CO_2-switchable. Its homopolymers, poly(N-(2-fluoroethyl amide)-N-(2-(diethylamino)ethyl)) acrylamide, or polyAM(F1EA-DEAE), are prepared through RAFT polymerization. These samples are thermo-responsive and their aqueous solutions exhibit thermo-induced phase transition behaviors at low critical solution temperature (LCST). It is important to point out that such homopolymers can reversibly interact with O_2 and CO_2 in aqueous solution, which in turn change their water solubility and shift their LCST to higher temperatures. This work demonstrates the first O_2 and CO_2 dual gas-switchable thermo-responsive homopolymer system with gas-switchable LCST, which can be fully recovered to the initial state by washing off the trigger gas with an inert gas or heating.

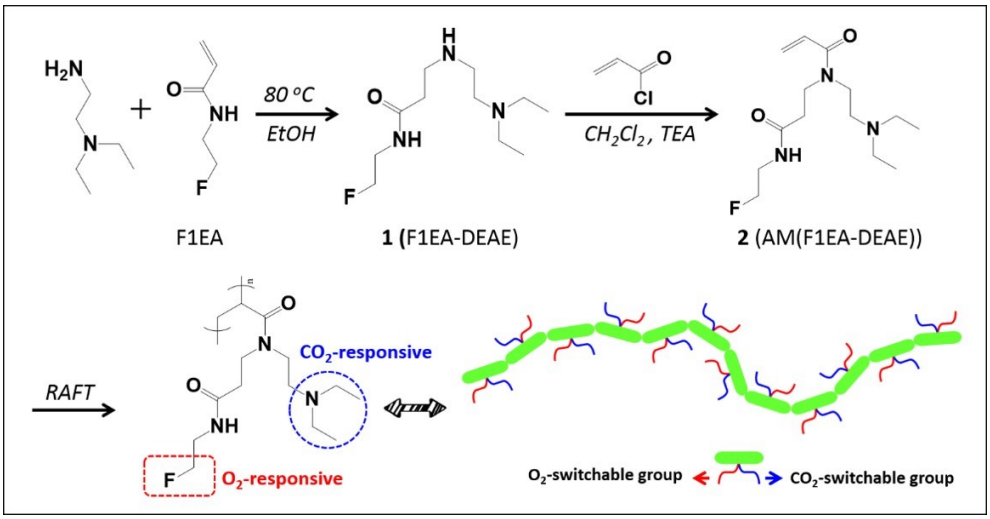

Figure 4-1. Synthesis route of polyAM-(F1EA-DEAE) homopolymers

§ 4.3 Experiments and Characterization

4.3.1 Materials

2-Fluoroethylamine hydrochloride (90%, Aldrich), acryloyl chloride (97%, Aldrich), N,N-diethylethylenediamine (99%, Aldrich), triethylamine (TEA, 99%, Aldrich), 4-(dimethylamino)pyridine (DMAP, 99%, Aldrich), dichloromethane (DCM, 98%, Aldrich), ethyl acetate (98%, Aldrich), hexane (99.5%, Aldrich), anhydrous ethanol (EtOH, Aldrich), methanol (MeOH, Aldrich), sodium chloride (NaCl, 99.5%, Aldrich), sodium sulfate (Na_2SO_4, 99%, Aldrich), 2-(dodecylthiocarbonothioylthio)-2-methylpropionic acid (DMP, 98%), dimethylformamide (DMF, 98%, Aldrich) were used as received. 2,2'-Azobis(2-methylpropionitrile) (AIBN, 98%, Aldrich) was recrystallized from methanol twice and stored in refrigeration prior to use. Milli-Q grade water prepared from Barnstead Nanopure Diamond system was used in all

aqueous solution preparation. CO_2, O_2, and N_2 gases were controlled by FMA-A2100 flow meters (Omega) to maintain a constant gas flow of 10 mL/min.

4.3.2 Experiment

4.3.2.1 Synthesis of N-fluoroethyl acrylamide (F1EA)

F1EA was synthesized using the method described by Lee et al.[1] Specifically, 2-fluoroethylamine hydrochloride (10 g, 123.4 mmol), TEA (27.63 g, 185.1 mmol), DMAP (1.21 g, 9.87 mmoL, 8 mol%) and CH_2Cl_2 (130 mL) were added into a 250 mL round-bottom flask and immersed in an ice salt-water. Acryloyl chloride (13.96 g, 154.3 mmol) diluted with 20 ml dichloromethane was then added dropwise under stirring within 20 min. The solution was allowed to react for 24 hours at room temperature. The solution was then washed with brine three times and the organic layer was dried with Na_2SO_4 and evaporated under reduced pressure. The residue product was purified by column chromatography with hexane and ethyl acetate mixture (V:V=1:5, with 1 vol. % TEA) as eluent, giving a light yellow oily liquid F1EA (7.83g, yield 66.64%). ^{1}H NMR in Figure 4-S1: δ (ppm): 4.4, 4.6 (2H, FC***H₂***CH_2), 3.4 (2H, FCH_2C***H₂***), 5.68, 6.36, 6.58 (3H, C***H***=C***H₂***).

4.3.2.2 Synthesis of N-(2-fluoroethyl amide)-N-(2-(diethylamino)ethyl) (F1EA-DEAE)

F1EA (3.5 g, 30 mmol) and DEAE (4.17 g, 36 mmol)) were dissolved in 25 mL anhydrous ethanol under vigorous stirring. The mixture was stirred under reflux at 80 ^{o}C and reacted for 72 hours. The solvent ethanol was evaporated under reduced pressure. The residue was purified by column chromatography on silica gel with DCM and MeOH (V:V=3:2, with 1 vol. % TEA) as eluent, giving orange oily liquid F1EA-DEAE **1** product (6.25 g, yield 73.19%). ^{1}H NMR in Figure 4-S2: δ (ppm): 4.3, 4.4 (2H, FC***H₂***CH_2), 3.4 (2H, FCH_2C***H₂***), 8.03 (1H, CON***H***), 2.83 (2H, $NHCH_2CH_2CONH$), 1.98 (1H, ***H***NCH_2CH_2CONH), 2.52 (2H, $HNCH_2C$***H₂***$CONH$), 2.5 (2H, HNC***H₂***$CH_2N(C_2H_5)_2$), 2.39 (2H, $HNCH_2C$***H₂***$N(C_2H_5)_2$), 1.00 (6H, $N(CH_2C$***H₃***$)_2$), 2.46 (4H, $N(C$***H₂***$CH_3)_2$.

4.3.2.3 Synthesis of N-(2-fluoroethyl amide)-N-(2-(diethylamino)ethyl) acrylamide (AM(F1EA-DEAE))

AM-(F1EA-DEAE) was synthesized through amidation reaction of acryloyl chloride and the intermediate **I** (F1EA-DEAE). Specifically, F1EA-DEAE (8.1g, 233 g/mol, 34.73 mmol), TEA (7.77g, 149.19 g/mol, 52.10 mmol), DMAP (8 mol%) and CH_2Cl_2 (20 mL) were added into a 50 mL round-bottom flask, which was immersed in an ice salt-water. Acryloyl chloride (3.93 g, 43.42 mmol) diluted with 5 mL dichloromethane was then added dropwise under stirring within 20 min. The solution was allowed to react for 24 hours at room temperature. The solution was then washed with brine three times and the organic layer was dried with Na_2SO_4 and evaporated under reduced pressure. The residue was purified by column chromatography on silica gel with DCM and MeOH (V:V=3:2, with 1 vol. % TEA) as eluent, giving light yellow oily liquid

AM(F1EA-DEAE) **2** product (3.62 g, yield 36%). ^{1}H NMR in Figure 4-1 a): δ (ppm): 4.3, 4.4 (2H, FC***H₂***CH_2), 3.4 (2H, FCH_2C***H₂***), 5.68, 6.36, 6.58 (3H, C***H***=C***H₂***), 3.24 (2H, NC***H₂***CH_2CONH), 2.66 (2H, NCH_2C***H₂***CONH), 3.06 (2H, NC***H₂***$CH_2N(C_2H_5)_2$), 2.53 (2H, NCH_2C***H₂***$N(C_2H_5)_2$), 1.00 (6H, $N(CH_2C$***H₃***$)_2$), 2.46 (4H, $N(C$***H₂***$CH_3)_2$.

4.3.2.4 Preparation of Poly(N-(2-fluoroethyl amide)-N-(2-(diethylamino)ethyl) acrylamide) (PolyAM(F1EA-DEAE))

PolyAM-(F1EA-DEAE) homopolymers having three different molecular weights were synthesized from reversible addition-fragmentation chain transfer (RAFT) polymerization with 2-dodecylsulfanylthiocarbonylsulfanyl-2-methylpropionic acid (DMP) as the chain transfer agent and 2,2'-azobisisobutyronitrile (AIBN) as the initiator (Scheme 4-S1). The recipe was fixed to [Monomer]:[DMP]:[AIBN]=100:1:0.4 by using DMF as the solvent. Specially, AM(F1EA-DEAE) (542 mg, 1.89 mmol), DMP (6.93 mg, 0.019 mmol), AIBN (1.25 mg, 0.08 mmol) and 0.5 ml of DMF were charged into a 2 mL flask sealed with rubber stopper. The solution was degassed with N_2 for 30 min under stirring. After that, the flask was placed into an oil bath of 80 ^oC and the polymerization was carried out for 16, 24 and 48 hours. The product was precipitated in cold diethyl ether upon vigorous agitation, which was repeated three cycles to remove the unreacted monomers for purification of the polymer product. At the end, the polymer was vacuum dried at room temperature until constant weight.

3.3.3 Characterization

^{1}H NMR spectra of all the samples were collected in $CDCl_3$ on Broke AV600 MHz NMR spectrometer. ^{13}C NMR of the AM(F1EA-DEAE) monomer in $CDCl_3$ and ^{19}F NMR of P1 in D_2O under O_2 and N_2 treatment were taken on Broke AV200 MHz NMR spectrometer. The molecular weight and the polydispersity index of the homopolymers were collected from Waters 2690 Seperations Module by using THF as effluent at a flow rate of 1mL/min. The LCST of polymer aqueous solution (0.5, 1.0, 2.0 mg/mL) was monitored by Cary 300 UV-vis spectrophotometer at 500 nm wavelength. The heating process was set from 5 to 85 °C at 1 °C/min temperature acceleration. Each sample was treated with specific gas of O_2, CO_2 and N_2 under the protection of ice-bath for 1 hour and sealed in closed vial during measurement.

§ 4.4 Results and Discussion

The fluorinated acrylamide monomer F1EA (Figure 4-S1) was synthesized following the procedure described by Lee et al.[33] The critical intermediate N-(2-fluoroethyl amide)-N-(2-(diethylamino)ethyl) (**1**: F1EA-DEAE) was synthesized from an Aza-Michael addition reaction between F1EA and N,N-diethylethylenediamine in ethanol at 80 ^{o}C. Thus, both O_2 and CO_2 switchable moieties (F1EA and DEAE, respectively) were incorporated into this intermediate. The ^{1}H NMR spectra in Figure 4-S2 confirmed the structures of both fluoroethyl amide (F1EA) and diethylamino)ethyl (DEAE) functional groups in the intermediate **1** (F1EA-DEAE). Then, the multi-responsive functional monomer N-(2-fluoroethyl amide)-N-(2-(diethylamino)ethyl) acrylamide, i.e. **2** AM(F1EA-DEAE), was synthesized from an amidation reaction

between acryloyl chloride and the intermediate **1** (F1EA-DEAE). The molecule structure was confirmed by the ^{1}H NMR and ^{13}C NMR spectra in Figure 4-1. Specifically, the proton analysis in Figure 4-2 (a) confirmed the signal peak integration of $I_a:I_{(b+e+f)}:I_c:I_{(d+g+h)}:I_i:I_{(j+k+l)}$ = 2:6:1:8:6:3, suggesting successful preparation of the targeted monomer **2**.

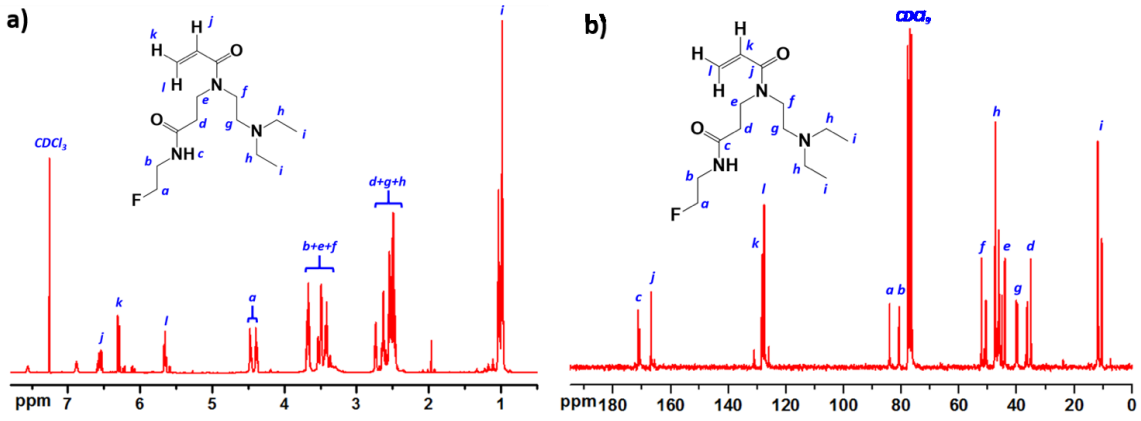

Figure 4-2. ^{1}H NMR (a) and ^{13}C NMR (b) spectra of AM (F1EA-DEAE) monomer in $CDCl_3$.

Poly(N-(2-fluoroethyl amide)-N-(2-(diethylamino)ethyl) acrylamide) homopolymers, polyAM(F1EA-DEA), having three different molecular weights were prepared through RAFT polymerization of AM(F1EA-DEAE) with 2-dodecylsulfanylthiocarbonylsulfanyl-2-methylpropionic acid (DMP) as the chain transfer agent (CTA) and 2,2'-azobisisobutyronitrile (AIBN) as the initiator (Figure 4-S3). The recipe was fixed to [Monomer]:[DMP]:[AIBN]=100:1:0.4 for all the polymerization runs conducted in DMF at 80 ^{o}C for different time periods in order to control the polymer molecular weight. The reaction mixtures were sampled for ^{1}H

NMR characterization immediately after the polymerization was stopped. The monomer conversion (mol %) was estimated from "$(A_{4.4}/2\text{-}A_{5.5})/(A_{4.4}/2) \times 100\%$" based on the areas of characteristic peaks at 5.5 ppm ("C***H₂***=CH-" proton of unreacted AM(F1EA-DEAE) monomer) and 4.4 ppm ("F-C***H₂***-" protons of both unreacted AM(F1EA-DEAE) monomer and poly(AM(F1EA-DEAE)) homopolymer). The polymer molecular weights were then estimated from "(100 x conversion (mol%) × 287 + 364) g/mol". Figure 4-S4 shows the ^{1}H NMR spectra of the **P1** homopolymer after purification, to confirm the macromolecular structure. The samples were also characterized by GPC measurements, as seen from Figure 4-S5. The GPC results agreed with the molecular weights from the NMR analysis and provided the polydispersity index (PDI) data. Table 4-1 summarizes a series of polyAM(F1EA-DEAE) homopolymers with narrow molecular weight distribution prepared through RAFT polymerization.

Table 4-1. Synthesis and characterization of polyAM(F1EA-DEAE) homopolymers.

Sample	*Reaction time (Hours)*	*^{1}H NMR [a]*		*GPC [b]*		*LCST [c]*		
		Con. (mol%)	*M_n (g/mol)*	*M_n (g/mol)*	*PDI*	*N_2*	*O_2*	*ΔLCST(O_2)*
P1	16	64	18700	18100	1.14	38	52	14
P2	24	75	21900	20300	1.19	40	55	15
P3	48	94	27300	26300	1.21	45	61	16

Note: [a]Monomer conversion (Con.%) and molecular weight (Mn) of polyAM(F1EA-DEAE) homopolymers estimated from ^{1}H NMR spectra of the reaction mixture right after polymerization. [b]Molecular weight (Mn) and polydispersity index (PDI) of the homopolymers

determined by GPC. [c]LCST of the homopolymer aqueous solution (1 mg/mL) pretreated by N_2 or O_2 at 10 mL/min for 1 hour.

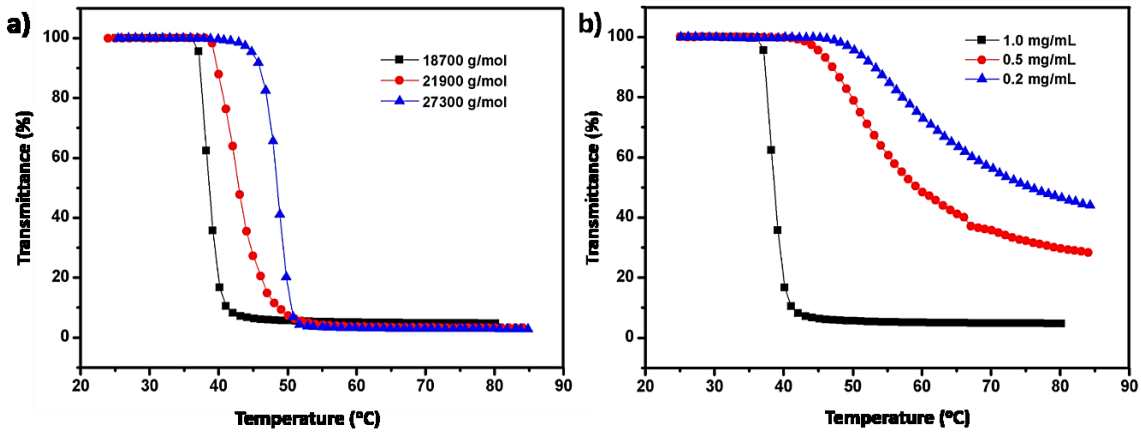

Figure 4-3. a) Temperature based transmittance curves of the aqueous solution (1 mg/mL) of polyAM(F1EA-DEAE) homopolymers having different molecular weights. b) PolyAM(F1EA-DEAE) homopolymer (P1: 18700 g/mol) aqueous solution at different concentrations.

The resulted polyAM(F1EA-DEAE) homopolymers exhibited very good water solubility at room temperature, which showed light yellow transparent color in aqueous solution (Figure 4-4 a). An abrupt increase in turbidity at a certain temperature was clearly observed with temperature increase, demonstrating the thermo-responsive phase transition behavior. The temperature based transmittance changes of polymer aqueous solution were measured by Cary 300 UV-vis spectrophotometer at 500 nm wavelength. The LCST was defined as the temperature, at which 5% decrease of the transmittance was reached. Figure 4-3 (a) shows the transmittance versus temperature curves for the aqueous solutions (1 mg/mL) of polyAM(F1EA-DEAE) homopolymers having different molecular weights. As the

molecular weight increased from 18700 g/mol (**P1**) to 21900 g/mol (**P2**) and 27300 g/mol (**P3**), the inherent LCST of the homopolymer increased from 38 °C to 40 °C and 45 °C. This was resulted from two competing factors: "end-group effect" and "dilute effect".[12, 36] On one side, the chain-end carboxyl group from DMP initiator contributed to the hydrophilicity of polyAM(F1EA-DEAE), which could be significant especially for the low molecular weight sample. On the other side, at the same mass concentration, the higher molecular weight sample had the lower molar concentration and thus contained fewer polymer chains in the aqueous solution, leading to the higher LCST. The "dilute effort" appeared to be dominating, as shown in Figure 4-3 (a). Such "dilution effect" was further be proved from LCST curves for polyAM(F1EA-DEAE) homopolymer (**P1**) aqueous solution with different homopolymer concentrations. As shown in Figure 4-3 (b), homopolymer aqueous solution with lower polymer concentration exhibit higher LCST.

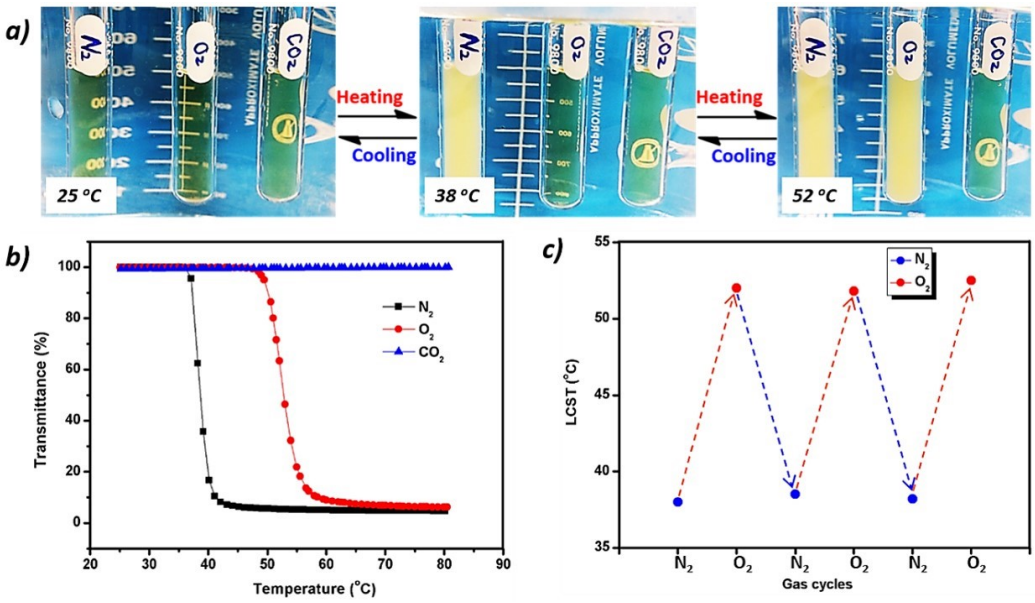

Figure 4-4. a) Photograph of polyAM(F1EA-DEAE) homopolymer (P1) aqueous solution (1 mg/mL) at different temperatures. The polymer solutions were pretreated with N_2, O_2 and CO_2 respectively for 1 hour at 10 ml/min under ice bath protection. b) Temperature-based transmittance curves of the homopolymer aqueous solution (1 mg/mL) under N_2, O_2 and CO_2 treatment. C) Reversibility of LCST shift induced by O_2-treatment.

It was also demonstrated that the polyAM(F1EA-DEAE) homopolymer exhibited O_2 and CO_2 dual gas-switchable thermo-responsive properties. The LCST of polymer aqueous solution could be effectively switched by treatment with trigger gases (O_2 and CO_2) at 10 ml/min for 60 min, and recovered by treatment with inert gas N_2. Figure 4-4 (a) shows that the P1 aqueous solution treated with N_2, O_2 and CO_2 exhibited distinct turbidity difference at different temperatures (25, 38 and 52 ^oC). N_2 was used to remove the trigger gas (O_2 or CO_2) dissolved in the polymer solution, as the control sample for comparison. The O_2 and CO_2 treatment increased the polymer water solubility and shifted its transmittance-to-turbidity transition to higher temperature. These observations could be confirmed from the temperature-based transmittance curves shown in Figure 4-4 (b). The inherent LCST (under N_2 treatment) of the polymer was determined to be 38 ^oC, which increased to 52 ^oC after 1 hour O_2 treatment under ice-bath protection. CO_2 treatment of 1 hour made the polymer totally water soluble and there was no LCST transition found in the transmittance versus temperature curve. It should be pointed out that the gas-induced LCST shift could be regulated by controlling the gas (CO_2) treatment time.[11] Table 4-1 lists the change of LCST induced by O_2 treatment, also seen the LCST curves from Figure 4-S6. With the increase in molecular weight, the LCST of **P1**, **P2** and **P3**

polymers increased 14, 15 and 16 ^{o}C, respectively. The effect of polymer molecular weight on LCST appeared to be minor.

The O_2-induced LCST increase could be attributed to the van der Waals intermolecular interaction between dissolved O_2 molecules and the fluorine atoms of F1EA component, which increased the hydrophilicity of the polymer. This can be proved from the ^{19}F NMR spectra of **P1** in deuterium oxide (Figure 4-S7) after N_2 and O_2 treatment, the fluorine peaks at -72.15 ppm under N_2 condition downshifted to -71.93 ppm after O_2 treatment. This result is in agreement with the previous studies, suggesting that the coordination between the fluorinated moiety (F1EA) with O_2 affect the electron distribution around fluorine atoms, and thus change the chemical shift.[26, 37-38] The CO_2-triggered LCST increase was resulted from the protonation of the tertiary amine group in DEAE by CO_2 dissolved in water, which significantly increased hydrophilicity of the polymer.[11, 35] Both O_2 and CO_2 induced LCST increases were recoverable by washing off the trigger-gas through N_2 purging for about 30 min or boiling the aqueous solution for 2 min. Since the polymer became totally water soluble after CO_2-treatment, there was thus no LCST measurable in the temperature range. Figure 4-4 (c) shows the O_2-induced LCST shift and recovery cycles for P1 aqueous solution (1 mg/m). The O_2-induced LCST switching was reversible and repeatable for numerous cycles, without any loss of the O_2-responsive properties.

It is worth mentioning that F1EA is just one example of many O_2-switchable monomer candidates. Its homologues N-(2,2-difluoroethyl)acrylamide (F2EA) and N-(2,2,2-trifluoroethyl)acrylamide (F3EA),[33-34] could also be good candidates for preparation of O_2-switchable homopolymers.

§ 4.5 Conclusion

In conclusion, we demonstrated O_2 and CO_2 dual gas-switchable thermo-responsive homopolymers through the monomer design by combining O_2-switchable F1EA and CO_2-swictbale DEAE into a single monomer. PolyAM(F1EA-DEAR) homopolymer was then synthesized by RAFT polymerization. The polymer exhibited an outstanding thermo-responsive property. Its inherent LCST could be reversibly triggered to different temperature levels. O_2-treatment increased water solubility of the polymer and shifted LCST to a higher temperature. CO_2-treatment made the polymer totally water soluble. This LCST shift was fully recoverable by removing the trigger gas with an inert gas washing or heating. This work provides an effective monomer design approach for preparation of O_2-responsive homopolymers.

§ 4.6 References

[1] Morse, A. J.; Armes, S. P.; Thompson, K. L.; Dupin, D.; Fielding, L. A.; Mills, P.; Swart, R. *Langmuir*, **2013**, 29 (18), 5466-5475.

[2] Zhao, Y. *Macromolecules*, **2012**, 45 (9), 3647-3657.

[3] Jean-Franc ¸ois Lutz; Akdemir, O. z. r.; Hoth, A. *J. Am. Chem. Soc.*, **2006**, 128, 13046-13047.

[4] Zhao, B.; Moore, J. S. *Langmuir*, **2001**, 17, 4758-4763.

[5] Murdan, S. *Journal of Controlled Release*, **2003**, 92 (1-2), 1-17.

[6] Thevenot, J.; Oliveira, H.; Sandre, O.; Lecommandoux, S. *Chemical Society reviews*, **2013**, 42 (17), 7099-7116.

[7] Paek, K.; Yang, H.; Lee, J.; Park, J.; Kim, B. *J. ACS Nano*, **2014**, 8 (3), 2848-2856.

[8] Li, C.; Liu, S. *Chemical Communications*, **2012**, 48 (27), 3262-3278.

[9] Sander, J. S.; Studart, A. R. *Langmuir*, **2013**, 29 (49), 15168-15173.

[10] Thavanesan, T.; Herbert, C.; Plamper, F. A. *Langmuir*, **2014**, 30 (19), 5609-5619.

[11] Han, D.; Tong, X.; Boissière, O.; Zhao, Y. *ACS Macro Letters*, **2012**, 1 (1), 57-61.

[12] Jiang, X.; Feng, C.; Lu, G.; Huang, X. *ACS Macro Letters*, **2014**, 3 (11), 1121-1125.

[13] Liu, Y.; Jessop, P. G.; Cunningham, M.; Eckert, C. A.; Liotta, C. L. *Science*, **2006**, 313, 958-960.

[14] Heldebrant, D. J.; Yonker, C. R.; Jessop, P. G.; Phan, L. *Energy & Environmental Science*, **2008**, 1, 487-493.

[15] Zhang, Q.; Yu, G.; Wang, W. J.; Li, B. G.; Zhu, S. *Macromolecular Rapid Communications*, **2012**, 33 (10), 916-921.

[16] Zhang, Q.; Yu, G.; Wang, W. J.; Yuan, H.; Li, B. G.; Zhu, S. *Langmuir*, **2012**, 28 (14), 5940-5946.

[17] Mihara, M.; Jessop, P.; Cunningham, *Macromolecules*, **2011**, 44 (10), 3688-3693.

[18] Zhang, Q.; Wang, W.-J.; Lu, Y.; Li, B.-G.; Zhu, S. *Macromolecules*, **2011**, 44 (16), 6539-6545.

[19] Pinaud, J.; Kowal, E.; Cunningham, M.; Jessop, P. *ACS Macro Letters*, **2012**, 1 (9), 1103-1107.

[20] Su, X.; Jessop, P. G.; Cunningham, M. F. *Macromolecules*, **2012**, 45 (2), 666-670.

[21] O'Neill, C.; Fowler, C.; Jessop, P.; Cunningham, M. *Green Materials*, **2013**, 1 (1), 27-35.

[22] Lei, L.; Zhang, Q.; Shi, S.; Zhu, S. *Langmuir*, **2015**, 31 (7), 2196-2201.

[23] Feng, A.; Zhan, C.; Yan, Q.; Liu, B.; Yuan, J. *Chemical Communications*, **2014**, 50 (64), 8958-8961.

[24] Yan, Q.; Zhao, Y. *Angewandte Chemie*, **2013**, 52 (38), 9948-9951.

[25] Roth, P. J.; Quek, J. Y.; Zhu, Y.; Blunden, B. M.; Lowe, A. B. *Chemical Communications*, **2014**, 50 (67), 9561-9564.

[26] Zhang, Q.; Zhu, S. *Macromolecular Rapid Communications*, 2014, 35 (19), 1692-1696.

[27] Zhang, Q.; Zhu, S. *ACS Macro Letters*, **2014**, 3 (8), 743-746.

[28] Akamol Klaikherd, C. N.; Thayumanavan, S. *J. AM. CHEM. SOC*., **2009**, 131, 4830-4838.

[29] Zhuang, J.; Gordon, M. R.; Ventura, J.; Li, L.; Thayumanavan, S. *Chemical Society reviews*, **2013**, 42 (17), 7421-7435.

[30] Schattling, P.; Jochum, F. D.; Theato, P. *Polym. Chem*., **2014**, 5 (1), 25-36.

[31] Jochum, F. D.; zur Borg, L.; Roth, P. J.; Theato, P. *Macromolecules*, **2009**, 42 (20), 7854-7862.

[32] Tang, X.; Liang, X.; Gao, L.; Fan, X.; Zhou, Q. *Journal of Polymer Science Part A: Polymer Chemistry*, **2010**, 48 (12), 2564-2570.

[33] Bak, J. M.; Kim, K.-B.; Lee, J.-E.; Park, Y.; Yoon, S. S.; Jeong, H. M.; Lee, H.-i. *Polym. Chem*., **2013**, 4 (7), 2219-2223.

[34] Bak, J. M.; Lee, H.-i. *Journal of Polymer Science Part A: Polymer Chemistry*, **2013**, 51 (9), 1976-1982.

[35] Yan, Q.; Zhao, Y. *Chemical Communications*, **2014**, 50 (79), 11631-11641.

[36] Yu, B.; Chan, J. W.; Hoyle, C. E.; Lowe, A. B. *Journal of Polymer Science Part A: Polymer Chemistry*, **2009**, 47 (14), 3544-3557.

[37] Choi, J. Y.; Kim, J. Y.; Moon, H. J.; Park, M. H.; Jeong, B. *Macromolecular Rapid Communications*, **2014**, 35 (1), 66-70.

[38] Suvorov, B. A. *Russian Journal of General Chemistry*, **2003**, 73 (1), 126-129

§ 4.7 Supporting information

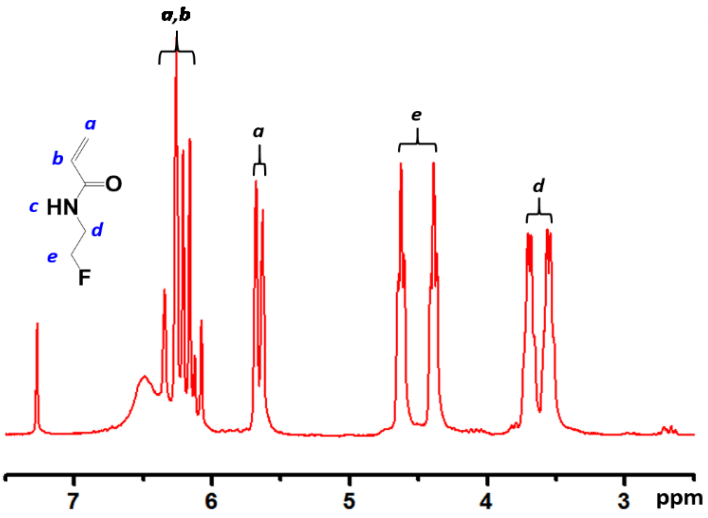

Figure 4-S1. ^{1}H NMR spectra of F1EA in $CDCl_3$.

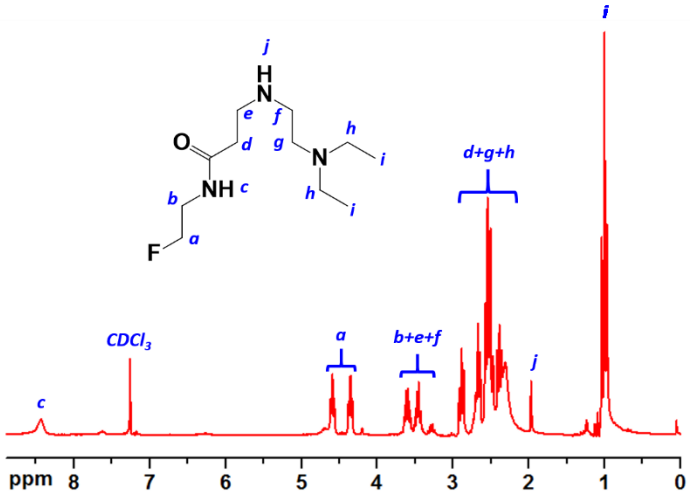

Figure 4-S2. ^{1}H NMR spectra of F1EA-DEAE in $CDCl_3$.

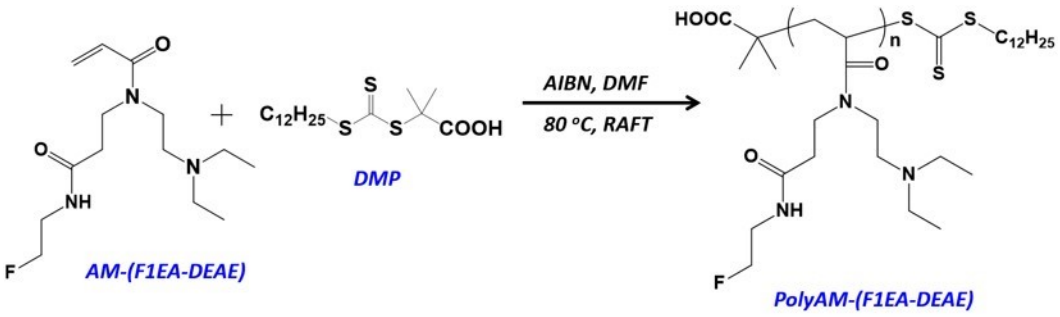

Scheme 4-S3. Synthesis route of polyAM(F1EA-DEAE) homopolymer from RAFT polymerization.

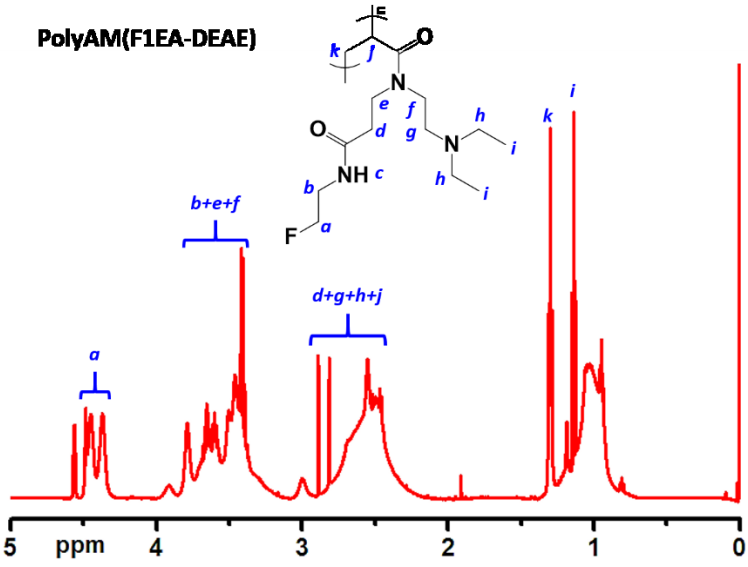

Figure 4-S4. ^{1}H NMR spectra of PolyAM(F1EA-DEAE) in $CDCl_3$.

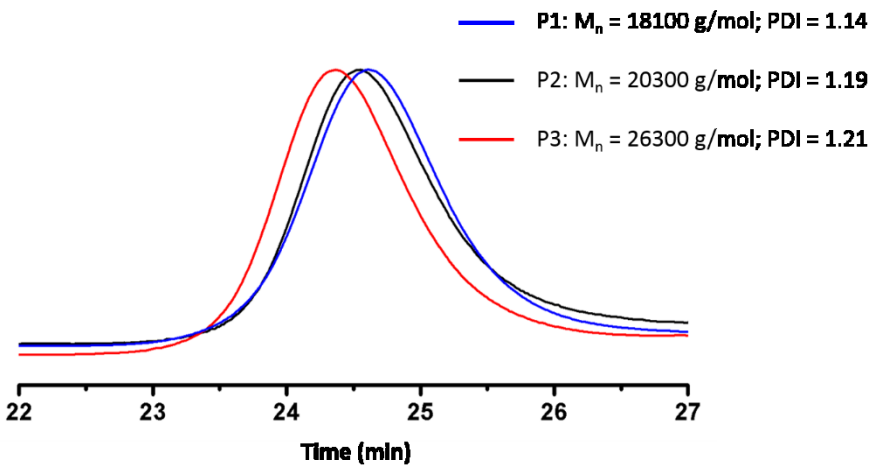

Figure 4-S5. GPC characterization of polyAM(F1EA-DEAE) homopolymers: P1, P2 and P3.

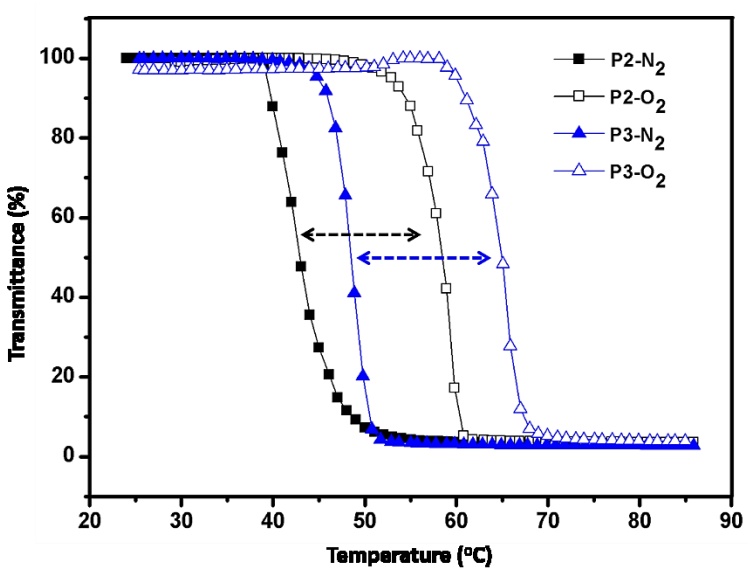

Figure 4-S6. Temperature based transmittance curves of the P2 (21900 g/mol) and P3 (27300 g/mol) homopolymer aqueous solution (1 mg/mL) under N_2 and O_2 treatment.

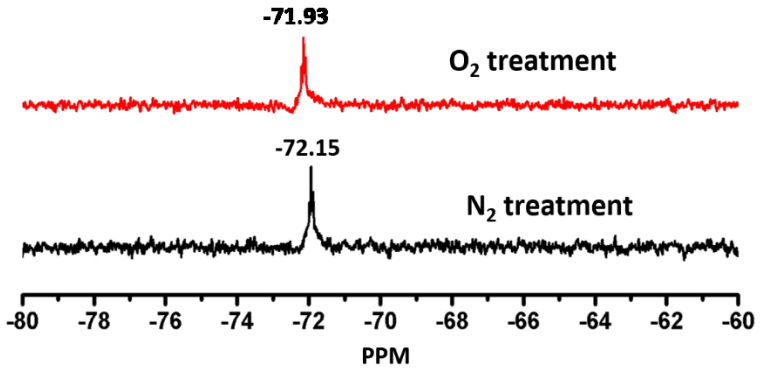

Figure 4-S7. ^{19}F NMR spectra of P1 in D_2O under N_2 and O_2 treatment.

5 O_2 AND CO_2- DUAL GAS-SWITCHABLE MICROGELS

In this chapter, we developed the first O_2 and CO_2 dual-gas switchable microgel system. This chapter is reproduced from the manuscript of "Oxygen and carbon dioxide dual gas-responsive and switchable microgels prepared from emulsion copolymerization of fluoro- and amino-containing monomers" published in Lei Lei, Qi Zhang, Susan Shi, Shiping Zhu "Oxygen and Carbon Dioxide Dual Gas-Responsive and Switchable Microgels Prepared from Emulsion Copolymerization of Fluoro- and Amino-Containing Monomers" *Langmuir*, **2015**, 31 (7), pp 2196–2201 (DOI: 10.1021/la504829j), and with the permission from ACS publisher.

Author contributions

Dr. Shiping Zhu provided the original idea of this work. Lei Lei did all the experiments and prepared the first manuscript under Dr. Zhu's supervision. Dr. Qi Zhang provided

valuable help and discussion on organization of the manuscript. Dr. Zhang and Dr. Shuxian Shi revised the first manuscript and Dr. Zhu did final revision before submission.

§ 5.1 Abstract

We report herein the design and preparation of microgels that are responsive to both O_2 and CO_2 gases. The microgels were synthesized through soap-free emulsion copolymerization of O_2-responsive monomer 2,3,4,5,6-pentafluorostyrene (FS) and CO_2-responsive monomer 2-(diethylamino) ethyl methacrylate (DEA) with N,N'-methylenebis(acrylamide) (BisAM) as the cross-linker. The P(DEA-*co*-FS) microgels dispersed in aqueous solution could undergo volume phase transitions triggered by either O_2 and/or CO_2 aeration. The particles were very responsive to CO_2, while their responsivity to O_2 was moderate. Microgels having different levels of the responsivity could be designed and prepared by varying the FS content in the copolymer. The phase transitions were also highly reversible and the initial states of microgels could be easily recovered by "washing off" the trigger gases with N_2. Multi-cycle O_2, CO_2 and N_2 aerations were applied and no loss in the dual gas-responsivity and switchability was observed.

§ 5.2 Introduction

Over the years, stimuli-responsive polymers have attracted increasing attention with high potential in various application areas.[1, 2] Stimuli-responsive microgels, as one of the most important examples, have been developing very rapidly for potential applications, such as controlled delivery-release,[3,4] oil recovery,[5] water treatment,[6] Pickering emulsion,[7, 8] and so on. Upon treatment with stimulus or triggers, chemical properties of these "smart" microgels could be reversibly changed through interactions between polymer chains and solvent molecules, leading to dramatic volume phase transition (VPT) and thus making them useful switchable materials. The most studied types of highly effective stimulus and triggers are temperature, pH, and light. While advantageous in some specific areas, each type has general drawbacks in use.[7, 8, 9] For example, when strong base and acid are employed to regulate pH, problems associated with buffer contamination and salt accumulation could occur.[7, 9] Change of temperature with a large volume system is slow and is limited of heat transfer rate. Light inducement is constrained by the depth of radiation. Seeking and design of stimulus and triggers operational with large-volume systems at mild conditions are worth of much research effort in developing smart materials.

Recently, the advent of gas stimuli/trigger has offered great opportunities.[10, 11, 12] Compared to other stimulus, gases are easy to operate in large volume systems, which are promising in industrial applications. Among the gas triggers, CO_2 has raised great

interest, with steady increase in publications. CO_2 is a weak gaseous acid, and it could react with amidine,[13, 14, 15, 16] amine,[17] and carboxyl groups,[18] to increase or decrease their hydrophilicity. Moreover, CO_2 could be easily washed off by simply bubbling of inert gas like N_2, without any accumulation to the system. In the recent years, several CO_2 switchable materials have been reported. For example, Jessop et al.[14, 15, 19] and Wang et al.[20, 21] designed and developed CO_2-switchable latexes. The latex particles could be reversibly coagulated by N_2 bubbling and re-dispersed by CO_2 bubbling. These innovations potentially benefit the latex separation, storage and transportation. Armes et al.[7] prepared poly(2-(diethylamino)ethylmethacrylate-*co*-poly(ethyleneglycol) methacrylate) microgel, which underwent reversible latex-to-microgel transition triggered by CO_2/N_2 aeration. When this microgel was used as switchable surfactant for Pickering emulsions, CO_2 purging for 4 h was needed for a complete demulsification. N_2 purging alone was not enough to recover the Pickering emulsion. Very recently, Wang et al.[22] reported a switchable Pickering emulsifier, which could be used to reversibly control the stability of Pickering emulsions by alternatively CO_2/N_2 purging.

CO_2-stimulated transformation of morphologies has received much attention in the study of the switchable materials.[23] Zhao et al. systematically studied CO_2-triggered self-assembling of block copolymers. The hydrophilic-hydrophobic balance and shift of block copolymers with CO_2 induction were examined,[17, 24] which provided the foundation for the stimuli-responsive self-assembling.[23] Various self-assembled

morphologies from block copolymers responsive to CO_2 aeration, such as, expansion of spheres and vesicles,[25] stretch of folded nanofibers,[26] and compartmentalization of lamellar vesicles.[26] Poly(ethylene oxide)-*b*-poly((N-amidine)dodecylacrylamide)-*b*-polystyrene copolymers were synthesized and self-assembled into rigid tubular geometry, which could be transformed into vesicle and sphere back and forth by alternative CO_2 and inert gas aeration.[27] In addition, Yuan et al.[12, 28] developed thermo and CO_2 dual-responsive triblock copolymers poly[(N,N-diethylaminoethyl methacrylate)-*b*-(N-isopropylacrylamide)] and poly(N-isopropylacrylamide)-*b*-poly(ε-caprolactone)-*b*-poly(N,N-dimethylaminoethylmethacrylate), both could be reversibly turned from vesicle to spherical micelle and expanded vesicle by respective thermal and CO_2 treatment. Furthermore, Feng et al.[11] synthesized the block random copolymer of poly(ethylene oxide)-*b*-poly(2-(diethylamino) ethylmethacrylate-*co*-styrene) and demonstrated self-assembled vesicle structures responsive to CO_2 inducement (from vesicle to micelle).

Besides CO_2, O_2-responsive polymers have also attracted growing interest. Very recently, O_2-sensitive pentafluorophenyl end-capped poly(ethylene glycol) was reported by Jung et al.[29] Interactions between oxygen and C-F bond increased the solubility of PF-PEG-PF and as a result, shifted its lower critical solution temperature (LCST) from 24.5 to 26 ^oC. Zhang et al.[30] reported a new design of fluorinated polymers, based on commercially available 2,2,2-trifluoroethyl meth-acrylate (FMA) and N,N-dimethylaminoethyl methacrylate (DMA). The LCST of the copolymers in

aqueous solutions increased dramatically from 24.5 to 50 °C, which provided a big operation window for the O_2-switchable materials. Later on, Zhang et al.[31] prepared O_2 and CO_2 dual-responsive nano-aggregates of fluoro- and amino-containing copolymers. This type of copolymers could self-assemble into vesicles, which underwent various shape transformations upon O_2 and CO_2 treatments. With O_2 bubbling, the vesicles expanded eight times in volume, while CO_2 bubbling collapsed the vesicular morphology and transformed it into small spherical micelle.

Continuing our effort in preparation of smart materials, in this study, we designed and demonstrated a microgel system responsive to both CO_2 and O_2. These microgels were synthesized through soap-free emulsion copolymerization of CO_2-switchable monomer 2-(diethylamino) ethyl methacrylate (DEA) and O_2-swtichable monomer 2,3,4,5,6-pentafluorostyrene (FS). N,N'-methylenebis(acrylamide) (BisAM) was used as the cross-linker (Scheme 4-1). The volume phase transitions (VPT) of the microgels were induced and regulated by both CO_2 and O_2 aerations. Moreover, the trigger gases could be easily washed off by simply bubbling inert gas N_2. To our best knowledge, this is the first dual gas-switchable microgel system that is sensitive to both O_2 and CO_2. It should be pointed out that this work is very different from the previous work, which was based on self-assembly of amine- and fluorine- containing copolymers,[29, 30, 31] it represents the first $O_2/CO_2/N_2$ switchable microgel particle system of cross-linked polymer network from an emulsion polymerization, which is much more industrially relevant.

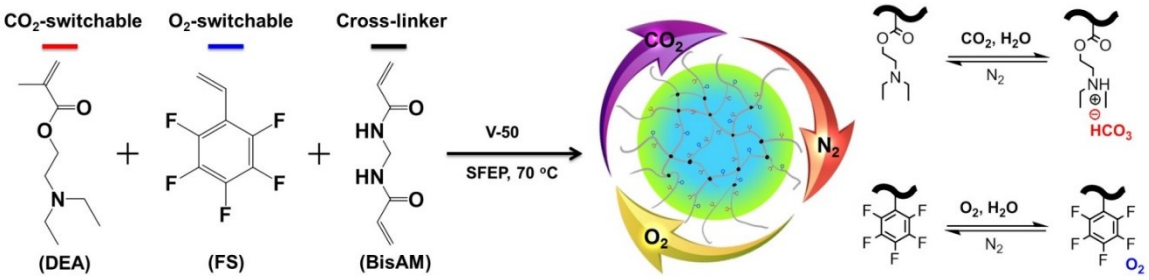

Figure 5-1. Synthesis route of P(DEA-*co*-FS) microgel, and schematic representation of its CO_2 and O_2 responsive behavior.

§ 5.3 Experiments and Characterization

5.3.1 Materials

2-(Diethylamino)ethyl methacrylate (DEA, 99%, Aldrich) and 2,3,4,5,6-pentafluorostyrene (FS, 99%, Aldrich) were passed through an inhibitor remover column and stored under freeze prior to use. N, N'-Methylenebis(acrylamide) (BisAM, 99%, Aldrich) and 2,2'-azobis(2-methylpropionamidine) dihydrochloride (V-50, 99%, Aldrich) were used as received. Milli Q grade water generated from Barnstead Nanopure Diamond system was used for all aqueous solution preparation. CO_2, O_2 and N_2 gases were controlled by FMA-A2100's flow meters (Omega®) to maintain constant gas flow of 10 mL/min.

5.3.2 Experiment

5.3.2.1 Preparation of P(DEA-*co*-FS) microgels

Poly(2-(diethylamino) ethyl methacrylate-*co*-2,3,4,5,6-pentafluorostyrene) microgels (in short, P(DEA-*co*-FS)) having different compositions were prepared via an aqueous surfactant free emulsion polymerization by using 2,2'-azobis(2-methylpropionamidine) dihydrochloride (V-50) as cationic initiator. FS content within the microgels were regulated between 0, 2, 5, 10, 15 and 50 wt% based on the total monomer mass (m_{DEA}+m_{FS}). All microgel samples had 2 wt% cross-linker BisAM in the recipe (with respect to the total monomer mass). Take the microgel with 5 wt% FS content as a synthesis example. 1.9 g of DEAEMA, 0.1 g of FS and 40 mg of BisAM were charged into a 100 mL round-flask. 45 mL of Milli Q water was then added. The flask was sealed with rubber stopper connected with gas inlet and outlet needles. The reaction mixture was magnetically stirred at 300 rpm and degassed with N_2 flow. Meanwhile, the reactor was gradually heated to 70 ^{o}C. After 30 min, the pre-degassed initiator aqueous solution (40 mg of V-50 in 5 mL of water) was injected into the flask to start the polymerization. Within 10 min, the reaction system turned from translucent into creamy white. The reaction was continued for 9 hours and stopped by exposing the latex to air and cooling down to room temperature. The system pH during the polymerization process was about 8.3, which make sure the P(DEA-*co*-FS) microgel were prepared in their latex state. The particle size and distribution of the latex was characterized by DLS. The P(DEA-*co*-FS) microgel latexes were purified through dialysis (Dialysis membrane D0655, Aldrich; 12.4 KD of MWCO) against deionized water (DI water) in order to remove residual monomers and oligomers. The

dialysis water (pH about 6.8) was changed twice every day for 5 days. The microgel latexes were dialyzed in their slightly swollen microgel state.

5.3.2.2 CO_2 and O_2 responsivity tests of P(DEA-*co*-FS) microgels

The purified P(DEA-*co*-FS) microgel dispersions were diluted with DI water to 0.5 mg/mL and pretreated with N_2 before the tests. The dispersions were purged with two cycles of different gases in the order of "$N_2 \rightarrow CO_2 \rightarrow O_2 \rightarrow N_2 \rightarrow O_2 \rightarrow CO_2 \rightarrow N_2$" at a constant flow rate of 10 mL/min. Each gas aeration was continued for one hour and after which, the microgel dispersions were sampled for the DLS test.

5.3.2.3 Swellability tests of P(DEA-*co*-FS) microgels

The swelling ratios of P(DEA-*co*-FS) microgels with different FS contents under CO_2 or O_2 treatment were estimated from the DLS measurement. N_2-treated microgel latexes were taken as reference. The changes in swelling ratio were followed in bubbling constant CO_2 and O_2 flow (10 mL/min) into 15 mL of microgel dispersions (0.5 mg/mL) for one hour in glass tubes. The particle sizes before and after gas treatment were recorded and the corresponding swelling ratios were calculated from $\alpha_{CO2} = V_{CO2}/V_{N2} = (D_{CO2}/D_{N2})_3$ and $\alpha_{O2} = V_{O2}/V_{N2} = (D_{O2}/D_{N2})_3$, where "$D_{CO2}$" and "$D_{O2}$" represent hydrodynamic diameters of the microgels after CO_2 and O_2 treatment; and "α_{CO2}" and "α_{O2}" are corresponding swelling ratios. "D_o" is the hydrodynamic diameter of the latex particles, right after the polymerization, while "D_{N2}" refers to the diameter of the particles after dialysis purification and N_2 treatment.

5.3.3 Characterization

The changes in turbidity of the microgel dispersions after N_2, O_2, and CO_2 treatments were followed by recording transmittance of the dispersions at 550 nm using UV-Vis (Brookhaven, DU 800) Spectrophoto Meter. The hydrodynamic diameters of the microgels at different swelling states were detected at 22 °C using Particle Size Analyzer (Brookhaven, 900Plus), equipped with 35 mW red diode laser source at 600 nm wavelength with a detection angle of 90 °. The samples were equilibrated for 180 s before detection, then conducted for 180 s with 30 s interval between measurements. Each measurement was performed 3 times. TEM images were recorded to characterize the changes in particle size and morphology of the microgels before and after gas treatments. One drop of phosphotungstic acid (PTA) aqueous solution (0.2 wt%) was added to 1.5 mL of microgel dispersions pretreated by N_2, O_2 and CO_2 for the purpose of staining purpose. The trace amount of PTA did not change pH of the solutions (remained 7.2) and did not cause particle swelling. After that, the microgel dispersion was drop coated on copper grid and immediately freezed by liquid nitrogen. The microgel sample was freeze-dried before the TEM tests. TEM images were recorded using JEOL-1200ex instrument.

§ 5.4 Results and Discussion

5.4.1 Preparation and characterization of P(DEA-co-FS) microgels

Table 5-1 summarizes the experimental conditions and particle size data from the "one-shot" soap-free emulsion copolymerization of CO_2-switchable monomer DEA and O_2-swtichable monomer FS with BisAM as the cross-linker. The pH value of the reaction system was about 8.3 before polymerization, which were initiated by cationic initiator V-50 at 70 ^oC and lasted for 9 hours. All the runs turned from translucent to creamy white within 10 min after initiator injection and yielded stable latexes. The amounts of cross-linker, initiator and total monomer were kept the same, while the weight percent of FS varied from 0~50 %. The microgels right after polymerization had the number-average particle diameters between 192 nm and 373 nm, with relatively narrow size distribution (≤ 0.09). The microgel diameter decreased with the increased FS content. This could be attributed to hydrophobicity of the FS units and their strong C-F intramolecular forces,[27] leading to much solid microgel structures. The D_{N2} values were smaller than D_o's because of the removal of oligomers and unreacted monomers in the dialysis purification. The total monomer conversions determined by a gravimetric method ranged from 55-70 wt%. Take Run 3 as an example, after polymerization, the comonomer (FS) conversion in P(DEA-*co*-FS) microgel estimated from the total monomer conversion and polymer composition was about 78 wt%.

Table 5-1. Experimental conditions of the emulsion copolymerization of DEA and FS with BisAM, and particle sizes of the resulting P(DEA-*co*-FS) microgels

Run[a]	FS[b] (wt%)	D_0[c] (nm)	PDI[c]	D_{N2}[d] (nm)	O_2		CO_2	
					D_{O2}[d]	α_{O2}[e]	D_{CO2}[d]	α_{CO2}[e]
1	0	373	0.068	352	—	—	1040	25.8
2	2	271	0.041	262	346	2.30	690	18.3
3	5	243	0.074	215	370	5.10	495	12.2
4	10	223	0.047	208	307	3.22	416	8.00
5	15	212	0.065	194	205	1.18	335	4.36
6	50	192	0.051	151	156	1.10	163	1.26

Note: a: Run 1-6 were conducted with 2 wt% BisAM cross-linker at 70 ºC for 9 h. b: With respect to the total monomer weight of FS and DEA. c: Hydrodynamic diameter and particle size distribution of the microgel latexes right after polymerization. d: "D_{CO2}", "D_{O2}" and "D_{N2}" represent hydrodynamic diameters of the microgels after CO_2, O_2 and N_2 treatment. e: "α_{CO2}" and "α_{O2}" represent the swelling ratio of microgel after CO_2 and O_2 treatment.

5.4.2 CO_2 and O_2 responsivity of P(DEA-co-FS) microgels

The CO_2 and O_2 responsivity of P(DEA-*co*-FS) microgels were thoroughly investigated by taking the microgel with 5 wt% FS (Run 3) as example. The N_2-saturated microgel dispersions were used as the initial latex. A constant CO_2 or O_2 flow at 10 mL/min was purged into the dispersion to trigger the responses, which were later expelled by purging N_2 (10 mL/min) to recover the system to initial state.

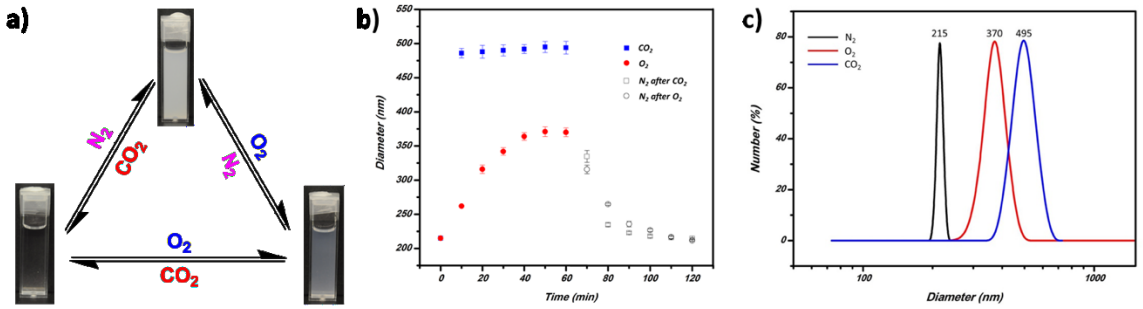

Figure 5-2. Gas responsive characterization of P(DEA-*co*-FS) microgel (Run 3) dispersions (0.5 mg/mL) upon N_2, CO_2 and O_2 treatments. a) Digital photos. b) Change of particle diameter with time (every 10 min) in the CO_2 (blue square) or O_2 (red circle) induced swelling, and the N_2 (black square and circle) assisted deswelling processes. c) DLS data of the microgel dispersions before (black) and after treatment with CO_2 (blue) and O_2 (red), respectively.

Optical changes of the microgel dispersion after CO_2, O_2 and N_2 treatment were shown in Figure 5-2 a). The original microgel dispersion (top) was creamy-white, which became clear gradually after 30 min purging with O_2 (right). O_2 appeared to be not as efficient as CO_2 (left), which took only about 10 min to become transparent. The microgel dispersion remained as stable dispersion after treating with O_2 and CO_2, no particle coagulation was observed. Turbidity measurement confirmed the optical changes. The transmittance of the initial microgel dispersion at 550 nm was 13.3 %, and it increased to 79.9 % and 84.1 % after 1 hour of O_2 and CO_2 aeration, respectively. This dramatic transmittance increase is caused by the refractive index decrease due to microgel swelling.

The changes of microgel diameter with time were monitored by dynamic light scattering during gas-response and recovery processes in every 10 min, Figure 5-2 b)

shows both swelling and deswelling kinetics of Run 3 sample towards CO_2/O_2 and N_2 treatments. Each gas treatment was continued for 60 min to ensure fully replacement of the previous trigger gas and saturation of the new gas. As it can be seen, in only 10 min of purging initial microgel dispersion (215 nm) with CO_2, the latex was swelled to more than 95 % (486 nm) of its total diameter expansion. Further CO_2 purging leveled off the diameter at about 495 nm. This CO_2 induced microgel swelling was recovered by 95% in 20 min of N_2 purging. The total recovery to the initial latex state required 60 min N_2 purging. In comparison, purging O_2 for 40 min swelled the microgel particles by 95% (364 nm), which was slower than CO_2 trigger process (10 min). Similarly, applying longer O_2 treatment time slightly increased the diameter to a constant value at 370 nm, which could be fully recovered within 60 min by N_2 purging. Figure 5-2 c) also showed the increased hydrodynamic diameters from the initial microgel after the O_2 and CO_2 treatments. The particle size distributions were clearly unimodal. These changes in both turbidity and particle size demonstrated the responsivity of P(DEA-*co*-FS) microgels to CO_2 and O_2.

Transmission electron microscopy (TEM) was applied to further visualize volume expansion of the microgels upon gas stimulus. Phosphotungstic acid (PTA) aqueous solution was used as the staining agent. A typical spherical particle morphology was observed for the original microgel, as shown in Figure 5-3 a). As measured from the TEM images, the average particle size of the original microgel was approximately 193 ± 16 nm. After treated with O_2, the particle size increased to around 338 ± 32 nm

(Figure 5-3 b). After treated with CO_2, the microgels expanded to 455 ± 45 nm (Figure 5-3 c). These TEM images clarified the obvious particle size increase without aggregation could clearly be observed. The particle size results were somewhat smaller than those obtained from DLS measurement, this is because the hydrodynamic diameters of the microgel obtained from DLS included the thickness of electrical double layer, which was absent in TEM test. Thus, it can be concluding that volume expansion of the microgel were caused by the individual microgel swelling, not their coalesce/aggregation.

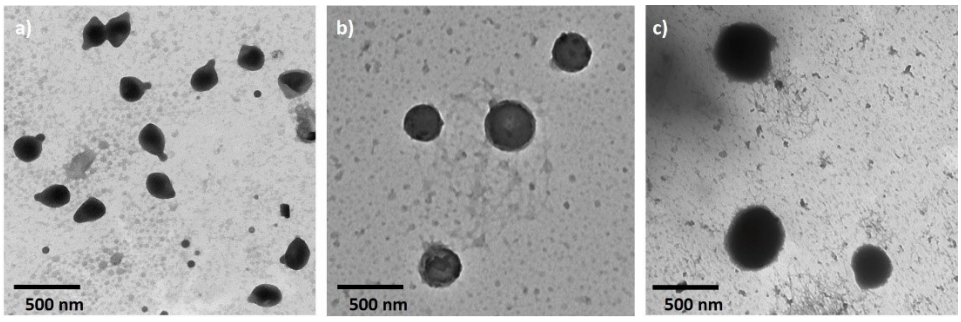

Figure 5-3. TEM images of P(DEA-*co*-FS) microgels (Run 3): a) after N_2 treatment; b) after O_2 treatment; c) after CO_2 treatment.

Reversibility of the volume expansion with CO_2 and O_2 treatments was then examined to see if the dual gas switchable process could be reversed by purging the system with inert gas N_2. The gas replacement process was repeated by two cycles of gas aeration in the order of "$N_2 \rightarrow CO_2 \rightarrow O_2 \rightarrow N_2 \rightarrow O_2 \rightarrow CO_2 \rightarrow N_2$". Figure 5-4 shows changes of the particle size as measured by DLS, during the two cycles of gas treatments. The data

was very reproducible, which clearly demonstrated good switchability of the P(DEA-*co*-FS) microgels by O_2, CO_2 and N_2 bubbling.

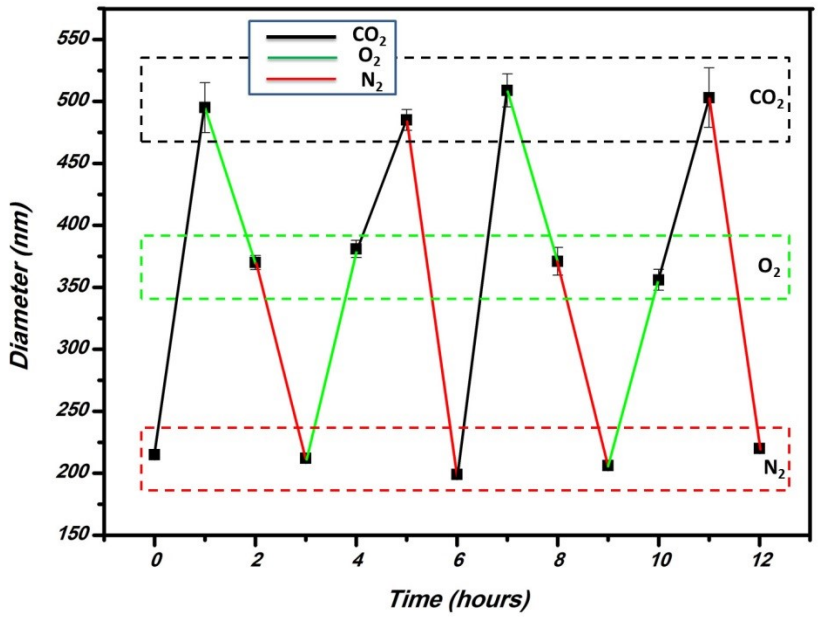

Figure 5-4. Changes in the particle size of P(DEA-*co*-FS) microgels (Run 3) during two cycles of CO_2, O_2 and N_2 treatments.

It has become clear that both CO_2 and O_2 could effectively drive the volume expansion of the microgels. Typically, when P(DEA-*co*-FS) microgel dispersion was treated by CO_2, the system transferred from milky white to nearly transparent (see Figure 5-2 a). This was because the tertiary amine groups of DEA were easily protonated by CO_2 dissolved in aqueous solution.[23] In order to balance the osmatic pressure generated by the charges, water molecules swelled into the microgel network, which reduced the system's light scattering index and led to the creamy-to-transparent conversion.[32] This process could be easily reversed by N_2 aeration, which expelled the dissolved CO_2

and the hydrodynamic volume of the microgel particles returned to the original value. In the O_2-triggered volume transition, the fluorinated component enhanced O_2 solubility in water.[33, 34, 35] Interactions between the dissolved O_2 molecules and the fluorine atoms in the polymer improved hydrophilicity of the material,[30, 31] and thus facilitated water absorption and swelling of the microgels. The dissolved O_2 molecules could also be easily washed off by N_2 bubbling to recover original state of the microgels. It should be pointed out that the particle size distribution increased after it was treated by active gas (CO_2 and O_2) to their swollen state. The distribution went back to its original level after N_2 purging. DLS and TEM results suggested no agglomeration happened during $CO_2/O_2/N_2$ cycles. It can also be pointed out that our experiment results verified that pure PDEA microgel latex was not responsive to O_2 and pure PFS latex was not responsive to CO_2. DEA and FS units in P(DEA-*co*-FS) microgel were one to one stimuli-responsive toward CO_2 and O_2, respectively.

5.4.3 Effect of FS content on swellability of P(DEA-co-FS) microgels

The CO_2 and O_2 responsivity of P(DEA-co-FS) microgels stemmed from the corresponding functional monomers (DEA and FS). The composition of the microgel was critical to the gas triggered swelling properties. All the microgel samples synthesized in this work had the fixed cross-linker content of 2 wt% BisAM. The FS content was varied from 0, 2, 5, 10, 15 to 50 wt% to regulate the O_2/CO_2 triggered swelling ratio.

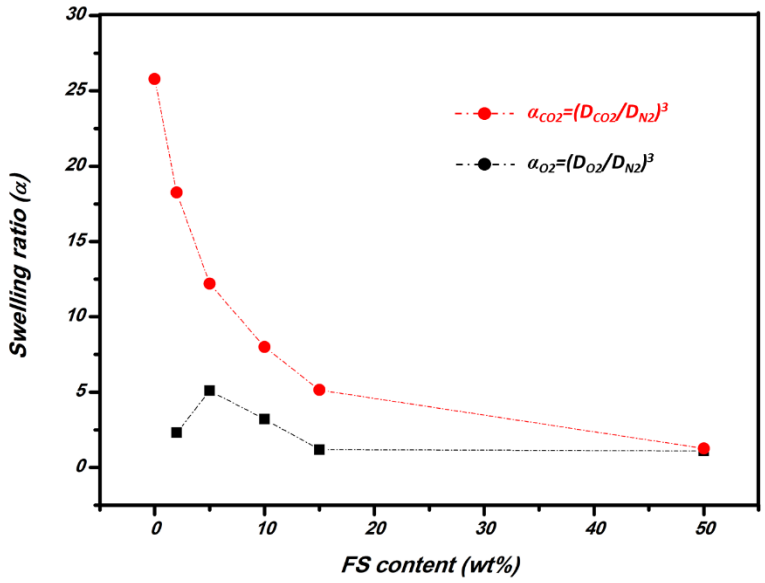

Figure 5-5. Change of the swelling ratio in CO_2 and O_2 treatment of P(DEA-*co*-FS) microgels with respect to the FS content.

Figure 5-5 shows a clear trend of the change in swelling ratio with respect to the microgel composition. Pure PDEA microgels, prepared in the absence of FS content (corresponding to 0 wt% of FS), gave a CO_2-induced swelling ratio of 25.8. Adding 2 wt% FS content made the microgel responsive to both CO_2 and O_2. The O_2-induced swelling ratio was 2.30, while the CO_2-induced swelling ratio decreased from 25.8 to 18.3. The swelling mechanisms towards CO_2 and O_2 were different: CO_2 protonated amine group while O_2 interacted with fluorine moiety. Introduction of the FS content reduced the number of functional groups responsive to CO_2. The fluorine moieties also provided constraints on volume expansion of the microgel in the CO_2-induced swelling. When the FS content increased to 5 wt%, the O_2-induced swelling ratio reached to its highest level, while the CO_2-induced ratio continued to decrease.

Further increasing the FS content to 10 wt% reduced the swelling ratios triggered by both O_2 and CO_2. Swellability of the microgels stemmed from O_2-fluro interactions was relatively low, compared to that of amine group by CO_2. PFS is also a super-hydrophobic polymer. Too much hydrophobic component prevented the network from volume expansion. When the FS content reached 15 wt%, the O_2-induced swelling ratio decreased to only 1.18, but it could still be swollen with CO_2 treatment (α_{CO2} = 4.36). With 50 wt% FS content, the microgel became insensitive to CO_2 or O_2 inducement. It becomes clear that P(DEA-*co*-FS) microgels having different levels of CO_2 and O_2 dual responsivity could be designed by varying the FS content. It should be pointed out that the latexes containing pure PFS were not oxygen responsive and the particles did not change their size after treated with O_2 for even hours.

§ 5.5 Conclusion

The microgels were prepared through soap-free emulsion copolymerization of 2,3,4,5,6-pentafluorostyrene (FS) and 2-(diethylamino) ethyl methacrylate (DEA) with 2 wt% N,N'-methylenebis(acrylamide) (BisAM) as the crosslinking agent. The FS content varied from 0, 2, 5, 10, 15 to 50 wt%, based on the total monomer mass. The microgels thus synthesized contained fluoro- and amino- moieties and were responsive to both O_2 and CO_2. The particles dispersed in aqueous solution underwent significant volume expansion with O_2 and/or CO_2 aeration. The swelling ratio strongly depended on the FS content. With 5 wt% FS, the microgel particles increased from 215 nm to 370 nm in diameter when bubbled with O_2 and to 495 nm when bubbled

with CO_2. These volume phase transitions were reversible and could be easily recovered by N_2 aeration. When bubbled with N_2, both the O_2- and CO_2-treated 5 wt% FS particles shrank to 215 nm. The particle sizes associated with O_2, CO_2 and N_2 treatments were definite and repeatable, regardless of the order of gas aeration and the number of cycles applied. It is believed that this work represented the first report on the design and preparation of dual gas-responsive and switchable microgels.

§ 5.6 References

[1] Stuart, M. A. C.; Huck, W. T. S.; Genzer, J.; Müller, M.; Ober, C.; Stamm, M.; Sukhorukov, G. B.; Szleifer, I.; Tsukruk, V. V.; Marek Urban; Winnik, F.; Zauscher, S.; Luzinov, I.; Minko, S. *Nature Materials* **2010**, 9, 101-113.

[2] Roy, D.; Cambre, J. N.; Sumerlin, B. S. *Progress in Polymer Science* **2010**, 35 (1-2), 278-301.

[3] Smeets, N. M. B.; Hoare, T. *Journal of Polymer Science Part A: Polymer Chemistry* **2013**, 51 (14), 3027-3043.

[4] Oh, J. K.; Drumright, R.; Siegwart, D. J.; Matyjaszewski, K. *Progress in Polymer Science* **2008**, 33 (4), 448-477.

[5] Eckford, R.; Fedorak, P. *Petroleum Biotechnology: Developments and Perspectives* **2004**, 151, 307-340.

[6] Brostow, W.; Hagg Lobland, H.; Pal, S.; Singh, R. P. *Journal of Materials Education* **2009**, 31 (3-4), 157-166.

[7] Morse, A. J.; Armes, S. P.; Thompson, K. L.; Dupin, D.; Fielding, L. A.; Mills, P.; Swart, R. *Langmuir* **2013**, 29 (18), 5466-5475.

[8] Morse, A. J.; Dupin, D.; Thompson, K. L.; Armes, S. P.; Ouzineb, K.; Mills, P.; Swart, R. *Langmuir* **2012**, 28 (32), 11733-11744.

[9] Fielding, L. A.; Edmondson, S.; Armes, S. P. *Journal of Materials Chemistry* **2011**, 21 (32), 11773-11780.

[10] Zhang, Q.; Zhu, S. P. *Macromol. Rapid Commun.* **2014**, 35 (19), 1692-1696.

[11] Liu, H.; Guo, Z.; He, S.; Yin, H.; Fei, C.; Feng, Y. *Polym. Chem.* **2014**, 5, 4756-4763.

[12] Feng, A.; Zhan, C.; Yan, Q.; Liu, B.; Yuan, J. *Chem. Commun. (Camb)* **2014**, 50 (64), 8958-8961.

[13] Quek, J. Y.; Davis, T. P.; Lowe, A. B. *Chemical Society Reviews* **2013**, 42 (17), 7326-7334.

[14] Liu, Y.; Jessop, P. G.; Cunningham, M.; Eckert, C. A.; Liotta, C. L. *Science* **2006**, 313 (5789), 958-960.

[15] Mihara, M.; Jessop, P.; Cunningham, M. *Macromolecules* **2011**, 44 (10), 3688-3693.

[16] Su, X.; Jessop, P. G.; Cunningham, M. F. *Macromolecules* **2012**, 45 (2), 666-670.

[17] Han, D.; Tong, X.; Boissière, O.; Zhao, Y. *ACS Macro Lett.* **2012**, 1, 57-61.

[18] Fischer, V.; Landfester, K.; Muñoz-Espí, R. *ACS Macro Lett.* **2012**, 1 (12), 1371-1374.

[19] Pinaud, J.; Kowal, E.; Cunningham, M.; Jessop, P. *ACS Macro Lett.* **2012**, 1 (9), 1103-1107.

[20] Zhang, Q.; Yu, G.; Wang, W. J.; Li, B. -G.; Zhu, S. P. *Macromol. Rapid Commun.* **2012**, 33 (10), 916-921.

[21] Zhang, Q.; Yu, G.; Wang, W. J.; Yuan, H.; Li, B.-G.; Zhu, S. P. *Macromolecules* **2013**, 2013, 1261-1267.

[22] Liu, P.; Lu, W.; Wang, W.-J.; Li, B.-G.; Zhu, S. P. *Langmuir* **2014**, 30 (34), 10248-10255.

[23] Yan, Q.; Zhao, Y. *Chem. Commum.* **2014**, 50, 11631-11641.

[24] Han, D.; Boissiere, O.; Kumar, S.; Tong, X.; Tremblay, L.; Zhao, Y. *Macromolecules* **2012**, 45 (18), 7440-7445.

[25] Yan, B.; Han, D.; Boissière, O.; Ayotte, P.; Zhao, Y. *Soft Matter* **2013**, 9 (6), 2011-2016.

[26] Yan, Q.; Zhao, Y. *J. Am. Chem. Soc.* **2013**, 135 (44), 16300-16303.

[27] Yan, Q.; Zhao, Y. *Angew. Chem. Int. Ed.* **2013**, 52 (38), 9948-9951.

[28] Liu, B.-w.; Zhou, H.; Zhou, S.-t.; Zhang, H.-j.; Feng, A.-C.; Jian, C.-m.; Hu, J.; Gao, W.-p.; Yuan, J.-y. *Macromolecules* **2014**, 47 (9), 2938-2946.

[29] Choi, J. Y.; Kim, J. Y.; Moon, H. J.; Park, M. H.; Jeong, B. *Macromol. Rapid Commun.* **2013**, 35 (1), 66-70.

[30] Zhang, Q.; Zhu, S. P. *Macromol. Rapid Commun.* **2014**, 35 (19), 1692-1696.

[31] Zhang, Q.; Zhu, S. P. *ACS Macro Lett.* **2014**, 743-746.

[32] Pelton, R.; Hoare, T. Microgels and their synthesis: An introduction. In Microgel Suspensions: Fundamental and Applications, Femandez-Nieves, A.; Hans M. Wyss; Mattsson, J.; Weitz, D. A., Eds.; *WILEY-VCH*, **2011**.

[33] Dias, A. M. A.; Freire, M.; Coutinho, J. A. P.; Marrucho, I. M. *Fluid Phase Equilibria* **2004**, 222-223, 325-330.

[34] Wesseler, E. P.; Iltis, R.; Clark, L. C. *Journal of Fluorine Chemistry* **1977**, 9, 137-146.

[35] Riess, J. G. Chemistry, and Some Physiology. *Chem. Rev.* **2001**, 101, 2797-2919.

6 O_2 AND CO_2- DUAL GAS-SWITCHABLE MICROGEL-COLLOIDOSOME

This chapter is the continue work of chapter 5. Based on the O_2 and CO_2 dual-gas switchable microgels, microgel-colloidosomes are prepared from Pickering emulsion template and used as microcapsules for hierarchical control-release of water soluble cargo molecules. This chapter is reproduced from the published work in Lei Lei, Qi Zhang, Susan Shi, Shiping Zhu "Breathable microgel-colloidosome: Gas-switchable microcapsules with O_2 and CO_2 tunable shell permeability for hierarchical size-selective control-release" *Langmuir*, **2017**, 33 (24), pp 6108–6115 (DOI: 10.1021/acs.langmuir.7b01092) with the permission from ACS publisher. The supporting information referred in the manuscript is attached at the end of this chapter.

Author contributions

The idea of this work is generated from the discussion with Dr. Qi Zhang. Lei Lei did all the experiments and prepared the first manuscript under the supervision of Dr. Shiping Zhu. Dr. Zhang and Dr. Shuxian Shi provided valuable discussion and first revision of the manuscript. Dr. Zhu did the final revision before submission.

§ 6.1 Abstract

Microcapsules enabling precise delivery and controlled release are highly desirable. However, it is still challenging to control the release profile by regulating the microcapsule shell permeability. In this work, gas-switchable microgel-colloidosome (MGC) with oxygen (O_2) and carbon dioxide (CO_2) dual gas-tunable shell permeability has been developed and tested for control-release of water-soluble cargo molecules, based on size exclusion mechanism. The O_2 and CO_2 dual gas-switchable poly(2-(diethylamino)ethyl methacrylate-*co*-2,3,4,5,6-pentafluorostyrene), P(DEA-*co*-FS), microgels having surface modified with amino group ($–NH_2$) were synthesized and used to stabilize oil-in-water (O/W) Pickering emulsions. The oil soluble poly(propylene glycol) diglycidyl ether (PPGDGE) was added as an inter-microgel cross-linker. The cross-linking between adjacent microgel particles at the water-oil interface was achieved through the amine-epoxy reaction of PPGDGE with the amine groups at the particle surface. Fluorescent-labelled dextran model cargo molecules of 10 kDa (D_1) and 2000 kDa

(D_2) were uploaded under CO_2 treatment and locked inside the MGC with N_2 treatment. The O_2 and CO_2 dual-gas switchable properties offered the MGC with tunable shell permeability, which allowed the hierarchical release of D_1 and D_2 based on size exclusive mechanism. This work provides a robust method for preparation of gas-switchable microcapsules with tunable permeability and size-exclusive hierarchical release profile, promising for multiple ingredient controllable release, separation, and reaction.

§ 6.2 Introduction

For decades, microcapsules that enable accurate encapsulation, delivery and control-release of active or sensitive ingredients (e.g. chemical and biological molecules) are of great interest and motivation for both academic research and pharmaceutical industry.[1-2] Encapsulation increases stability and lifetime of the active cargoes and protect them against harsh environment. The encapsulation also facilitates accurate delivery and controlled release to avoid side effects of miss-targeting and over-dosage of active cargoes.[2] Various microcapsules have been developed from block copolymer self-assembling (vesicles/polysomes),[3] polymer precipitation by phase separation,[4] interfacial polycondensation,[5] layer-by-layer polyelectrolyte deposition,[6-8] and so on.

Colloidosome is one of the most studied microcapsules, with its shell built by self-assembled colloid particles at oil/water interface template from Pickering emulsion.[2,

[9-10] Technically, almost all particles (e.g. microgels,[11-14] silica sols,[15] polystyrene latexes,[1, 16-17] Au[18], Fe_3O_4[19] and metal-organic framework (MOF)[20] nanoparticles) capable of stabilizing Pickering emulsion droplets can be used as building blocks for preparation of colloidosomes. The size of colloidsome could be controlled by oil and water phase selection, regulating the oil/water phase fraction, the concentration of particulate stabilizer (building block), the homogenization speed, and so on.[9-10] Subsequent processing for robust colloidosome fabrication, such as colloidosome transfer (remove emulsion template) and purification, normally requires reinforcement (locking) of the particle shell, which can be realized by thermo annealing,[17] chemical cross-linking,[1, 16, 21] and physical bridging through trapping of high molecular weight polymers.[13] The colloidosomes made from coagulated or fused colloid particles process semipermeable features, allowing entrapped cargo ingredients to diffuse through, with a diffuse rate controlled by shape, orientation, and uniformity of the interstices between encapsulants and colloid shell membrane, based on a size exclusive mechanism.[9-10, 13] Breaking or dissolution of the microcapsule shell would result in an immediate release of the encapsulated ingredient, while a sustained release is often preferable.[22] Thus, control over release profile of the core ingredients represents a critical challenge in the development of microencapsules.

Due to the flexibility of microgels, microgel-colloidosome (MGC) with tunable swellbility (shell permeability) can be prepared as smart microencapsules for

controlled release in response to external triggers such as pH- [11-12, 16] and thermo-,[13-14, 21] and magnetic.[15, 19, 23] For example, using poly(N-isopropylacrylamide) (PNIPAM) microgel particles, Shah et al. reported thermo-responsive MGC with reversible thermo-induced size changes through microfluidic W/O emulsion template.[14] Cayre et al. reported pH-responsive MGC from polystyrene latex surface modified with poly(dimethylaminoethyl methacrylate) (PDMA).[1] The microgel particles on emulsion droplet surface were chemically cross-linked either by 1,2-bis-(2-iodoethoxy)ethane (BIEE, amine in DMA reacted with iodo-end group in BIEE) or by poly(propylene glycol) diglycidyl ether (PPGDGE, amine in DMA reacted with epoxy-end groups in PPGDGE). Both encapsulation and controlled release of dextran molecules were achieved by regulating pH of the environment.[1] An alternative method for smart colloidosome preparation is to encapsulate some stimuli-responsive absorbent objects within colloidosome to capture and release cargos upon the treatment of external triggers. Sander et al. prepared pH and magnetic dual-responsive colloidosomes.[15] Fe_3O_4 nanoparticles incorporated in the shell led migration of the colloidosome to a target position under magnetic field. The pH regulation controlled on-off desorption and release of cargo molecules from the absorbent particles.

Among all stimuli, gas-switchable polymers have attracted tremendous attention in the recent years. Carbon dioxide (CO_2) is the most reported trigger gas.[24-28] After hydrolysis in water, CO_2 can reversibly react with amine, amidine, guanidine and

imidazole moieties and regulate their hydrophilicity.[25, 28] Another gas trigger is O_2, which can reversibly interact with fluorinated groups in aqueous solution through van de Walls interaction and increase water solubility of the fluorinated monomers.[29-33] These gas-switchable processes are "green" and efficient, without buffer contamination and fully reversible without loss of switchability. Moreover, O_2 and CO_2 possess great biocompatibility and membrane permeability, making them desirable candidates for biomedical applications such as controlled drug release and tissue engineering. O_2 and CO_2 dual-gas switchable microgels has been reported.[33] The microgels can swell to different levels upon O_2 and CO_2 treatment respectively, and recover to their initial states by wash off the trigger gases with N_2. In this work, using such O_2 and CO_2 dual-gas switchable microgel particles as building block, we prepared microgel-colloidosomes (MGC) with tailored shell permeability through microgel-stabilized oil-in-water (O/W) Pickering emulsion. The adjacent microgel particles at the MGC shell were crosslinked with an oil soluble cross-linker. The internal oil core phase and the excess microgels in the aqueous phase were removed through centrifuge-washing cycles. The prepared MGCs were tested as smart microcapsules for control-release of water-soluble ingredients. Dextran molecules of 10 and 2000 kDa were successfully loaded into the MGCs using CO_2 to maximize the shell permibility. A hierarchical release of D_1 and D_2 molecules was demonstrated by treating the MGC with O_2 and CO_2, respectively. To our best knowledge, this work represents the first gas-switchable MGC system. The O_2 and CO_2 dual gas-tunable shell

premibility and hierarchical release profile of the MGC are promising for applications of the multi-drug delivery systems.

§ 6.3 Experiments and Characterization

6.3.1 Materials

2-(Diethylamino)ethyl methacrylate (DEA, 99%, Aldrich) and 2,3,4,5,6-pentafluorostyrene (FS, 99%, Aldrich) were passed through an inhibitor remover column and stored under freeze prior to use. N, N'-methylenebis(acrylamide) (BisAM, 99%), 2, 2' -azobis(2-methylpropanimidamide) dihydrochloride (V-50, 99%), N-(3-aminopropyl) methacrylamide hydrochloride (APMA), fluorescein O-methacrylate (97%,), poly(propylene glycol) diglycidyl ether (PPGDGE, MW = 640 g/mol), hexadecane (>99%), FITC–dextran (**D_1**: M_w = 10 kDa), and blue-dextran (**D_2**: M_w = 2000 kDa) were purchased from Aldrich and used as received. Ethanol (99.5%) was purchased from Commercial Alcohols in ON, Canada. Milli-Q grade water was generated from Barnstead Nanopure Diamond system.

6.3.2 Experiments

6.3.2.1 Preparation of O_2 and CO_2 dual-gas switchable microgels

The O_2 and CO_2 dual-gas switchable poly(2-(diethylamino)ethyl methacrylate-*co*-2,3,4,5,6-pentafluorostyrene), also known as P(DEA-co-FS) microgels, were prepared from surfactant free emulsion polymerization, as described in our previous work.[33] A

typical preparation procedure for the microgels with 5 wt% FS (MG-F5) was described as follows for the reader's convenience. DEA (1900mg, mol), FS (100 mg), BisAM (40 mg, 2 wt%), APMA (60 mg, 3 wt%) and 38 mL Milli-Q water were added into a 100 mL round-flask. The flask was finely sealed with rubber stopper and connected with gas inlet/outlet needles. The reaction mixture was immersed in oil bath and magnetically stirred at 300 rpm. The system was also degassed with N2 flow and preheated to 70 ^{o}C at the same time. After 30 min, the predegased V-50 (100 mg, 5wt%) aqueous solution (2 mL) was injected into the system to start polymerization. The reaction was conducted for 4 hours and stopped by cooling down the flask in an ice-bath. The microgel was purified through dialysis (12.4 kDa of MWCO) against deionized (DI) water. The hydrodynamic diameter of microgel particles was determined by DLS.

The O_2 and CO_2-switchability of the microgels were characterized by measuring their hydrodynamic particle sizes before and after O_2 or CO_2 treatment, respectively. The microgel aqueous dispersion (1 mg/mL) was treated with O_2 and CO_2 gas bubbling at 10 mL/min for 1 hour before DLS characterization.

6.3.2.2 Preparation of microgel colloidosomes

The microgel-colloidosomes (MGC) were prepared by using the microgel-stabilized O/W Pickering emulsion templates. The Pickering emulsions were prepared by using P(DEA-*co*-FS) microgels as particulate stabilizer in aqueous dispersion (10 mg/mL, 7

mL), hexadecane (3 mL) dispersed with PPGDGE (0.5 wt% based on the microgel mass) as oil phase. The mixture was homogenized by IKA T18 Ultra-Turrax at 20000 rpm for 2 min. The final O/W emulsion was insulated at 40 ^{o}C for 24 hours to complete inter-microgel (MG-MG) cross-linking (amine-epoxy reaction) and formation of colloid shell for the MGC.

The MGC samples were purified by removing excess microgel particles and extracting core oil phase through a solvent exchange method. After each centrifuge at 4000 rpm for 10 min, the supernatant was removed and the MGC was washed with ethanol/water (1/3 = v/v) mixture. The system was mixed thoroughly with Vortex for 30 min before another centrifuge-wash cycle. The centrifuge and washing cycle were conducted for at least 5 times. The final MGC samples were kept in aqueous solution before test and use.

6.3.2.3 Gas-triggered microgel-colloidosome control-release

The purified MGCs were used as gas-switchable microcapsules for control-release tests of fluorescent-labelled dextrans having different molecular weights (D1: Mw = 10 kDa and D2: Mw = 2000 kDa) as the cargo molecules. Specifically, MGC was first dispersed in an aqueous solution containing 1 wt% of both D1 and D2 molecules, which was then treated with CO_2 at 10 mL/min for about 2 hours. This process expanded MGC and allowed the dextran molecules penetrate through the shell and

loaded into the MGC. The dextran contents of D1 and D2 at different loading stages were monitored by UV-vis spectrometer absorption at 485 nm and 630 nm, respectively. The sample solution was balanced in the instruction for 2 min before each measurement. The excess dextran (D1 and D2) molecules were removed by subsequent centrifugation and washing cycles for 3 times. The loading efficiency (LE) was calculated from "$LE=(C_0-C)/C_0$ ", where the "C_0" and "C" are the initial and final dextran concentration (D1 and D2) in the mother solution at the loading stage. Subsequently, the MGC aqueous dispersion was charged with N_2 to remove the trigger gas CO_2 and to lock D1 and D2 inside MGC microcapsules (MGC*, with symbol * meaning loaded). The MGCs loaded with cargo molecules (MGC*) were purified by centrifuge, with the supernatant removed and then washed with degassed DI water to remove excess dextran molecules.

MGC-F5 (microgel colloidosome prepared from P(DEA-co-FS) microgel containing 5 wt% FS) loaded with (D1 and D2) dextran molecules (MGC*-F5) was prepared as smart microcapsule for O_2 and CO_2 gas-triggered control-release tests. The MGC-F5* sample was divided into three aliquots of the same volume and diluted with an equal amount of degassed DI water. They were then treated with N_2 (as control gas), O_2 and CO_2, respectively at 10 mL/min. The dextran (D1 and D2) concentrations in the environment solution at different release stages (time) were monitored by UV-vis spectrometer at 485 nm and 630 nm, respectively.

6.3.3 Characterization

The hydrodynamic particle size and distribution of microgels before and after trigger gas (O_2 and CO_2) treatment were measured by particle size analyzer (Brookhaven, 900Plus). All the microgel-stabilized O/W Pickering emulsions, microgel-colloidosomes (MGC) and the MGC loaded with dextran (MGC*) were characterized by fluorescence microscope. The fluorescence images were acquired from Zeiss LSM 510 Meta Confocal Microscope (Zeiss, Gottingen, Germany). The fluorescence images presented cross-section views of the MGC microcapsules, which were used to distinguish if the cargo dextran molecules were located on surface or encapsulated in core of the MGC. One drop of the MGC or MGC* aqueous dispersion was placed onto a glass slide and covered with another cover slice for observation. MGC morphologies were characterized by JEOL JSM 7000 Scanning Electronic Microscopy (SEM) at 3 kv accelerating voltage. The cargo molecule D1 and D2 concentrations at different stages in the environment solution during loading or releasing were detected by UV-vis spectrometer absorption at 485 nm and 630 nm, respectively. Samples were balanced for 2 min before each measurement.

§ 6.4 Results and Discussion

6.4.1 Preparation and characterization of O_2 and CO_2 dual gas-switchable microgels

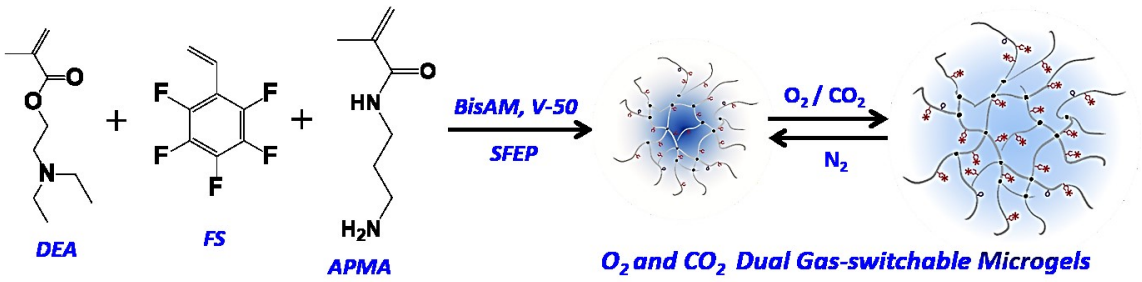

Figure 6-1. Synthetic route of the O_2 and CO_2 dual gas-switchable P(DEA-*co*-FS) microgel with surface modified by amino (–NH_2) groups.

P(DEA-*co*-FS) microgels having different chemical compositions were prepared from surfactant free emulsion copolymerization of FS and DEA, as described in our previous work.[33] As illustrated in Figure 6-1, 2 wt% BisAM was used as cross-linker and 3 wt% APMA as surface amino-agent in preparation of all the microgels (based on the total monomer mass). The FS content in the microgel varied from 5, 40 to 80 wt% (based on the total monomer mass), in order to regulate gas switchability of the microgel as listed in Table 6-1. The gas-switchable properties of different P(DEA-*co*-FS) microgels were reflected from the changes in their hydrodynamic diameters before (D_{N2}) and after O_2 (D_{O2}) or CO_2 (D_{CO2}) treatment at 10 mL/min for 60 min. Table 6-1 and Figure 6-S1 summarize the microgel diameters characterized by DLS, after treated with different trigger gases. The corresponding swelling ratios were estimated from on the diameters, e.g. the O_2-swelling ratio $\alpha_{O2} = (\frac{D_{O2}}{D_{N2}})^3$.

Table 6-1. Prepared P(DEA-*co*-FS) microgels and their gas-switchable properties

MGs	*Composition (DEA:FS, wt./wt.)*	D_{N2} [a] *(nm)*	*PDI*	O_2		CO_2	
				D_{O2} [b]	α_{O2} [c]	D_{CO2} [d]	α_{CO2} [e]
MG-F5	95:5	80	0.105	142	5.59	191	13.6
MG-F40	60:40	83	0.095	89	1.23	137	4.50
MG-F80	20:80	84	0.089	85	1.04	86	1.11

Note: [a, b, d] The hydrodynamic diameters of the microgels under N_2, O_2 and CO_2 treatment, respectively. [c,e] Swelling ratio of the microgels under O_2 and CO_2 treatment, defined as: $\mathbf{a_{O2}} = (\frac{D_{O2}}{D_{N2}})^3$ (same equation is applicable to "$\mathbf{a_{CO2}}$").

As shown in Table 6-1, the microgels having different FS contents gave distinct O_2- and CO_2- switchable properties, consistent with our previous studies.[33] P(DEA-*co*-FS) microgel containing 5 wt% FS (MG-F5) showed O_2 and CO_2 dual gas-switchability, with the hydrodynamic volume changed upon O_2 and CO_2 treatment, exhibiting swelling ratios of 5.59 and 13.6, respectively. Increasing the FS content to 40 wt% decreased the volume changes to α_{O2} = 1.23 and α_{CO2} = 4.5, due to inherent hydrophobicity of the fluorinated monomer FS. However, the microgel containing 80 wt% FS (MG-F80) almost lost its gas-switchable properties and acted as solid latex particles.

The hydrodynamic volume changes of P(DEA-*co*-FS) microgels upon O_2 and CO_2 treatments were due to interactions between the trigger gases and function groups in the microgels. CO_2 dissolved in aqueous solution induced protonation of the tertiary amine group in DEA and significantly increased the microgel hydrophilicity. The

dissolved O_2 molecules interacted with the fluorine atoms of FS through Van der Waals forces, which improved microgel hydrophilicity, facilitated water absorption and thus, promoted size expansion of the microgel upon trigger gas treatment.[29-30, 33] It should be noted that the size expansion induced by both O_2 and CO_2 could be recovered to their initial states by washing off the trigger gas with an inert gas (N_2) or heating.

6.4.2 Microgel-colloidosome preparation and purification

All the microgels were employed as building blocks for the preparation of microgel-colloidosomes (MGC) using microgel-stabilized oil-in-water (O/W) Pickering emulsions as templates. Figure 6-2 (a) schematically illustrates the MGC preparation procedure. Firstly, the O/W Pickering emulsion was prepared using an aqueous dispersion of the microgel (5 mg/mL) as water phase and PPGDGE-containing hexadecane as an oil phase (a-I). The oil phase fraction was fixed to 30 vol.% (based on total volume). During emulsification, the shear force of homogenization promoted migration of the microgel particles to oil/water interface, to minimize surface energy of the system, thus preventing the internal phase oil droplets from coalescence (a-II).

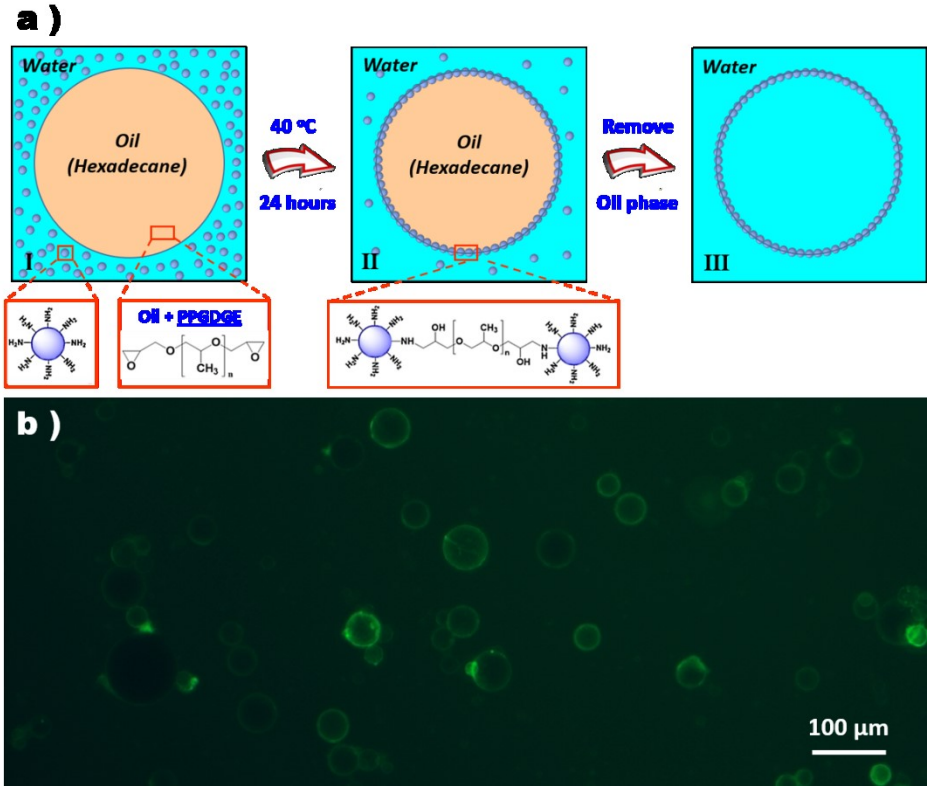

Figure 6-2. a) Schematic illustration of the microgel-colloidosome (MGC) preparation. b) Fluorescence microscope images of MGC-F5 cross-linked with 0.5 wt.% of PPGDGE. The microgel MG-F5 was labeled by fluorescence monomers.

In order to prepare robust MGCs and prevent them from disassembling during subsequent purification and control-release application, all the microgel particles were surface modified with amino group (-NH_2) by adding 3 wt% APMA (based on monomer mass) during the microgel preparation. PPGDGE containing epoxy end groups (-CH(-CH_2-O-)) inter-crosslinked the self-assembled microgel particles at the oil/water interface through amino–epoxy reaction, as illustrated in Figure 6-2 (a-II). The MGCs prepared in this work exhibited monolayer architecture. Since the microgel particles were dispersed in the continuous aqueous phase and the cross-linker

PPGDGE was dissolved in the internal oil core phase, the linking of adjacent microgel particles was realized through inter-microgel crosslinking, only occurred at the oil/water interphase, which avoided possible inter-droplet cross-linking or fusing. This amino-epoxy reaction has been well reported and it was easily realized at 40 ^{o}C for 24 hours.[1, 34] Such MG-MG cross-linking fixed the microgel particles on the oil/water interface, acting as a permeable microgel-shell for the MGC microcapsules, as illustrated in Figure 6-2 (a-II). It was worth to note that microgel without surface – NH_2 modification cannot be used as the building block for MGC preparation by using the same method. After preparation, the MGCs were purified by centrifuge to remove the supernatant, which contained excess microgel particles. The oil hexadecane core phase was extracted by washing with 10 times of ethanol/water (1:3) solution. This centrifuge-washing process was repeated for 5 cycles. The MGC was then dispersed in DI water to form the water-in-water microcapsules for subsequent uses, as shown in Figure 6-2 (a-III). The gas-switchable properties of the colloidal MGC shell enabled the regulation of shell permeability through O_2 and CO_2 treatment respectively.

Figure 6-2 (b) shows the fluorescence image for an aqueous dispersion of MGC-F5 cross-linked with 0.5 wt% PPGDGE (based on the microgel mass). The microgel particles labeled with fluorescein O-methacrylate (0.01 wt%) were inter-MG cross-linked, integrating the colloid shell of the MGCs and exhibiting green shell in the water-in-water structure. The mass content of PPGDGE cross-linker in MGC-F5 preparation varied from 0.5, 1.0 to 2.0 wt% (refer to Figure 6-S2). All the MGCs

remained intact after CO_2 treatment, with standing the maximum swelling of MGs. The change in size of MGC before and after CO_2 treatment was barely noticed. In order to minimize the effect of inter-microgel cross-linking on the gas-responsive properties, MGC-F5 cross-linked with 0.5 wt% PPGDGE was used in the following gas-triggered loading and control-release experiments.

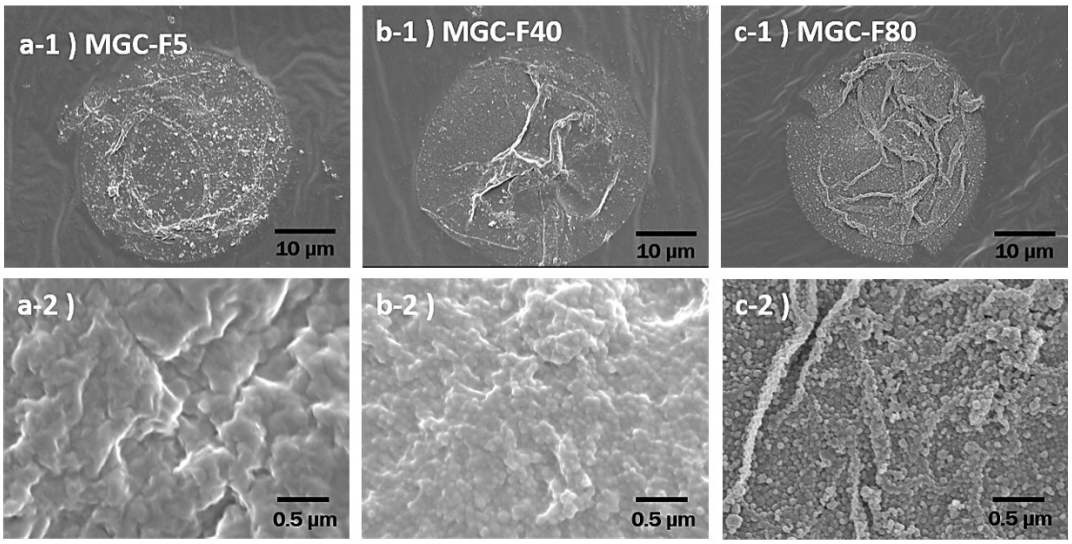

Figure 6-3. a) SEM images of MGCs prepared from P(DEA-*co*-FS) microgels with 5, 40 and 80 wt% FS content. a-1, 2) MGC-F5, FS = 5 wt%; b-1, 2) MGC-F40, FS = 40 wt%; 3) MGC-F80, FS = 80 wt%.

Figure 6-3 shows SEM images of the MGCs with 5, 40 and 80 wt.% FS content. The microgel particles in the MGC shell were cross-linked with 0.5 wt% PPGDGE. All three MGCs exhibited finely collapsed sphere structure. Figure 6-S3 shows a collection of MGC-F5, MGC-F40 and MGC-F80 microcapsules. The wrinkles were due to extraction of the core phase during SEM sample preparation, demonstrating elastic properties of the colloid shell. From the magnified SEM images, an increased degree of microgel

fusion was in the order of a-2), b-2) and c-2). This feature of morphology was attributed to the different chemical composition of the microgels. Microgel with higher FS fraction resulted in MGC with less surface microgel fusion.

6.4.3 O_2 and CO_2 dual gas-switchable control-release of MGC

6.4.3.1 Loading MGCs with cargo molecules

The MGCs prepared from different microgels were used as smart microcapsules for gas-triggered control-releases. The water soluble FITC–dextran (D1) and blue-dextran (D2) having different molecular weights and labeled with distinct fluorescences (D1: Mw=10 kDa, 485 nm; D2: Mw=2000 kDa, 630 nm) were selected as the model cargo molecules for the control-release experiments.

The first step in the control-release experiment was to load the cargo molecules into the MGC microcapsules. As schematically illustrated in Figure 6-3 a), the MGC was first dispersed in an aqueous mother solution containing 1 wt% of both D1 and D2 cargo molecules (a-I). The dispersion was then treated with CO_2 at 10 mL/min for about 2 hours, which facilitated the dextran molecules penetrate through MG shell into MGC (a-II). This permeation was driven by the difference of chemical potential between the continuous phase and the MGC core phase. Subsequently, the MGC was treated with N_2 for 1 hour to remove CO_2 and to lock the cargo molecules inside MGC microcapsules (a-III). Lastly, excess D1 and D2 in the mother solution or weakly attached on the MGC surface were removed through centrifuge and washing with degassed water for 3

cycles.

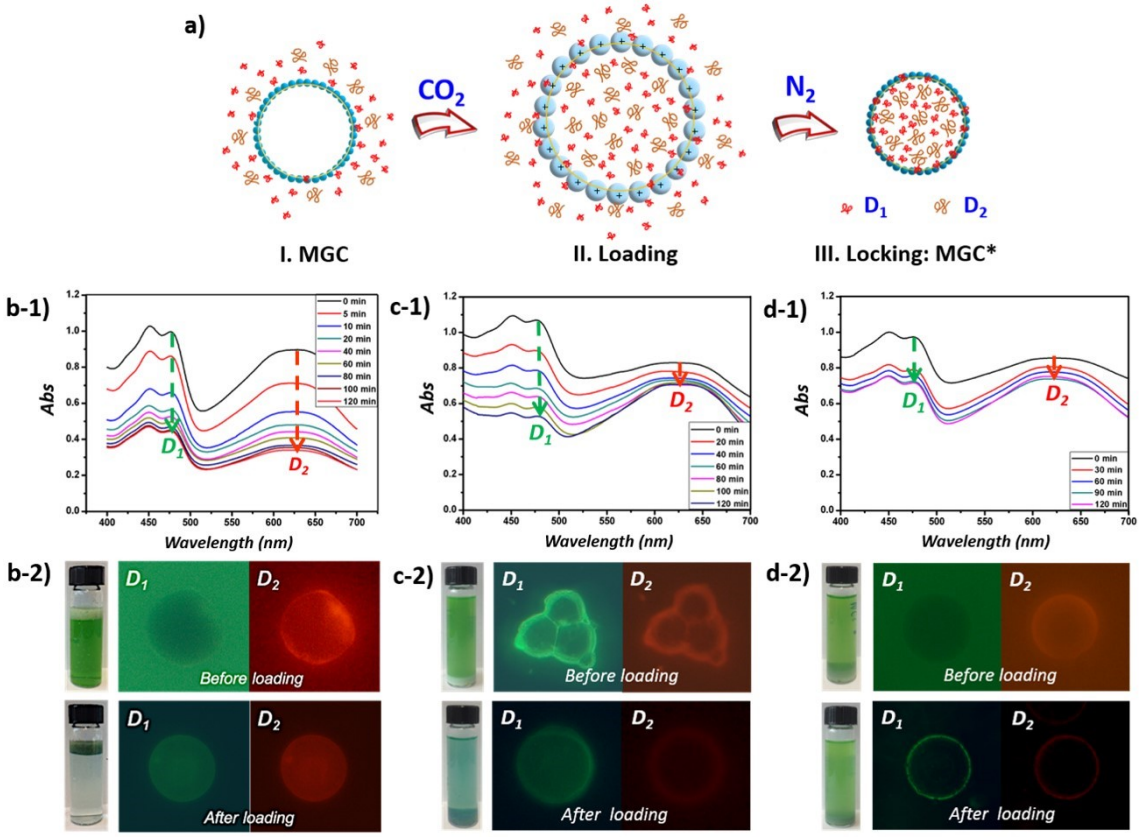

Figure 6-4. a) Schematic illustration of MGC loading-lock process with cargo molecules under CO_2 treatment. The loading and encapsulation process of MGC-F5 (b-1), MGC-F40 (c-1) and MGC-F80 (d-1) recorded by UV-vis spectrometer detection of D1 (485 nm) and D2 (630 nm) content in the mother solution. The photo and fluorescence images of MGC-F5 (b-2), MGC-F40 (c-2) and MGC-F80 (d-2) before and after D1 and D2 loading and encapsulation.

The cargo molecules D1 and D2 possessed UV-vis absorption at 485 and 630 nm, respectively. The loading and encapsulation process of MGC-F5 was recorded by monitoring D1 and D2 concentration in the mother solution through UV-vis spectrometer. The UV-vis absorption curves, as shown in Figure 6-4 b-1), suggested that both D1 and D2 concentrations decreased dramatically during the loading

process, with 56.12 wt% and 63.64 wt% loading efficiencies reached in less than 2 hours. The loading of cargo molecules into MGC-F5 microcapsule was also evident from the photo and fluorescence images in Figure 6-4 b-2). A dramatic color decrease of the mother solution from dark green before loading to barely transparent after loading could be observed in the photo images (left). The MGC-F5 layer float on the top of the aqueous solution turned from white before loading to dark green after loading. In the fluorescence images (right), the dark MGC microcapsule was surrounded by D1 (green) and D2 (red) molecules in the mother solution before loading, which migrated and penetrated into MGC-F5 microcapsule after loading, showing highlighted green and red color. The contraction of MGC-F5 after CO_2 removal concentrated D1 and D2 in the internal aqueous core phase.

The cargo molecules were also loaded into MGC-F40 and MGC-F80, as shown in Figure 6-4 c) and d). The loading efficiency for MGC-F40 reached 50.56 wt% and 14.91 wt% (Figure 6-4 c-1) in 2 hours for D1 and D2, respectively. For MGC-F80, the loading efficiency reached to the maximum of 25.58 % and 13.61 wt % (Figure 6-4 d-1) for D1 and D2 in 1.5 hours. Further extension to 2 hours did not increase the loading efficiency. As showed from the MGC-F80 loading fluorescence images (right) in Figure 6-4 d-2), highlighted green (D1) and red (D2) shells with dark internal cores were found both before and after MGC-F80 loading, no apparent color difference were found in the mother solution. Considering that MG-F80 was not gas-switchable (refer to Section 3.1 and Table 6-1), it was thought that D1 and D2 decreased from the

mother solution were not encapsulated in the core of MGC-F80, but load on the MGC surface. Assuming the same amount of the D1 and D2 were loading on the surface of MGC-F40, about 25 wt% D1 and 1.30 wt% D2 were encapsulated in MGC-F40. As shown in Figure 6 c-2), the photo images (left) exhibited a color transition from dark green to blue after loading of the cargo molecules. The D1 molecule (yellow color) penetrated into MGC-F40, leading to the yellow color (D1) extracted from the dark green mother solution (D1 and D2 mixture aqueous solution) and migrated to the MGC, left the blue D2 ingredient in the mother solution. This could be verified from the fluorescence images (right) which showed that the D1 molecule penetrated into MGC-F40, highlighted with green color after loading. There was no D2 (red) in the internal core of MGC-F40. Based on the same surface loading assumption, about 31 wt% (D1) and 49wt% (D2) encapsulation efficiencies were reached for MGC-F5 within 2 hours, respectively. Both D1 (green) and D2 (red) were found in the inner core of MGC-F5 after loading, as shown in the fluorescence image of Figure 6-4 b-2).

It was worth to clarify the difference between “loading efficiency” and “encapsulation efficiency” described above. The “loading efficiency” means “the D1 and D2 cargo molecules decreased from the mother solution were loaded both on the surface and inner core (encapsulate) of the MGC”, while “encapsulation efficiency” only referred to “the D1 and D2 encapsulated within the inner core of MGC”. It becomes then clear that D1 and D2 encapsulation was based on a size exclusion mechanism. Driven by the difference of concentrations in the mother solution and in inner core phase of MGCs,

the cargo molecules penetrated the MG-MG colloid shell. It was the swellbility of P(DEA-*co*-FS) microgels that regulated the permeability of MGC shell upon the treatment of trigger gas O_2 and CO_2. Depending on the copolymer composition, MGC-F5 encapsulated both D1 and D2; MGC-F40 encapsulte mainly D1 but little D2; MGC-F80 encapsulate no cargo molecules due to its lack of gas responsitivity.

6.4.3.2 Gas-triggered control-release of D1 and D2 cargo molecules loaded inside MGC-F5

MGC-F5 samples encapsulated with 31 wt% D1 and 49 wt% D2 (MGC-F5*) were employed to investigate the gas-triggered control-release properties of MGC-F5*. MGC-F5* microcapsules were divided into three equal aliquots and dispersed in 8 mL degassed DI water prior to the control-release test. The dispersion samples were bubbled with inert gas N_2, and trigger gases O_2 and CO_2, respectively. The D1 and D2 concentrations in the environment solution at different stages were monitored by UV-vis spectrometer at 485 nm (D1) and 630 nm (D2), as summarized in Figure 6-5.

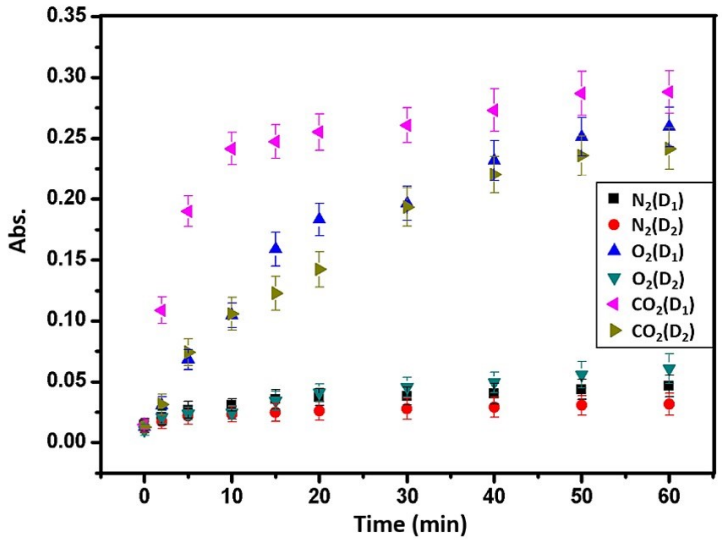

Figure 6-5. a) Gas-triggered MGC-F5* microcapsule releasing profile recorded by UV-vis spectrometer at 485 nm (D1) and 630 nm (D2).

As a control sample, MGC-F5* treated with N_2 for 60 min released very little D1 and D2, as seen from Figure 6-5. Distinct releases of the cargo molecules (D1 or/and D2) were clearly detected in the environment solutions, treated with trigger gas O_2 and CO_2, respectively. Treated with O_2, D1 started to release in 5 min, and a balance at 0.26 was reached in 60 min. In contrast, very little D_2 release (0.061) was detected, even after long time O_2 bubbling. This size exclusion based release was due to the shell permeability. The O_2-induced swelling of the microgels allowed penetration of the smaller D1 but not the larger D_2. Treating with CO_2 resulted in more severe swelling of the microgels and thus opened up the shell to allow both D1 and D2 release. It was noticed that D1 releases much faster at the early stage with 0.24 D1 achieved within the first 10 min. The maximum D1 release of 0.29 was reached in 60 min of CO_2 treatment. Compared to D1, D2 release was slower (0.22 in 40 min), with its maximum

concentration at 0.24 reached after 60 min CO_2 treatment. It was also found that a small content of D1 and D2 could be detected from the mother solution after the freshly prepared MGC-F5* sample was exposed to atmosphere and stored over long time (over weeks). This might be attributed to the absorption of CO_2 from open air, which gradually promoted the release of D1 and D2 from the MGC*.

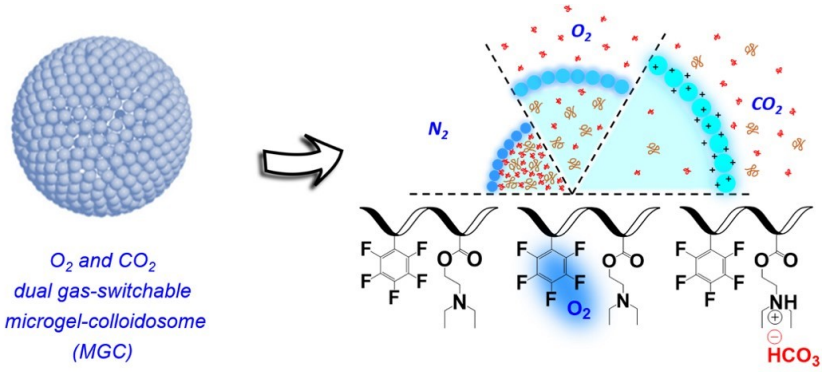

Figure 6-6. Schematic illustration of gas (O_2 and CO_2)-triggered hierarchical releases of MGC-F5* microcapsule encapsulated with water-soluble cargo molecules having different molecule weights.

As illustrated in Figure 6-6, it was found that O_2 only triggered the release of D1 from MGC-F5* microcapsule, while CO_2 was capable to induce the release of both D1 and D2. N_2 did not work as a gas-trigger. The hierarchical release profile of the cargo molecules was based on a size exclusion mechanism. O_2 and CO_2 could reversibly interact with the functional groups of P(DEA-*co*-FS) microgels (fluorine atoms and ternary amines, respectively), increasing hydrophilicity and induce microgel swelling.

§ 6.5 Conclusion

In conclusion, the microgel colloidosomes (MGC) with tunable shell permeability were prepared using O_2 and CO_2 dual-gas switchable P(DEA-*co*-FS) microgels, which were surface modified with amine groups (-NH_2). In MGC preparation, the microgel-stabilized oil-in-water Pickering emulsion was used as template with the adjacent microgel particles crosslinked by oil soluble PPGDEMA through amine-epoxy reaction. The MGC was purified by washing off excess microgel particles and by extraction of the oil core phase. The successful encapsulation of dextran cargo molecules having different sizes (molecule weight: 10 and 2000 kDa) into MGC-F5 was demonstrated, with the shell permeability maximized by CO_2-induced swelling of the microgels. Removing CO_2 trigger gas led to contraction of the MGC and locking of cargo molecules inside. Treated MGC-F5* with O_2 and CO_2 respectively, a hierarchical release profile of D_1 and D_2 was observed. The release was based on a size exclusion mechanism. The switchability of the microgels upon O_2 and CO_2 treatment resulted distinct shell permeabilities to release D_1 and D_2 hierarchically from MGC-F5*. Such gas-switchable MGC microcapsules with tunable shell permeability are promising for control-release of multiple ingredients.

§ 6.6 References

[1] Cayre, O. J.; Hitchcock, J.; Manga, M. S.; Fincham, S.; Simoes, A.; Williams, R. A.; Biggs, S., *Soft Matter* **2012**, 8 (17), 4717-4724.

[2] Yow, H. N.; Routh, A. F., *Soft Matter* **2006**, 2 (11), 940-949.

[3] Xu, J.; Li, J.; Yang, Y.; Wang, K.; Xu, N.; Li, J.; Liang, R.; Shen, L.; Xie, X.; Tao, J.; Zhu, J., *Angewandte Chemie* **2016**, 55 (47), 14633–14637.

[4] Tiarks, F.; Landfester, K.; Antonietti, M., *Langmuir* **2001**, 17, 908-918.

[5] Bouchemal, K.; Briançon, S.; Perrier, E.; Fessi, H.; Bonnet, I.; Zydowicz, N., *International Journal of Pharmaceutics* **2004**, 269 (1), 89-100.

[6] Caruso, F.; Caruso, R. A.; Mohwald, H., *Science* **1998**, 282, 111-114.

[7] Donath, E.; Sukhorukov, G. B.; Frank Caruso; Davis, S. A.; Möhwald, H., *Angew. Chem. Int. Ed.* **1998**, 37, 2201-2205.

[8] Decher, G., *Science* **1997**, 277, 1232-1237.

[9] Thompson, K. L.; Williams, M.; Armes, S. P., *Journal of colloid and interface science* **2015**, 447, 217-228.

[10] Dinsmore, A. D.; Hsu, M. F.; M. G. Nikolaides; Marquez, M.; Bausch, A. R.; Weitz, D. A., *Science* **2002**, 298, 1006-1009.

[11] Wang, W.; Milani, A. H.; Carney, L.; Yan, J.; Cui, Z.; Thaiboonrod, S.; Saunders, B. R., *Chemical communications* **2015**, 51 (18), 3854-3857.

[12] Morse, A. J.; Madsen, J.; Growney, D. J.; Armes, S. P.; Mills, P.; Swart, R., *Langmuir* **2014**, 30 (42), 12509-12519.

[13] Berger, S.; Zhang, H.; Pich, A., *Advanced Functional Materials* **2009**, 19 (4), 554-559.

[14] Shah, R. K.; Kim, J. W.; Weitz, D. A., *Langmuir* **2010**, 26 (3), 1561-1565.

[15] Sander, J. S.; Studart, A. R., *Langmuir* **2013**, 29 (49), 15168-15173.

[16] Thompson, K. L.; Armes, S. P.; Howse, J. R.; Ebbens, S.; Ahmad, I.; Zaidi, J. H.; York, D. W.; Burdis, J. A., *Macromolecules* **2010**, 43 (24), 10466-10474.

[17] Cayre, O. J.; Noble, P. F.; Paunov, V. N., *Journal of Materials Chemistry* **2004**, 14 (22), 3351-3355.

[18] Liu, D.; Zhou, F.; Li, C.; Zhang, T.; Zhang, H.; Cai, W.; Li, Y., *Angewandte Chemie* **2015**, 54 (33), 9596-9600.

[19] Duan, H.; Wang, D.; Sobal, N. S.; Giersig, M.; Kurth, D. G.; Mohwald, H., *Nano Lett.*, **2005**, 5 (5), 949-952.

[20] Zhu, H.; Zhang, Q.; Zhu, S., *Advanced Materials Interfaces* **2016**, 3 (18), 1600294.

[21] Tamate, R.; Ueki, T.; Yoshida, R., *Angewandte Chemie* **2016**, 55 (17), 5179-5183.

[22] Romero-Cano, M. S.; Vincent, B., *Journal of Controlled Release* **2002**, 82, 127-135.

[23] Sander, J. S.; Studart, A. R., *Soft Matter* **2014**, 10 (1), 60-68.

[24] Han, D.; Tong, X.; Boissière, O.; Zhao, Y., *ACS Macro Letters* **2012**, 1 (1), 57-61.

[25] Yan, Q.; Zhao, Y., *Chemical communications* **2014**, 50 (79), 11631-11641.

[26] Liu, Y.; Jessop, P. G.; Cunningham, M.; Eckert, C. A.; Liotta, C. L., *Science* **2006**, 313, 958-960.

[27] Zhang, Q.; Wang, W.-J.; Lu, Y.; Li, B.-G.; Zhu, S., *Macromolecules* **2011**, 44 (16), 6539-6545.

[28] Liu, H.; Lin, S.; Feng, Y.; Theato, P., *Polym. Chem.* **2017**, 8, 12-23.

[29] Lei, L.; Zhang, Q.; Shi, S.; Zhu, S., *ACS Macro Letters* **2016**, 828-832.

[30] Lei, L.; Zhang, Q.; Shi, S.; Zhu, S., *Polym. Chem*. **2016**, 7 (34), 5456-5462.

[31] Choi, J. Y.; Kim, J. Y.; Moon, H. J.; Park, M. H.; Jeong, B., *Macromolecular rapid communications* **2014**, 35 (1), 66-70.

[32] Zhang, Q.; Zhu, S., *Macromolecular rapid communications* **2014**, 35 (19), 1692-1696.

[33] Lei, L.; Zhang, Q.; Shi, S.; Zhu, S., *Langmuir* **2015**, 31 (7), 2196-2201.

[34] Acocella, M. R.; Corcione, C. E.; Giuri, A.; Maggio, M.; Maffezzoli, A.; Guerra, G., *RSC Adv.* **2016**, 6 (28), 23858-23865.

§ 6.7 Supporting information

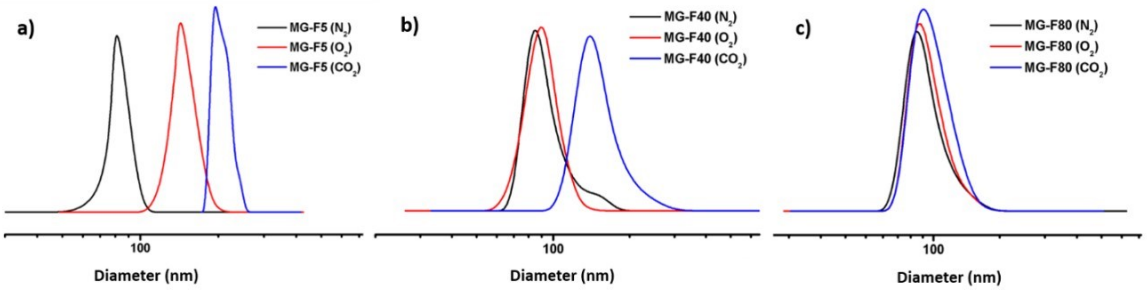

Figure 6-S1. Dynamic light scattering (DLS) characterization of the gas (O2 and CO2)-switchable hydrodynamic size for P(DEA-co-FS) microgels with different FS content. a) MG-F5 (FS = 5 wt%), b) MG-F40 (FS = 40 wt%), c) MG-F80 (FS = 80 wt%).

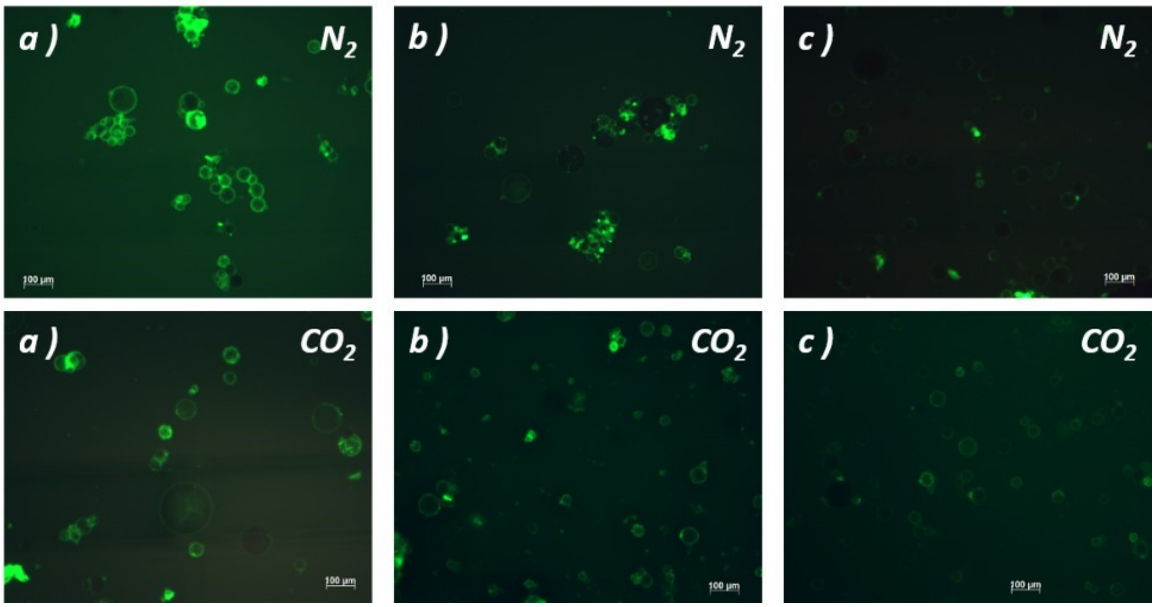

Figure 6-S2. Fluorescence microscope images of the microgel-colloidosomes (MGC-F5) with 0.5, 1.0 and 2.0 wt% PPGDEG (based on microgel mass) for inter microgel (MG-MG) cross-linking: before (N_2) and after CO_2 treatment.

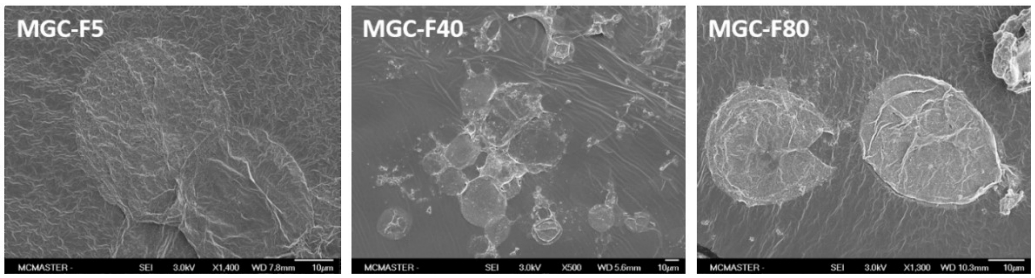

Figure 6-S3. SEM image of MGC-F5, MGC-F40 and MGC-F80.

7 CO_2-SWITCHABLE MEMBRANES USED FOR OIL/WATER SEPARATION

This chapter reports the generation of highly porous membrane with "open-cell" structure and CO_2-switchable surface wettability and their application on CO_2-controlled oil/water separation. This work is reproduced from a newly prepared manuscript of "Highly porous poly(high internal phase emulsion) membranes with "open-cell" structure and CO_2-switchable wettability used for controlled oil/water separation". The combination of stimuli-responsive functionality and novel macrostructure enable promising applications in the areas of control-release, smart separation, tissue engineering and so on.

Author contributions

The idea of this work is generated from the discussion with Dr. Qi Zhang. Lei Lei did all the experiments and prepared the first manuscript under the supervision of Dr.

Shiping Zhu. Dr. Zhang and Dr. Shuxian Shi provided valuable discussion and first revision of the manuscript. Dr. Zhu did the final revision before submission.

§ 7.1 Abstract

Polymer membranes with switchable wettability have promising applications in smart separation. Hereby, we report highly porous poly(styrene-co-N,N-diethylaminoethyl methacrylate) (i.e., poly(St-co-DEA)) membranes with "open-cell" structure and CO_2-switchable wettability prepared from water-in-oil (W/O) high internal phase emulsion (HIPE) templates. The "open-cell" porous structure facilitates fluid penetration through the membranes. The combination of CO_2-switchable functionality and porous microstructure enable the membrane with CO_2-switchable wettability from hydrophobic or superoleophilic to hydrophilic or superoleophobic through CO_2 treatment in an aqueous system. This type of membranes can be used for gravity-driven CO_2-controlled oil/water separation, in which oil selectively penetrates through the membrane and separates from water. After treated with CO_2 switching wettability of the membrane, a reversed separation of water from oil can be achieved. Such wettability switch is fully reversible and the membrane could be regenerated through simply removal of CO_2 and oil residual through drying. This facile and cost effective approach represents the development of first CO_2-switchable polyHIPE system, promising for smart separation in large volume.

§ 7.2 Introduction

Fresh water is very precious since 97% of the water on earth is inedible salt water, and one in four people in the world are suffering from safe water shortage. Organic liquid (oil) often contaminates water and separating oil for water is thus important for water purification and regeneration.[1] In general, oil/water separation can be classified as oil-removing, water-removing, and smart controllable separation.[2,3] Stimuli-responsive membranes with tunable wettability are promising for various applications such as oil/water separation,[2,4–7] anti-fouling,[8–10] cell capture and release,[11] and so on. The surface wettability of these advanced membranes is an important factor in the applications, which could be regulated by changing chemical composition and surface structure of the substance.[2,7,12,13]

By incorporating functional monomers and components, the physiochemical properties of membranes, such as surface microstructure and wettability, could be precisely manipulated through treating the membrane with an external stimulus like pH,[2,14] thermo,[7,14] electric-field,[15] and UV,[6,16] for on-off switching. For example, thermo and pH dual-controllable oil/water separation material has been reported by Cao et al.,[14] in which poly(dimethylaminoethyl methacrylate) (PDMAEMA) was coated on a steel mesh through light-initiated free radical polymerization. Due to the double responsiveness of PDMAEMA, water could pass through the mesh and be separated from the water/oil mixture at temperature below 55 ^{o}C and pH lower than 13. Otherwise, oil could permeate through and be collected. However, heating the

system is energy and time consuming and it is particularly true for large volume separation operation with limited heat transfer rates. The often-used pH regulation might also cause secondary contamination by acid and base addition. Recently, carbon dioxide (CO_2) has been widely reported as an abundant "green" gaseous stimulus,[17–19] which has been applied to various smart systems including redispersible latexes,[16,19] "breathable" microgels,[21,22] block polymer self-assembling and shape/morphology deformations.[23] Such stimuli-responsive features are attributed to the reversible reactions of CO_2 with such functional groups as amines, guanidines and amidines in aqueous solution, which regulate hydrophobicity/polarity properties without contamination.[23,24]

Surface structure (geometry and roughness) is another critical factor that affects fabrication of smart surfaces with specific wetting properties, as described by Wenzel model and Cassie-Baxter (C-B model).[12,25–27] Wenzel model reveals that surface roughness could enhance both wetting and anti-wetting properties of liquid on the surface.[25] C-B model extended Wenzel's analysis to porous surfaces and suggested that air trapped in porous roughness could facilitate preparation of anti-wetting surfaces.[26] The development of nanotechnology, polymer science and interfacial engineering provide a wide range of methods and technologies to prepare fibrous and porous membranes. For example, Che et al.[4] reported poly(methylmethacrylate-co-N,N-diethylamino ethylmethacrylate) (i.e., PMMA-co-PDEAEMA) nanofiberous membranes prepared from electro-spinning, a broadly used technology in fiber

production. Fibers with diameter ranged from nanometer to several micrometers could be drawn from polymer solutions and melts.[28,29] The wettability of membrane could be switched between hydrophilic and lipophilic by applying and removing CO_2 trigger. The combined nanoporous structure and CO_2-switchbility enable the membranes successful oil/water on-off separation. Using the same technology, Li et al.[2] deposited poly(methyl methacrylate)-b-poly(4-vinylpyridine) (i.e., PMMA-b-P4VP) block copolymer on a metal mesh and prepared pH-responsive fiber membranes. P4VP gave the membranes with pH-switchable surface wettability while PMMA provided mechanical strength and stability. The as-prepared membranes enabled highly efficient and reversible gravity-driven pH-controllable oil/water separation.

Compared to the fibrous membranes consisting of perpendicularly arranged fibers forming a network, porous membranes provide outstanding three-dimensional mechanical strength and stability against liquid flow and exhibit higher filtration efficiencies due to their irregular pore path.[5,30–32] High internal phase emulsion (HIPE) is an unique emulsion system consisting of more than 74 vol.% internal phase.[33,34] Highly porous materials could be obtained by curing or polymerizing continuous phase and extracting internal phase out of the emulsion, known as polyHIPE.[33,35–39] Based on morphology of the porous structure, polyHIPE could be classified as "open-cell" and "closed-cell", depending whether there are interconnected channels (aka, "windows") in/between the pores ("rooms").[40] The

porous morphology originated from the dispersed phase can be regulated by changing surfactant type and concentration, monomer composition, oil/water phase ratio, and so on.[33–37,40–42] Compared to electro-spinning membranes, polyHIPE is facile in preparation. HIPEs could be easily processed under ambient conditions and "cured" into complex shapes (e.g. monoliths, membranes and beads) by casting in template moulds and polymerization under mild conditions.[32–35,39] Jing et al.[43] prepared open-cell porous polystyrene (PS) monolith templates from water-in-styrene HIPEs. This ultra-low density monolith could reversibly absorb and release (squeezed out) spilled organic liquid (e.g. mineral oil and dichloromethane) from water, which is promising for purification of oil contamination. Polystyrene HIPE with both closed-cell and open-cell porous structures have also been reported by Yu et al.[5] The open-cell polyHIPE products are highly gas permeable due to their interconnected porous structure. The closed-cell polyHIPE was used for reversible absorption separation of oil from water, exhibiting a higher dichloromethane (CH_2Cl_2) absorption capacity (33 g/g) than its open-cell electro-spinning counterpart (20.21 g/g).[43] It is believed that the closed-cell structure helps to hold more organic phase, but may restrict the rate of absorption, which took about 1 min to reach its maximum capacity.[5]

Oil/water separation has been realized by either filtration separation or absorption separation. Fibrous membranes are often used for filtration separation while porous materials are used for absorption separation.[2–6,14,16] Filtration separations are more

applicable for continuous oil-water separation operation. Porous membranes are rarely used for liquid filtration separation due to a high pressure drop issue.[16] This work reports a facile method for fabrication of highly porous membranes with "open-cell" structure and CO_2-switchable wettability. Such poly(styrene-co-N, N-diethylaminoethyl methacrylate) (i.e., poly(St-co-DEA)) HIPE membranes are prepared from polymerizing the continuous oil phase of W/O high internal phase emulsion templates and extracting the dispersed aqueous phase. The "open-cell" porous structure enables fluid penetration through the membranes. The combined CO_2-switchable functionality and microporous "open-cell" structure provide the membranes with CO_2-switchable wettability between hydrophobic or superoleophilic and hydrophilic or superoleophobic. Such membranes could be used for reversible CO_2-controlled oil/water separation. This work represents the first CO_2-switchable polyHIPE system, which is cost-effective for the preparation of large volume porous separation device with consistent porous quality and switchable wettability.

§ 7.3 Experiments and Characterization

7.3.1 Materials

Styrene (St, 99%, Aldrich), 2-(diethylamino)ethyl methacrylate (DEA, 99%, Aldrich) and divinylbenzene (DVB, 80%, Aldrich) were passed through an inhibitor remover column (Aldrich) and stored at 4 ^oC prior to use. Span 80, calcium chloride ($CaCl_2$, Aldrich) and potassium persulfate (KPS) were purchased from Aldrich and used as

received. Ethanol (95%), hexane (95%) and chloroform (99.5%) purchased from Caledon Laboratory Chemicals are used as received. Milli-Q grade water was generated from Barnstead Nanopure Diamond system and used for all aqueous solution/phase preparation.

7.3.2 Experiments

7.3.2.1 Preparation of poly(St-*co*-DEA)-HIPE

All polyHIPE membranes were prepared from polymerization of the water-in-oil (W/O) HIPEs. Take poly(St-*co*-DEA)-HIPE with 30 wt.% DEA content (based on total monomer and cross-linker mass) as an example. The oil phase was prepared by adding St (2.4 g), DEA (1.2 g), DVB (0.4 g) and Span-80 (1.4g, 35 wt.%) into a 50 mL plastic (polypropylene) tube. The water solution (36 mL, 90 vol.%) of KPS (0.08 g) and $CaCl_2$ (0.4 g) was degased with N_2 for 30 min. HIPE was prepared by homogenizing the oil phase at 20000 rpm, during which the aqueous phase was slowly added by syringe within 5 min. Homogenization was continued for another 2 min after the complete addition of water phase. The freshly prepared HIPE was casted in a homemade Teflon membrane model (diameter "D" = 50 mm, thickness "d" = 0.5) and closed. The model was then cured in an oven at 70 ^{o}C for 48 hours to complete the polymerization, resulting in a white solid polyHIPE membrane. The membrane was washed in Soxhlet apparatus with ethanol for 48 hours to remove the residual monomer and surfactant, and dried in vacuum overnight at room temperature.

7.3.2.2 CO_2-switchable oil-water separation

PolyHIPE membranes with 30 wt.% DEA content were used for CO_2-controlled oil/water separation. The membrane was trimmed into a circular shape with diameter about 47 mm and it was then fixed on to a filtration apparatus (Synthware Glass). A metal mesh was applied to support the membrane during filtration. Dry membrane and CO_2-treated membrane were used for the filtration of hexane/water and chloroform/water, respectively. Specifically, the membrane was first thoroughly dried and it was then immersed into H_2O for CO_2 treatment (bubbling). A mixture of 100 mL water and 100 mL oil (hexane or chloroform) was dumped onto the upside glass apparatus for oil/water filtration separation. After each use, the membrane was dried or treated with CO_2 for another cycle of use.

7.3.3 Characterization

The morphology of polyHIPE membranes was characterized by SEM. Each sample was coated with 5 nm of platinum prior for observation. The sizes of pores and cells and windows were counted and evaluated with the software Image J. The membrane wettability was characterized by an optical contact angle measurement instrument. Specifically, for waster contact angle measurement, 2 μL of DI water or CO_2-saturated DI water was applied to the sample in air and measured after 90s stable. Hexane was used for oil contact angle measurements, following the same procedure for water contact angle (WCA) testing. Specifically for underwater oil contact angle test, the membrane was immersed in water and treated with CO_2 before text. Oil (henxane)

droplet was extruded from the needle and attached the membrane surface for measurement. The static contact angle was the average value for three measurements at three different positions of the sample.

§ 7.4 Results and Discussion

7.4.1 Poly(St-co-DEA)-HIPE membrane preparation and surface morphology characterization

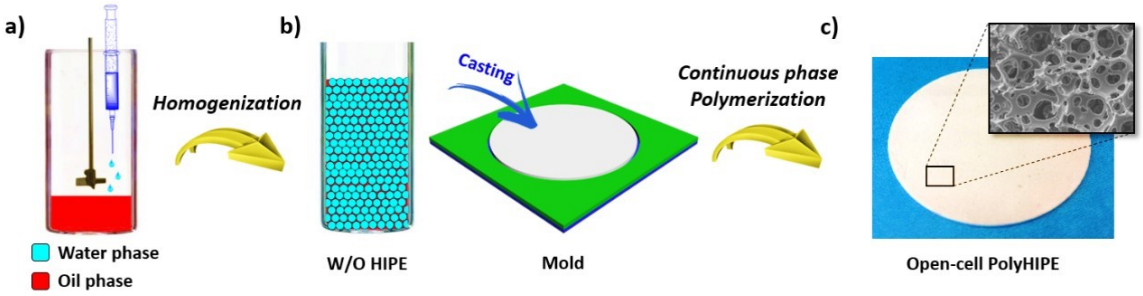

Figure 7-1. Synthetic illustration of poly(St-*co*-DEA)-HIPE membrane preparation. a) Water phase was added to system during oil phase homogenization for W/O HIPE preparation. b) The readily prepared HIPE was casted into a homemade membrane mold. c) Highly porous polyHIPE membrane with open-cell morphology was prepared by polymerizing the continuous phase of W/O HIPE.

7.4.1.1 PolyHIPE membrane preparation

The poly(St-*co*-DEA)-HIPE membranes with different DEA compositions were prepared from the water-in-oil (W/O) high internal phase emulsion (HIPE) template. The dispersed aqueous phase served as porogen, while the continuous oil phase including monomers is responsible for construction of the membrane frame-

work.[34,40,42] Figure 7-1 illustrates the process of highly porous polyHIPE membrane preparation. The oil phase contained monomers (DEA and St), cross-linker (DVB) and oil-soluble surfactant (Span-80). Specifically, St was used as a substrate monomer to provide the membrane with mechanical strength. DEA as CO_2-switchable monomer enabled the membrane with CO_2-switchable wettability.[17,23] As a classic oil soluble cross-linker, DVB copolymerized with St provided the membrane enough mechanical strength and prevented the membrane from dissolving in organic solvents. Oil-soluble Span-80 was used as surfactant to stabilize W/O HIPE. The aqueous phase volume fraction was fixed at 90 vol% and dissolved with thermal initiator $K_2S_2O_8$ and assistant stabilizer $CaCl_2$. For HIPE preparation, water phase was gradually added to the system during oil phase homogenization (Figure7-1a). The viscosity of the emulsion system increased dramatically as the aqueous phase was continuously added, suggesting the formation of HIPE. The readily prepared cream-gel like HIPE was casted into a homemade model (Figure7-1b) and cured by polymerizing the continuous oil phase of W/O HIPE at 80 ^oC. Poly(St-*co*-DEA)-HIPE membranes with varying compositions were fabricated and purified by washing the residual monomers and surfactants off with ethanol in Soxhlet apparatus, and vacuum-dried overnight at room temperature (Figure7-1c).

7.4.1.1 PolyHIPE porous structure characterization as function of chemical compostion

The morphology of poly(St-*co*-DEA)-HIPE membranes was characterized by SEM, as shown in Figure 7-2. Highly hierarchical porous membranes with "open-cell" structure were generated. The polymerization of monomer phase formed skeleton of the membrane. The first level of polyHIPE porosity, named "cell", was inherited from the porogen of water phase, which constructed the microcellular structure, as highlighted by the red cycle in Figure 7-2 (c-1). The interconnected "windows" between adjacent cells represent the second level of porosity, marked as yellow cycles, was caused by the volume contraction from monomer to polymer conversion, which induced thin film rapture between the adjacent emulsion droplets.[35,39] The diameters of cells and windows are denoted as "D" and "d", respectively. The surface ratio between windows and cells is defined as the "openness" of polyHIPE, which is critical for evaluation of consistent mass transfer through polyHIPE.

Table 7-1. Poly(St-*co*-DEA)-HIPE membrane preparation and characterization

Runs [a]	Recipe [b]		PolyHIPE morphology [c]				WCA [d]	
	St (g)	**DEA** (g)	**D** (μm)	**d** (μm)	**n**	**O (%)**	**Air**	**CO_2**
M10	3.2	0.4	4.82	1.42	7	35.08	152	22
M20	2.8	0.8	4.36	1.21	8	35.57	134	10
M30	2.4	1.2	4.21	1.17	9	40.13	126	0
M45	1.8	1.8	3.54	0.87	7	24.41	105	0

Note: [a] Name of the membranes, "M" represents "membrane", with the number indicating DEA content. e.g. "M10" refers to polyHIPE membrane with 10wt.% DEA based on the total mass of monomer and cross-linker. [b] Monomer composition for poly(St-*co*-DEA)-HIPE preparation. The oil phase includes St, DEA, DVB (0.4 g) and Span-80 (1.4 g, 35 wt.%). Water phase contains $K_2S_2O_8$ (0.08 g), $CaCl_2$ (0.4 g), H_2O (36 mL). [c] SEM characterization of polyHIPE membrane morphology: "D", cell diameter; "d", window diameter; "N", estimated number of windows in

each cell from "$N = n \cdot 2 \cdot \frac{2}{\sqrt{3}}$", in which "n" accounts for the average apparent number of windows counted in each cell;[39] "O", openness of the membrane, denoted as the ratio between window area and cell surface area as "$O = \frac{S_o}{S_c} = \frac{N \cdot S_w}{S_c} = \frac{N}{4} \cdot \frac{d^2}{D^2} = \frac{n}{\sqrt{3}} \cdot \frac{d^2}{D^2}$".[39] d CO_2-switchable water contact angle tested with DI water (air) or CO_2 saturated DI water in air condition.

Figure 7-2 presents SEM images of polyHIPE membrane samples composing different DEA contents. Their precursor HIPEs were stabilized with 35 wt% surfactant (Span-80) based on monomer (St/DEA) and cross-linker mass (DVB). As summarized in Table 7-1, it was found that both sizes of cells "D" and windows "d" decreased from 4.82 to 3.54 μm and 1.42 to 0.87 μm, respectively, as DEA content increased from 10 to 45 wt%. The average apparent number of windows "n" in each cell slightly increased from 7 to 9 as DEA content increased from 10 to 30 wt%. When DEA content continued to increase to 45 wt% in M45, about 7 apparent windows were found in each cell. Further increase in DEA caused cells collapsing and dramatically decreasing the window size. As seen from the cross-section crackles and surface roughness of the cells and windows, the rigidity of the membranes decreased as St component substituted by DEA. At the same time, the elasticity or softness of the membrane increased since more shrinks were generated around the windows where rupture of the film happened. On the other side, since the "open-cell" structure was required for mass transfer through the membrane, the area ratio of window and cell, defined as "openness", is critical to evaluate the mass transfer efficiency. As evaluated in Table 7-1, PolyHIPE with 30 wt% DEA content (M30) showed the highest openness of 40.13

%, suggesting that nearly half of the cells was open for mass transfer, which is promising for filtration separation.

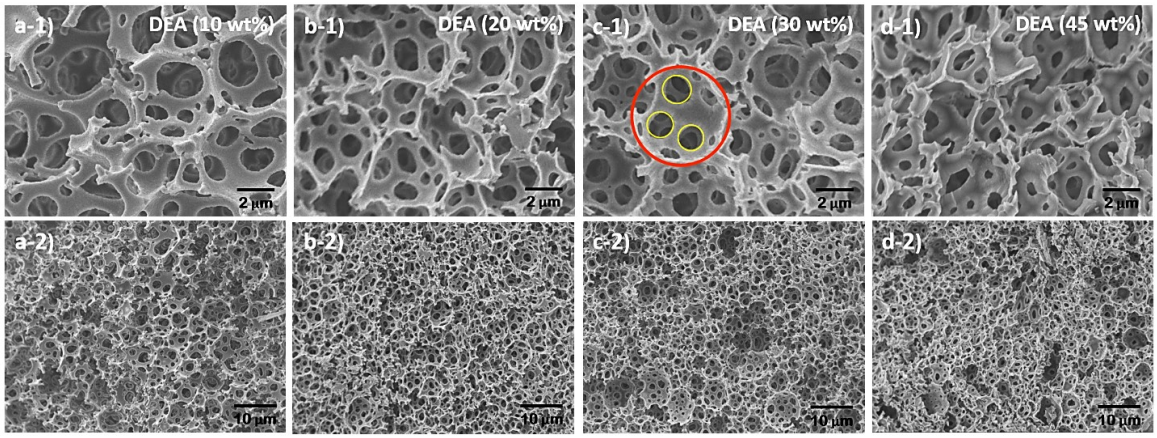

Figure 7-2. SEM images of poly(St-*co*-DEA)HIPE membranes composing different DEA contents. a-1,2) 10 wt%, b-1,2) 20 wt%, c-1,2) 30 wt%, d-1,2) 45 wt%.

PolyHIPE membranes prepared from 20 wt.% Span-80 stabilized HIPE were also presented as SEM images and characterization summarized in Figure 7-S1 and Table 7-S1, respectively. Large cavities could be found among the membranes, which might cause damage or defect during filtration separation. This was caused by the coalescence of emulsion droplets before or during HIPE curing, because less surfactant would decrease the stability of HIPE system.

7.4.2 CO_2-switchable wettability of polyHIPE membrane

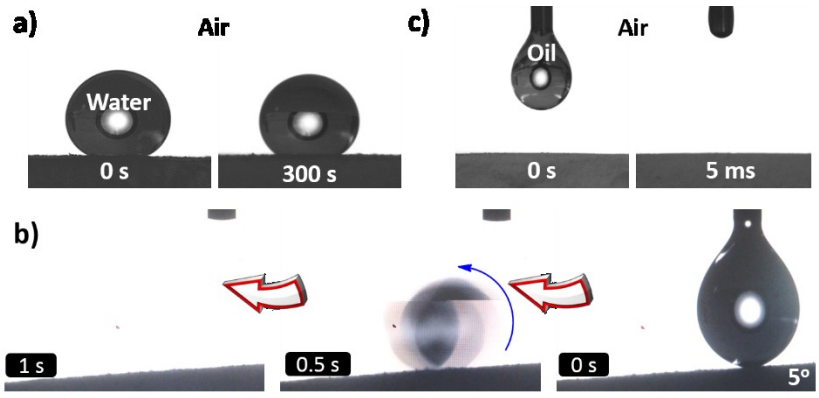

Figure 7-3. Contact angle measurement of P(St-*co*-DEA)-HIPE membrane, M10. a) WCA of 152° on the membrane surface at 0 and 300 second. b) The tumble process of water droplet at membrane surface at 5°. c) OCA at 0 and 5 ms, oil droplet immediately spread out on the membrane surface. As seen from video 7-S1.

The surface wettability of the membranes is determined by their chemical composition and geometry structure.[2,7,13] To probe the wettability of poly(St-co-DEA)-HIPE membranes, the water contact angle (WCA) was firstly measured in air. It was found that such highly porous membranes exhibited significantly higher WCA compared to their smooth film counterparts. As shown in Figure 7-3a, the membrane composing 10 wt% DEA (M10) was able to stand a spherical kindred water droplet with WCA of 152°. The WCA did not change even after 5 min, despite reduced droplet size due to water evaporation, suggesting that surface wettability of the membrane was very stable. Even under enforced attachment, the water droplet could be easily detached from the membrane. Furthermore, the water droplet could roll away with a sliding angle of less than 5° (Figure 7-3b and Video 7-S1). All these observations suggested superhydrophobicity of the membrane M10, even though both PS and PDEA have intrinsic WCA close or less than 90°.[44] This could be caused by the densely

3D microporous surface structure of the membrane, since the roughness geometry structure is the key consideration in construction of superhydrophobic surfaces, as described by C–B model.[2,3,26] Specifically, air trapped in the microporous membrane surface could dramatically reduce the contact area with water droplet, which increased repellency of the membrane against water droplets.

The oil wettability of the membrane was tested through oil (hexane) contact angle (OCA) measurement, as shown in Figure 7-3c. It was found that the oil droplet penetrated into the membrane, as soon as it attached the membrane surface, indicating the membrane was superlyophilic under air condition. The high affinity of the membrane toward oil was mainly caused by low surface tension of the oil and surface feature of the membrane. Specifically, PS and PDEA possessed surface energies of 40.7 and 33.7 mJ/m^2, respectively, much higher than the surface tension of hexane (18.43 mN/m).[45,46] Such surface enrichment components endowed the membrane high affinity to oil and oleophilicity. 3D microporous surface geometry also facilitated the oil affinity. Thus, both surface enrichment and microporous structure offered the membrane with great oleophilicity.[2,3]

Chemical composition is another factor that affects water wettability of polyHIPE membranes, as reflected from WCA values under DI water (air) summarized in Table 7-1. The difference in dimension of microporous structure for all the membranes was neglected here. As DEA component increased to 10, 20, 30 and 45 wt%, WCA of the

membrane decreased to 152, 134, 126 and 105, respectively. This was due to that PDEA had higher surface energy than PS and water (72 nN/m), the membrane with higher DEA content had more surface enrichment, which gave the membrane affinity to water. Furthermore, all the membranes exhibited great affinity to hexane. The oil droplet penetrated into the membrane immediately upon contact with membrane. Both surface energy enrichment and microporous structure resulted in the superlolephilicity of polyHIPE membranes.

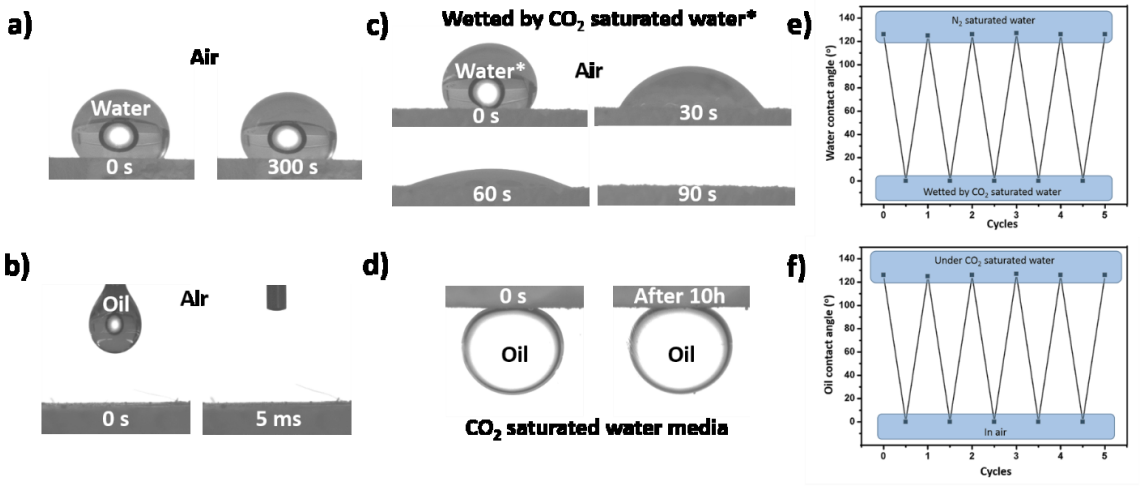

Figure 7-4. Contact angle measurement of P(St-*co*-DEA)-HIPE membrane M30. a) Image of the natural water contact angle at 0 and 300 seconds in air. b) Oil (hexane) contact angle at 0 and 0.5 ms in air. c) CO_2-saturated water contact angle at 0, 30, 60 and 90 second in air. d) Oil (hexane) contact angle under CO_2-saturated water. e) CO_2-induced reversible water wettability of the membrane between hydrophobic and superhydrophilic. f) CO_2-induced reversible oil wettability of the membrane between superoleophilic and underwater superoleophobic.

PDEA in poly(St-*co*-DEA)-HIPE membrane is a weak polybase with pKa about 7.3.[47] The wettability of PDEA-based membrane could be altered by manipulating CO_2-aqueous environment of the membrane, as a consequence for protonating and

deprotonating the tertiary amine group of DEA component.[4] PolyHIPE membrane with 30 wt% DEA (M30) was used to demonstrate CO_2-switchable membrane wettability toward water and oil in air. As presented in Figure 7-4a, water droplet with WCA of 126° was initially formed on top of the membrane, which did not change even after 5 min standing, despite a decrease in droplet size caused by water evaporation. However, oil (hexane) droplet would instantaneously penetrate into the membrane upon contact (Figure 7-4b). This super oil (hexane) affinity of the membrane was resulted from both surface energy and surface morphology of the membrane.

It is worth to note that wettability of the membrane M30 toward water and oil could be switched from hydrophobic or superoleophilic to hydrophilic or underwater susperoleophobic using CO_2-saturated water droplet or media. As shown in Figure 7-4c, CO_2-saturated water droplet could gradually spread out and wet the membrane surface within 90s. In this case, PDEA component of the membrane could be protonated when CO_2-saturated water was applied, which dramatically increased the membrane hydrophilicity and facilitated the water wetting process. CO_2-switchable water wettability for the other membranes is listed in Table 7-1, which were all measured after 90s of the droplet formation. With DEA component increase, the membrane became more affinity to water (decreased WCA from 152° to 105°) and increased CO_2-induced hydrophilicity.

The underwater oil behavior is presented in Figure 7-4d. The membrane was immersed in H_2O and treated with CO_2 for 30 min for saturation before OCA test. Oil (hexane) droplet could not wet the membrane underwater and a spherical oil droplet with OCA of 152° formed below the membrane surface. This super oil repellency state could be retained for more than 10 hours when the membrane was immersed in CO_2-saturated water, suggesting that the membrane exhibited very stable underwater superoleophobicity (Figure 7-4d). It is believed that PDEA component protonated by CO_2 in water could facilitate water diffusion through the membrane and prevent contact of oil droplet with membrane. The water molecules present in the membrane could reduce the membrane/oil contact area. On the other side, the water affinity and diffusion in CO_2-treated membrane could extrude air trapped in microspores. Similarly as described in C-B theory that air trapped in membrane increases membrane hydrophobicity,[26] the water presence in the membrane here generated the water/membrane/oil interface, and created the surface with underwater superoleophobicity and low-oil adhesion properties.

The wettability of the membranes could be recovered to the initial state by simply drying the membrane in air flow, which could remove CO_2 and deprotonate PDEA or remove oil residue and recover the membrane to its initial state. The membrane could be regenerated in this way and be prepared for another cycle of use. The wettability membrane toward water and oil could thus be reversibly altered between

hydrophobic or superoleophilic and hydrophobic or underwater superoleophobic, as seen from the reversible WCA and OCA cycles in Figure 7-4e and 4f.

7.4.3 CO_2-controlled oil/water seperation

The highly porous polyHIPE membranes with the highest openness (M30) and CO_2-induced wettability switch were used for oil/water separation. As proof of concept, polyHIPE membrane with 30 wt% DEA content (M30) and 5 mm thickness was used for controlled oil/water separation. Specifically, the membrane was supported by metal mesh and fix between two glass filtration apparatus with flange connection. A cone bottle was connected to the bottom for liquid collection, as shown from Figure 7-5. Oil (hexane stained with yellow color) of 200 mL and water mixture (volume ratio = 1:1) were poured into the upper glass apparatus. It was found that the mixture became phase separated before hexane spread and wet throughout the membrane. Hexane of lower density floated up to the top layer. Water in the lower layer could not wet and penetrate through the membrane since the membrane was initially hydrophobic. Although the membrane was superoleophilic at this state, hexane was isolated from the membrane by water layer which prohibited the oil/water separation. Considering that oil/water separation was intervened by water layer between hexane and membrane, another model oil (chloroform stained with red color) with higher density than water was used for the demonstration of oil/water separation (Figure 7-5a). At this time, chloroform spread over the membrane quickly since the membrane was initially superhydrophilic and hydrophobic. Chloroform in

the lower layer continuously penetrated through the membrane and even after the phase separation of chloroform/water mixture. However, water layer was repelled above the membrane after all chloroform passed through the membrane. This was because the membrane at this state was still encroached by oil phase, water molecules was repelled from wetting membrane. It is worth to note that the rate of separation was slow due to irregular porous paths and limited openness compared to fibrous films (Video 7-S2).[2,4] The filtration separation process could be accelerated by vacuuming the system.

When the membrane was immersed in water and treated with CO_2. The hexane/water separation could be successfully achieved. Water could immediately spread and wet the membrane because the protonation of PDEA component switched the membrane wettability from hydrophobic to hydrophilic, as schematically illustrated in Figure 7-5c. The membrane at this state was hydrophilic and superoleophobic. Water in the lower layer could continuously penetrate through the membrane and be collected in the flask. While after all the water phase passed through, the hexane layer was isolated at top of the membrane because water molecules wetted on the membrane and isolated it from wetting by oil (Figure 7-5b). The membrane used for the oil/water separation could be easily regenerated by drying the membrane for another cycle of use. Thus, the highly porous poly(St-*co*-DEA)-HIPE membranes with open-cell structure and CO_2-switchable wettability could be used for reversible oil/water separation.

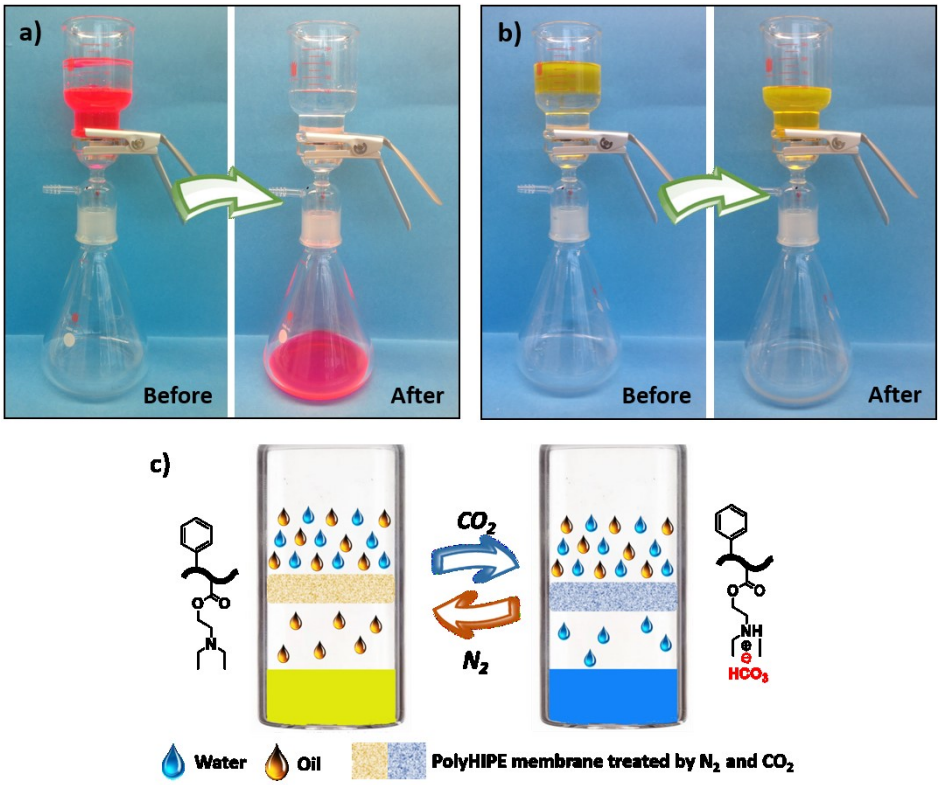

Figure 7-5. Images of CO_2-controlled oil/water separation. a) Water/chloroform (red) separated by dried membrane. b) Water/hexane (yellow) separation by CO_2 treated membrane. c) Schematic illustration of CO_2 controllable water/oil separation using poly(St-*co*-DEA)-HIPE membrane. The membrane wettability could be reversibly switched by CO_2 treatment between hydrophobic/superoleophilic (left) and hydrophilic/underwater superoleophobic (right), which allows the filtration of oil and water, respectively.

§ 7.5 Conclusion

In conclusion, poly(St-*co*-DEA)HIPE membranes with various DEA component have been prepared from W/O high internal phase emulsion (HIPE) templates. By polymerizing the continuous oil phase and extracting the water phase, highly porous polyHIPE membranes with "open-cell" structure could be obtained. The "open-cell" structure enabled consistent penetration of fluid through the membrane. The

combination of CO_2-switchable functionality DEA and microporous structure gave the membrane CO_2-switchable wettability toward water and oil. Specifically, the wettability of the membrane could be switched between hydrophobic or superoleophilic and hydrophilic or underwater superoleophobic, through drying or treating the membrane with CO_2 in aqueous system. Furthermore, such membranes (e.g., M30) could be used for CO_2-controlled oil/water separation. The membrane could easily be regenerated for multi-cycle uses, through simple drying the membrane to remove oil residue or CO_2 effect. This work represents a facile and cost-effective method for the preparation of large volume porous separation device with consistent porous quality and switchable wettability.

§ 7.6 References

[1] Shannon, M. A.; Bohn, P. W.; Elimelech, M.; Georgiadis, J. G.; Mariñas, B. J.; Mayes, A. M. *Nature* **2008**, 452 (7185), 301–310.

[2] Li, J. J.; Zhou, Y. N.; Luo, Z. H. *ACS Appl. Mater. Interfaces* **2015**, 7 (35), 19643–19650.

[3] Li, J. J.; Zhou, Y. N.; Jiang, Z. D.; Luo, Z. H. *Langmuir* **2016**, 32 (50), 13358–13366.

[4] Che, H.; Huo, M.; Peng, L.; Fang, T.; Liu, N.; Feng, L.; Wei, Y.; Yuan, J. *Angew. Chemie - Int. Ed.* **2015**, 54 (31), 8934–8938.

[5] Yu, S.; Tan, H.; Wang, J.; Liu, X.; Zhou, K. *ACS Appl. Mater. Interfaces* **2015**, 7 (12), 6745–6753.

[6] Kim, D. H.; Jung, M. C.; Cho, S.-H.; Kim, S. H.; Kim, H.-Y.; Lee, H. J.; Oh, K. H.; Moon, M.-W. *Sci. Rep.* **2015**, 5 (1), 12908, 1-12.

[7] Xue, B.; Gao, L.; Hou, Y.; Liu, Z.; Jiang, L. *Adv. Mater.* **2013**, 25 (2), 273–277.

[8] Cheng, C.; Ma, L.; Wu, D.; Ren, J.; Zhao, W.; Xue, J.; Sun, S.; Zhao, C. *J. Memb. Sci.* **2011**, 378 (1–2), 369–381.

[9] Han, Z.; Cheng, C.; Zhang, L.; Luo, C.; Nie, C.; Deng, J.; Xiang, T.; Zhao, C. *Desalination* **2014**, 349, 80–93.

[10] Meng, J.; Cao, Z.; Ni, L.; Zhang, Y.; Wang, X.; Zhang, X.; Liu, E. *J. Memb. Sci.* **2014**, 461, 123–129.

[11] Laloyaux, X.; Fautré, E.; Blin, T.; Purohit, V.; Leprince, J.; Jouenne, T.; Jonas, A. M.; Glinel, K. *Adv. Mater.* **2010**, 22 (44), 5024–5028.

[12] Zhao, H.; Law, K. Y.; Sambhy, V. *Langmuir* **2011**, 27 (10), 5927–5935.

[13] Wang, B.; Liang, W.; Guo, Z.; Liu, W. *Chem. Soc. Rev.* **2015**, 44 (1), 336–361.

[14] Cao, Y.; Liu, N.; Fu, C.; Li, K.; Tao, L.; Feng, L.; Wei, Y. *ACS Appl. Mater. Interfaces* **2014**, 6 (3), 2026–2030.

[15] Kwon, G.; Kota, A. K.; Li, Y.; Sohani, A.; Mabry, J. M.; Tuteja, A. *Adv. Mater.* **2012**, 24 (27), 3666–3671.

[16] Li, L.; Liu, Z.; Zhang, Q.; Meng, C.; Zhang, T.; Zhai, J. *J. Mater. Chem. A* **2015**, 3 (3), 1279–1286.

[17] Han, D.; Tong, X.; Boissiere, O.; Zhao, Y. *ACS Macro Lett.* **2012**, 1, 57–61.

[18] Y. Liu, P. G. Jessop, M. Cunningham, C. A. Eckert and C. L. Liotta, *Science*, **2006**, 313, 958-960.

[19] Zhang, Q.; Lei, L.; Zhu, S. *ACS Macro Lett.* **2017**, 6, 515–522.

[20] Zhang, Q.; Yu, G.; Wang, W. J.; Li, B. G.; Zhu, S. *Macromol. Rapid Commun.* **2012**, 33 (10), 916–921.

[21] Lei, L.; Zhang, Q.; Shi, S.; Zhu, S. *Langmuir* **2015**, 31 (7), 2196–2201.

[22] Li, M.; Lei, L.; Zhang, Q.; Zhu, S. *Macromolecular Rapid Communication*. **2016**, 37 (12), 957–962.

[23] Yan, Q.; Zhao, Y. *Chem. Commun.* **2014**, 50 (79), 11631–11641.

[24] Lei, L.; Zhang, Q.; Shi, S.; Zhu, S. *Polym. Chem.* **2016**, 7 (34), 5456–5462.

[25] Wenzel, R. N.. *J. Ind. Eng. Chem*. (Washington, D. C.) **1936**, 28, 988–994.

[26] Cassie, B. D.; Cassie, A. B. D.; Baxter, S. *Trans. Faraday Soc.* **1944**, 40 (5), 546–551.

[27] Tuteja, A.; Choi, W.; Ma, M.; Mabry, J. M.; Mazzella, S. A.; Rutledge, G. C.; McKinley, G. H.; Cohen, R. E. *Science* **2007**, 318 (5856), 1618–1622.

[28] Bhardwaj, N.; Kundu, S. C. *Biotechnol. Adv.* **2010**, 28 (3), 325–347.

[29] Huang, Z. M.; Zhang, Y. Z.; Kotaki, M.; Ramakrishna, S. *Compos. Sci. Technol.* **2003**, 63 (15), 2223–2253.

[30] Allard, J. F.; Herzog, P.; Lafarge, D.; Tamura, M. *Appl. Acoust.* **1993**, 39 (1–2), 3–21.

[31] Wojciech L. Suchanek, M. Y. Preparation of Fibrous , Porous Hydroxyapatite Ceramics from. *J. Am. Chem. Soc.* **1998**, 81, 765–767.

[32] Tebboth, M.; Menner, A.; Kogelbauer, A.; Bismarck, A. Polymerised High Internal Phase Emulsions for Fluid Separation Applications. *Curr. Opin. Chem. Eng.* **2014**, 4, 114–120.

[33] Lei, L.; Zhang, Q.; Shi, S.; Zhu, S. *J. Colloid Interface Sci.* **2016**, 483, 232–240.

[34] Cameron, N. R.; Sherrington, D. C. *Advances in Polymer Science*, **1996**, 126, 163–214.

[35] Cameron, N. R. *Polymer* (Guildf). **2005**, 46 (5), 1439–1449.

[36] Bokhari, M.; Carnachan, R. J.; Przyborski, S. A.; Cameron, N. R. *J. Mater. Chem.* **2007**, 17 (38), 4088–4094.

[37] Zhang, H.; Cooper, A. I. *Soft Matter* **2005**, 1 (2), 107–113.

[38] Bhumgara, Z. *Filtr. Sep.* **1995**, 32 (3), 245–251.

[39] Pulko, I.; Krajnc, P. *Macromol. Rapid Commun.* **2012**, 33 (20), 1731–1746.

[40] Zhang, T.; Xu, Z.; Guo, Q. *Polymer chemistry*, **2016**, 7, 7469-7476.

[41] Krajnc, P. *Polymers*, **2002**, 47 (3), 180–183.

[42] Cameron, N. R.; Barbetta, A. *J. Mater. Chem.* **2000**, 10 (11), 2466–2471.

[43] Jing, P.; Fang, X.; Yan, J.; Guo, J.; Fang, Y. *J. Mater. Chem. A,* **2013**, 1 (35), 10135–10141.

[44] Good, R. J.; Kotsidas, E. D. *J. Colloid Interface Sci.* **1978**, 66 (2), 360–362.

[45] Wu, S. *Delaware* **1989**, I (1960), 632–638.

[46] Shahalom, S.; Tong, T.; Emmett, S.; Saunders, B. R. *Langmuir* **2006**, 22 (20), 8311–8317.

[47] Smith, A. E.; Xu, X.; Kirkland-York, S. E.; Savin, D. A.; McCormick, C. L. *Macromolecules* **2010**, 43 (3), 1210–1217.

§ 7.7 Supporting information

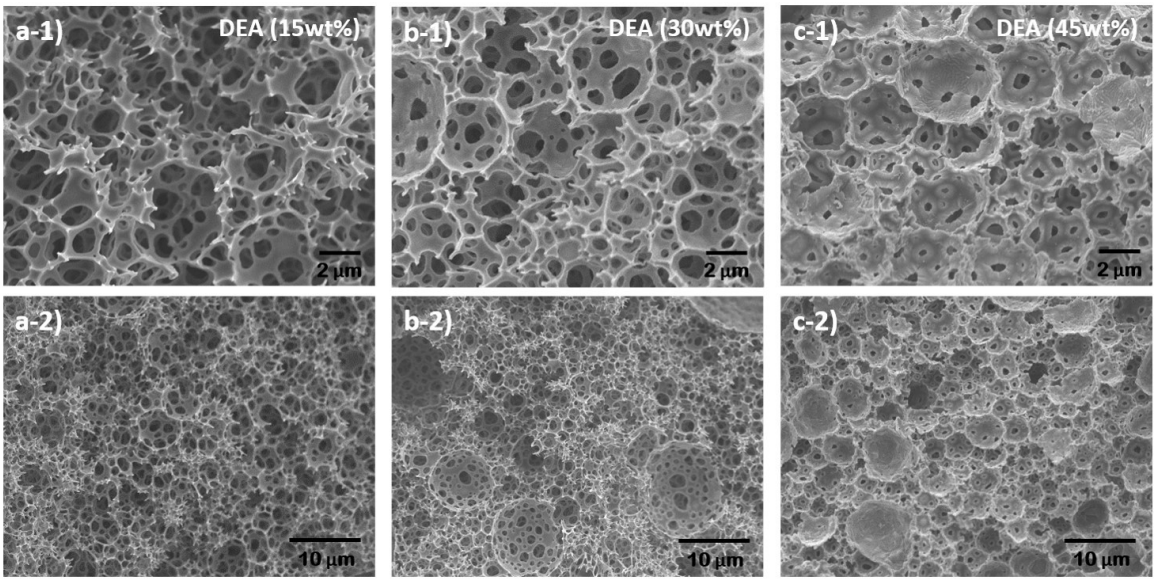

Figure 7-S1. SEM images of poly(St-*co*-DEA) HIPE membrane composing different DEA contents prepared from 20 wt% Span-80 stabilized HIPE. a-1,2) 15 wt%, b-1,2) 30 wt%, c-1,2) 45 wt%

Table 7-S1. The preparation and characterization of poly(St-*co*-DEA)-HIPE prepared from 20wt% Span-80 stabilized HIPE.

Runs	Recipe		PolyHIPE morphology			
	St (g)	DEA (g)	D (μm)	d (μm)	n	O (%)
1#	3.0	0.6	4.17	0.81	8	17.43
2#	2.4	1.2	4.05	0.67	9	14.22
3#	1.8	1.8	3.96	0.56	6	6.93

8 CONTRIBUTIONS AND PERSPECTIVES

In this chapter, the major contributions of this thesis study are highlighted. Some research perspectives and recommendations are also provided for future researchers in this emerging area.

§ 8.1 Major Contributions

The major contribulitions made by this study provide better understanding and application of O_2 and/or CO_2-swictachable functionalities in various polymer systems, as summerized below:

- The investigation of O_2-switchability of various flurinated monomers provides a comprehensive methodology for the development, selection and application of monomer candidates for O_2-switchable functional polymers.

- The combination of gas-switchability and thermo-responsivity enables the exhibition and comparison of gas-induced physicochemical changes by LCST shifting, which is applicable for both random copolymers and homopolymers.

- The first O_2 and CO_2 dual-gas switchable microgel system, and its building of microgel-colloidosomes, facilitates the development of microcapsules for hierarchical release of water soluble cargo molecules upon respective O_2 and CO_2 treatment.

- The first report of polyHIPE membrane with CO_2-tunable wettability and their proof-of-concept application for CO_2 controlled oil/water separation opens up a new area for preparation of smart membranes.

§ 8.2 Perspective and Recommendations

Stimuli-responsive polymers have attracted growing attentions due to their unique responsive properties and a wide range of potential applications. The introduction of gas triggers has greatly expanded the family of stimuli-responsive systems. Although significant progresses have been achieved over the past decade, the study on gas-switchable polymers is still at its early stage and there are many chanllenges remaining to be tackled. Following are some perspectives and recommendations for furture researchers in the areas of gas-switchable polymers.

Oxygen (O_2), carbon oxide (CO_x), nitrogen oxide (NO_x), sulfur oxide (SO_x), and hydrogen sulfide (H_2S) have been and will continue be the key gas triggers to study since they are highly relevant to our enviroment and health issues, as well as their tremedeous applications in material processing and biomedical area.[1] Based on the dosage applied during application, gas triggers could be devided into two catagries. For these "green" and aboundent gases like O_2 and CO_2, they are easily to be applied and remove from the system, suitable for large volume operations. These gases are more applicable for industry operations since gas triggered recycling and seperation could benefit in both energy/cost saving and production efficiency. For instance, reaction and seperation are both fundemental operations in chemical engineering. CO_2-switchable initiator,[2] catalysis,[3,4] and seperation[5,6] have be reported, but only in laboratory scale. More powerful gas-switchable system are highly disierable for industrail conditions. For the biological signal gas molecules like NO, CO, and H_2S, they are operated in trace level (μM) and very strict on dosage since dysregulation of signaling molecules could cause serious diseases.[7] The sensitivity and biocompatibility would be the direaction for further study. For example, the high sensitivity could be realized by developing novel responsive functionalities or through exquisite molecular chain structure design. [7–9]

In the aspect of fundentamental research, since all the gas-switchable systems are operated in liquid, expecically under aquous and moisture conditions, gas bubbling and interactions between gas molecules and trageted funcational moieties require

further mechanistic elucidation. The development of inexpensive and facile gas-responsive functional groups are also worth of much attention. Studies on gas molecule diffusion in polymer solution can greatly benefit realizing the potential applications of gas-switchable systems.

§ 8.3 References

[1] Zhang, Q.; Lei, L.; Zhu, S. *ACS Macro Lett.* **2017**, 6, 515–522.

[2] Su, X.; Nishizawa, K.; Bultz, E.; Sawamoto, M.; Ouchi, M.; Jessop, P. G.; Cunningham, M. F. *Macromolecules* **2016**, 49 (17), 6251–6259.

[3] Jessop, P. G.; Mercer, S. M.; Heldebrant, D. J. *Energy Environ. Sci.* **2012**, 5 (6), 7240.

[4] Hull, J. F.; Himeda, Y.; Wang, W.-H.; Hashiguchi, B.; Periana, R.; Szalda, D. J.; Muckerman, J. T.; Fujita, E. *Nat. Chem.* **2012**, 4 (5), 383–388.

[5] Zhang, Q.; Yu, G.; Wang, W. J.; Li, B. G.; Zhu, S. *Macromol. Rapid Commun.* **2012**, 33 (10), 916–921.

[6] Che, H.; Huo, M.; Peng, L.; Fang, T.; Liu, N.; Feng, L.; Wei, Y.; Yuan, J. *Angew. Chemie - Int. Ed.* **2015**, 54 (31), 8934–8938.

[7] Xu, M.; Liu, L.; Hu, J.; Zhao, Y.; Yan, Q. *ACS Macro Lett.* **2017**, 6 (4), 458–462.

[8] Yan, Q.; Sang, W. *Chem. Sci.* **2016**, 7 (3), 2100–2105.

[9] Zhang, J.; Hu, J.; Sang, W.; Wang, J.; Yan, Q. *ACS Macro Lett.* **2016**, 5 (8), 919–924.

APPENDIX: POROUS MATERIALS TEMPLATED FROM HIGH INTERNAL PHASE EMULSION WITH DOUBLE EMULSION MORPHOLOGY

This chapter introduces a promising emulsion application based on the microgels prepared in chapter 5. Advanced polymer materials with porous morphology have been prepared from the high internal phase Pickering emulsion stabilized by microgel particles. This chapter is reproduced from the published paper of Lei Lei, Qi Zhang, Susan Shi, Shiping Zhu "High internal phase emulsion with double emulsion morphology and their templated porous polymer systems" *Journal of Colloid and Interface Science*, **2016**, 483 (1), pp 232–240 with the permission from Elsevier. The supporting information referred in the test is attached at the end of this appendix. Because the work does not involve gas-switchable polymers, it is not included into the major body of the thesis. However, it is highly related to the development of chapter 6. It can be considered as the link of background for the chapter to rest of the thesis.

Author contributions

This work is originated from a novel emulsion morphology founded during microgel-stabilized HIPE preparation. Dr. Shiping Zhu, Dr. Qi Zhang and Dr. Shuxian Shi provided valuable discussion. Lei Lei did all the experiments and prepared the first manuscript. Dr. Zhang and Dr. Shi gave first revision of the manuscript and Dr. Zhu did the final revision before submission.

Abstract

This paper reports synthesis of the first high internal phase emulsion (HIPE) system with double emulsion (DE) morphology (HIPE-DE). HIPE is a highly concentrated but highly stable emulsion system, which has a dispersed/internal phase fraction over 74 vol%. DE represents an emulsion system that hierarchically encapsulates two immiscible phases. The combination of HIPE and DE provides an efficient method for fabrication of complex structures. In this work, HIPE-DE having a water-in-oil-in-water (W/O/W) morphology has been prepared for the first time via a simple one-step emulsification method with poly(2-(diethylamino)ethyl methacrylate) (PDEA) microgel particles as Pickering stabilizer. An oil phase fraction up to 90 vol% was achieved by optimizing the microgel concentration in aqueous phase. The mechanism of the DE formation has been elucidated. It was found that while PDEA microgels stabilized the oil droplets in water, small amount protonated DEA monomers acted as

surfactant and formed water-containing micelles inside the oil droplets. It was demonstrated that the W/O/W HIPE-DE could be precisely converted into porous polymer structures. With styrene as the oil phase in W/O/W HIPE-DE, porous polystyrene particles were obtained upon polymerization. With dissolved acrylamide as the aqueous phase and toluene as the continuous phase, porous polyacrylamide matrixes were prepared. Elevating temperature required for polymerization did not change the W/O/W HIPE-DE morphologies. This simple approach provides a versatile platform for synthesis of a variety of porous polymer systems.

Introduction

A high internal phase emulsion (HIPE) is also known as "gel emulsion". It is defined as an emulsion system, which contains more than 74 vol% internal/dispersed phase.[1, 2] The densely packed emulsion droplets are very stable in the system. HIPE has applications in food processing, cosmetic, pharmaceutical, and petroleum industries.[3-5] The two HIPE types reported so far, either water-in-oil (W/O) or oil-in-water (O/W), can be used as template for fabrication of highly porous polymeric scaffolds in tissue engineering and for preparation of filtration membranes by adding polymerizable monomers into the continuous phase.[6-8] Both molecular and particulate surfactants (Pickering emulsion) can be employed to stabilize HIPEs. Particulate stabilizers such as colloid particles possess many advantages over conventional molecular surfactants. First, colloid particles used in Pickering emulsion can be irreversibly adsorbed onto oil-water interface due to a high level of attachment

energy, resulting in stable emulsion having shelf life over months or even years.[9] Second, the size, structure, chemical composition and hydrophilicity of colloid particles can be easily pre-designed and controlled, which is important in the preparation of Pickering emulsions.[10] Furthermore, numerous functional groups can be introduced into particle surface, which provides a versatile platform for fabrication of stimuli-responsive Pickering emulsions and functionalization of the resulting materials.[11-14]

An emulsion system often suffers from catastrophic phase inversion with excessive increase in its internal phase volume fraction. Higher fraction of the internal phase has always been an objective in HIPE research.[15, 16] Recently, HIPE systems having an internal phase higher than 90 % have been reported by using inorganic titania or silica particle as Pickering stabilizer, while hydrophilicity of the particles must be modified prior to their use.[17,18] Organic microgels have also been used to stabilize HIPE systems. For example, Ngai et al.[16] prepared hexane-in-water (O/W) Pickering emulsion with an inner phase fraction up to 90% using poly(N-isopropylamide-co-methacrylic acid) (P(NIPAM-*co*-MAA)) microgels as the stabilizer. The HIPE was directly used as a template for preparation of porous microgel membranes by evaporating both the oil and water phases. The pore size and membrane porosity could be regulated by microgel concentration in the original Pickering emulsion.

On the other side, double emulsion (DE) represents a novel class of emulsion morphologies. It is a hierarchical multiphasic emulsion system, in which dispersed droplets of one liquid phase contain smaller droplets of another phase.[19] This fascinating and unique morphology can be of particularly useful as template for preparation of porous materials,[16] fabrication of multi-compartment structures,[20] and cargos for delivery of sensitive drugs.[4, 21] Unfortunately, double emulsion systems are considered to be thermodynamically unstable due to flocculation, coalescence, Ostwald ripening, etc.[22] Double emulsions are usually prepared through two-step procedures using two distinct surfactants (lipophilic and hydrophilic). For instance, a W/O emulsion is prepared first and it is then dispersed into an aqueous continuous phase to prepare the W/O/W double emulsion.[23] This approach is cumbersome and the second step emulsification may disrupt the prior emulsion droplets. Simplifying multicomponent encapsulation is of priority in the double emulsion study and one-step emulsification is most desirable.

Recently, double emulsion (DE) systems have been developed from one-step emulsification. Wang et al. reported several double emulsion systems and their corresponding resulted porous particles.[24-26] For example, polylactic acid (PLA) microspheres having interconnected chambers were generated based on a water-in-oil-in-water (W/O/W) double emulsion with 16.7 vol% oil phase fraction. The double emulsion was prepared from an oil-in-water emulsion, which consisted of polylactic acid (PLA)-containing dispersed dichloromethane phase and cetyltrimethyl

ammonium bromide (CTAB)-containing continuous water phase. It was proposed that electrostatic interactions between PLA (it has carboxylic acid moiety on one chain end and hydroxyl group on the other) and CTAB (it is a cationic surfactant) led to an influx of water from the external aqueous phase to pass through the oil-water interface, thus forming small water droplets within the large oil droplets.[24] Hayward et al.[20] reported another W/O/W double emulsion (also 16.7 vol% oil phase fraction) stabilized by amphiphilic block copolymer of polystyrene-block-poly(N-isopropylacrylamide) (PS-*b*-PNIPAM). Within the primary oil droplets, salt species derived from the block copolymer formed aggregates, osmotically driving water transfer from the continuous water phase into the dispersed oil droplets and form inner water droplets, thus resulting in a W/O/W double emulsion system. Particulate stabilizers have also been employed for preparation of Pickering double emulsion systems. Lee et al.[19] reported one-step formation of W/O/W double emulsion stabilized by amphiphilic Janus particles, with styrene and acrylic acid as the respective apolar and polar regions. This double emulsion could be destabilized to release encapsulant by simply increasing pH of the continuous phase.

The combination of high internal phase emulsion (HIPE) and double emulsion (DE) is expected to result in, either HIPE constituted of DE (HIPE-DE) or DE constituted of HIPE (DE-HIPE), which may provide a powerful approach for fabrication of complex structures. As schematically illustrated in Figure A1 b). Liu et al.[27] reported a good example of DE constituted of HIPE, in which a W/O/W double emulsion was prepared

via catastrophic phase inversion of W/O HIPE. This W/O/W double emulsion having high internal water phase was used as template to prepare polymer microspheres with an interconnecting porous structure. It must be pointed out that, although several double emulsion systems have been reported, their dispersed phase ratios were all far below 74 vol%. There has been no HIPE system reported so far, which contained a double emulsion morphology. The reported HIPE works were simple O/W and/or W/O systems. In this paper, we report the first synthesis of a high internal phase emulsion with double emulsion morphology (HIPE-DE) (Figure A1a) through one-step emulsification by using poly(2-(diethylamino)ethyl methacrylate) (PDEA) microgel particles as Pickering stabilizer. The oil phase fraction in this double emulsion system can be increased up to 90 vol% without collapsing. Such highly stable water-in-oil-in-water (W/O/W) HIPE-DE can be used as soft templates to prepare either porous particles or porous matrixes by respectively polymerizing the monomer-containing dispersed oil phase or the monomer-containing continuous aqueous phase. The objective of the present work is to study on the generation of HIPE-DE morphologies and to explore their potential applications for preparation of porous particles and matrixes.

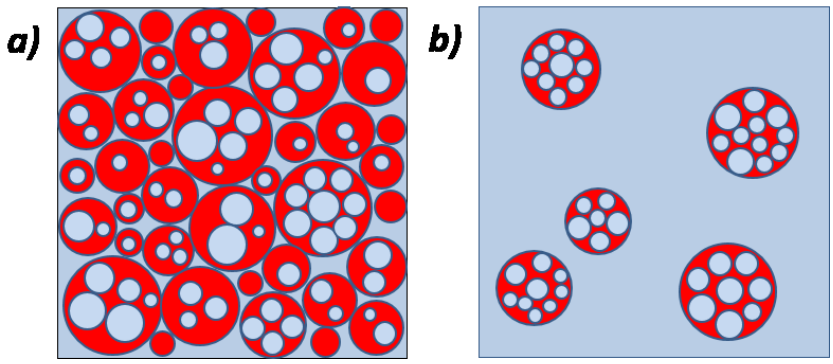

Figure A1. Schematic illustration of a) high internal phase emulsion constituted of double emulsion (HIPE-DE) and b) double emulsion constituted of high internal phase emulsion (DE-HIPE).

Experiments and Characterization

Materials

2-(Diethylamino)ethyl methacrylate (DEA, 99 %, Aldrich) and styrene (St, ≥ 99 %, Aldrich) were passed through an inhibitor remover column before use. N,N'-Methylenebis(acrylamide) (BisAM, 99 %, Aldrich), 2,2'-azobis(2-methylpropionamidine) dihydrochloride (V-50, 99 %, Aldrich), acrylamide (AA, 99 %, Aldrich), toluene (99.5 %, Aldrich) and Nile Red (Aldrich) were used as received without purification. 2,2'-Azobis(2-methylpropionitrile) (AIBN, 98%, Aldrich) was recrystallized from methanol twice and stored in refrigeration prior to use. Milli-Q grade water generated from Barnstead Nanopure Diamond system was used in preparation of all aqueous dispersions of microgels.

Experiment

PDEA microgel preparation: PDEA microgels with an average hydrodynamic diameter of 120 nm was prepared through surfactant-free emulsion polymerization (SFEP) as described in the previous work.[14] Specifically, 5.0 g DEA, 250 mg BisAM and 48 mL Milli Q water were charged into a 250 mL round-flask. The flask was sealed with rubber stopper and degassed with N_2 flow while magnetically stirred at 250 rpm.

Meanwhile, the reactor was gradually heated to 70 ºC. After 30 min, the pre-degassed initiator aqueous solution (400 mg V-50 in 2 mL water) was injected to start the polymerization and the reaction mixture was turned from translucent to creamy white within 5 min. The reaction was continued for 24 hours and stopped by exposing the latex to air and cooling down to room temperature. Microgel particle size and distribution were measured by dynamic light scattering (DLS). PDEA microgel particles were purified through dialysis purification (dialysis membrane D0655, Aldrich; 12.4 kDa of MWCO) against deionized (DI) water in order to remove residual monomers and oligomers. The dialysis water was changed twice every day for 5 days.

Pickering emulsion preparation: The readily prepared PDEA microgel aqueous dispersion (100 mg/mL) was diluted into various concentrations and used as the aqueous phase for Pickering emulsion preparation. Styrene stained by 0.01 wt % Nile Red was used as the oil phase. Different volume ratios of the aqueous and oil phases were charged into glass vials, followed by homogenization (IKA, Ultra-turrax T18 digital, S18N-10G) at 10000 rpm for 90 s. The Pickering emulsions stood still for 2 hours before their morphologies were characterized by confocal fluorescence microscope (CFM).

Porous polystyrene particles prepared from W/O/W HIPE-DE template: Pickering emulsions with styrene (oil phase) fraction of 85 vol% stabilized by 50 mg/mL PDEA microgel aqueous dispersion were polymerized into porous polystyrene particles.

AIBN of 5 wt% was dissolved in the styrene phase before homogenization. The resulted W/O/W HIPE-DE was polymerized at 90 ^{o}C for 24 h and vacuum dried. Scanning Electrical Microscope (SEM) and transmission electron microscopy (TEM) were used to visualize the morphologies of polystyrene particles.

Porous polyacryamine matrixes prepared from W/O/W HIPDE template: PDEA microgel aqueous dispersion (50 mg/mL) containing 20 wt% of acrylamide monomer (based on the microgel content) and 5 wt% of V-50 initiator (based on the monomer amount) was used as the aqueous phase. Toluene was used as the oil phase. The W/O/W HIPE-DE with oil phase fraction of 85 vol% was polymerized into porous polyacrylamide matrixes at 90 ^{o}C for 24 hours and vacuum dried to remove the internal oil phase (toluene). Scanning electrical microscope (SEM) was used to visualize the morphologies of polyacrylamide matrixes.

Characterization

The particle size and distribution of PDEA microgels were determined by a particle size analyzer (Brookhaven, 900Plus), which was equipped with 35 mW red diode laser source at 600 nm wavelength with a detection angle of 90°. The samples were equilibrated for 180 s before detection and were then conducted for 180 s with 30 s intervals between measurements. The emulsion morphologies and emulsion droplet sizes were characterized by confocal fluorescence microscope (CFM). The oil phase

was stained with Nile red (492/520 nm). CFM images were acquired from Zeiss LSM 510 Meta Confocal Microscope (Zeiss, Gottingen, Germany). One drop of the emulsion was trickled onto a glass slide and another cover glass was placed over it, to make the emulsion layer thin enough to enable the light/laser pass through. The morphologies of porous polymers were characterized by JEOL JSM 7000 Scanning Electronic Microscopy (SEM) and transmission electron microscope (JEOL-1200EX). In order to observe the porous structure of cross-section slice, the powdered samples of PS particles were infiltrated in Spurr's epoxy resin for 24 hours and transferred to embedding moulds, which were then polymerized overnight in a 60 ^{o}C oven. Thin sections were cut by Leica UCT ultra-microtome and placed to Cu grids. The sections were viewed in JEOL JEM 1200 EX TEMSCAN transmission electron microscope (JEOL, Peabody, MA, USA) operated at an accelerating voltage of 80kV. The images were acquired with AMT 4 megapixel digital camera (Advanced Microscopy Techniques, Woburn, MA).

Results and Discussion

High internal phase emulsion with double emulsion morphology (HIPE-DE)

We used poly(2-(diethylamino)ethyl methacrylate) (PDEA) microgel particles to stabilize the styrene-in-water emulsion. To our surprise, the resulting emulsion was not a simple styrene-in-water high internal phase emulsion (O/W HIPE). It was a styrene-in-water high internal phase emulsion containing water-in-styrene double

emulsion (W/O/W HIPE-DE). The water-in-oil-in-water (W/O/W) double emulsion morphology was clearly present, as it can be seen from the confocal fluorescence microscope (CFM) image in Figure A2. A number of small internal water droplets (black) are encapsulated in the primary oil droplets (red), which are dispersed in the continuous aqueous phase (black). The oil phase fraction in this double emulsion system can be increased up to 90 vol% without collapsing, thus resulting highly stable W/O/W HIPE-DE system. This is very different from the work of Stefanec et al,[28] in which a W/O HIPE was first prepared and it was then dispersed into an aqueous solution to generate the W/O/W double emulsion. The final emulsion product was a very dilute W/O/W emulsion. It is also different from the work of Liu et al,[27] in which a W/O/W double emulsion was prepared from phase inversion of W/O HIPE. Both literature works were dilute O/W double emulsions, but their W/O droplets had high internal water phase (i.e. DE-HIPE). In comparison, our work is a high internal phase emulsion exhibiting double emulsion morphology, in which the emulsion system contains very concentrated W/O/W emulsion droplets (HIPE-DE). As far as we know, this is the first report on a high internal phase emulsion having double emulsion morphology (HIPE-DE), and it is also the first demonstration of double emulsions stabilized by microgel particles as Pickering stabilizer, which could be readily prepared through one-step emulsification.

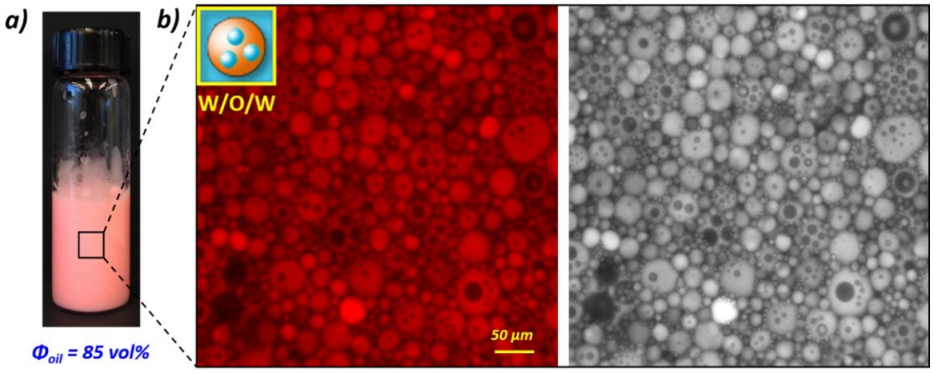

Figure A2. (a) Digital photo and (b) confocal fluorescence image of Pickering high internal phase emulsion with double emulsion morphology (HIPE-DE) stabilized by the readily prepared PDEA microgel aqueous dispersion (50 mg/mL) with an internal oil phase fraction of 85 vol%. Styrene stained by 0.01 wt% Nile red was used as the oil phase, showing red colour in confocal fluorescence image.

An examination of the emulsion literatures revealed that there were several microgel-stabilized HIPE systems reported, but no double emulsion morphologies have ever been observed.[16, 29-31] It is therefore worth much effort to further explore mechanisms of the double emulsion formation in such high internal phase emulsion systems. It must be pointed out that the microgel particles and their dispersions used as Pickering emulsifier, as well as the aqueous phase, in this work, were readily prepared with no further purification steps required. The PDEA microgels were prepared via an aqueous surfactant-free emulsion polymerization, as described in our previous work.[14] The particles had a number average diameter of 120 nm. In the preparation of PDEA microgels, the monomer conversion was 94 wt%, as determined by a gravimetric method. The unreacted DEA monomer was about 6 wt%.

We hypothesized that the unreacted DEA might be responsible for the formation of double emulsion morphology. In the literature, Xu et al. found that N-(4-vinylbenzyl)-N,N-dibutylamine (VBA) could be used for preparation of W/O/W emulsions. It was attributed to the amphiphilic feature of VBA, which was converted to a surfactant monomer N-(4-vinylbenzyl)-N,N-dibutylamine hydrochloride (VBAH) via acidification.[32] Similar to VBA, DEA has an intramolecular amphiphilic structure and it can be converted to DEAH through protonation of the tertiary amine group in DEA.[11, 14] The effect of DEA as surfactant on the double emulsion morphology was thus investigated.

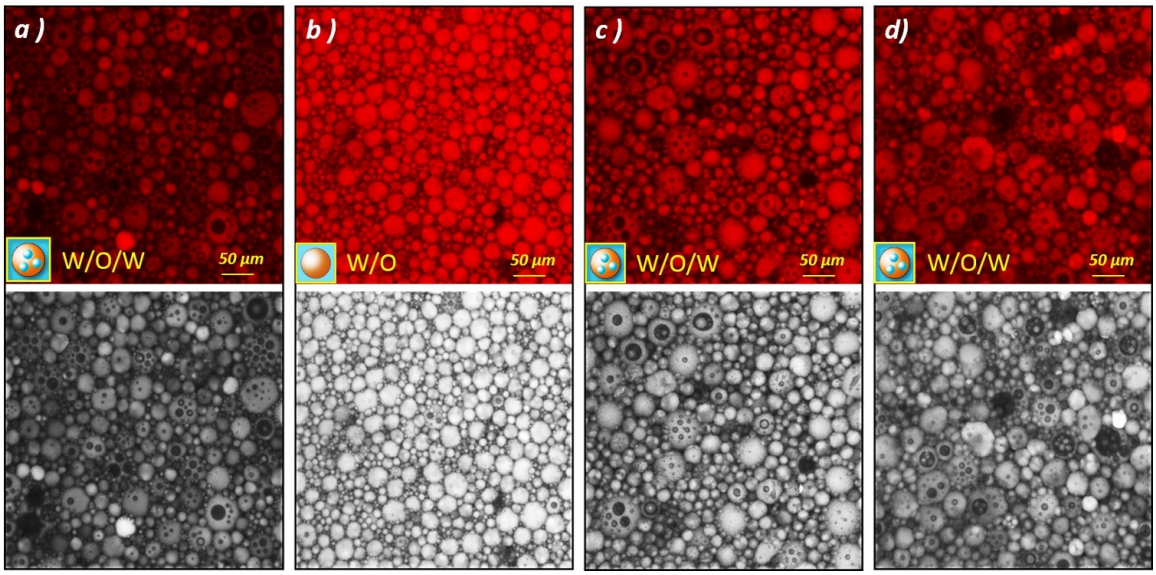

Figure A3.Confocal fluorescence images of PDEA microgel-stabilized Pickering HIPE-DEs having 85 vol% oil phase fraction prepared by 50 mg/mL PDEA microgel dispersion as the aqueous phase. (a) PDEA microgels before dialysis purification (same as Figure A1 (b)). (b) PDEA microgels after dialysis purification. (c) Adding 3 wt% and (d) 6 wt% fresh DEA (based on PDEA amount) to the dialysis-purified PDEA microgel aqueous dispersion. In the microgel

preparation, DEA conversion was 94%, with 6 wt% of the monomer unreacted and remained in the PDEA microgel sample.

Aqueous dispersion containing 50 mg PDEA microgel per milliliter of H_2O, before and after dialysis purification (to remove unreacted DEA), were used as the aqueous phase in preparation of the emulsions having 85 vol% of styrene as the oil phase. The Pickering emulsions were prepared with Ultra-turrax T18 homogenizer (IKA, 10 mm head) at 10000 rpm for 90s. pH and conductivity were used to measure the DEA monomer content in the PDEA microgel aqueous dispersion. Figure A3 shows the confocal fluorescence images of the prepared Pickering emulsions after standing for 2 hours. Interestingly, the PDEA microgel aqueous dispersion without dialysis gave high internal phase emulsions containing a large number of double emulsion droplets (Figure A3 (a)). The internal water phase concentration was obtained by counting the number of small water droplets (black) within the W/O (oil phase: red) droplets. In contrast, this double emulsion morphology was not seen in the emulsions prepared with the dialysis-purified PDEA microgel dispersion (Figure A3 (b)). This observation suggested that the unreacted DEA played a crucial role in the formation of W/O/W double emulsion morphology. We therefore purposely added small amount DEA monomer to the dialysis-purified PDEA microgel dispersion and prepared the high internal phase emulsions. Indeed, the double emulsion morphology was recovered. As shown in Figure A3, adding 3 wt% (c) or 6 wt% (d) of fresh DEA monomer (based on PDEA microgel amount) to the dialyzed microgel aqueous dispersion resulted in the double emulsion morphology. We have also suspected other residues in the

polymerization recipe such as the surfactant V-50 and the crosslinker BisAM. However, addition of V-50 and BisAM to the dialyzed microgel dispersion did not lead to the double emulsion generation. Thus, we concluded that it was the DEA monomer, in collaboration with the PDEA microgel, that resulted in the W/O/W HIPE-DE formation.

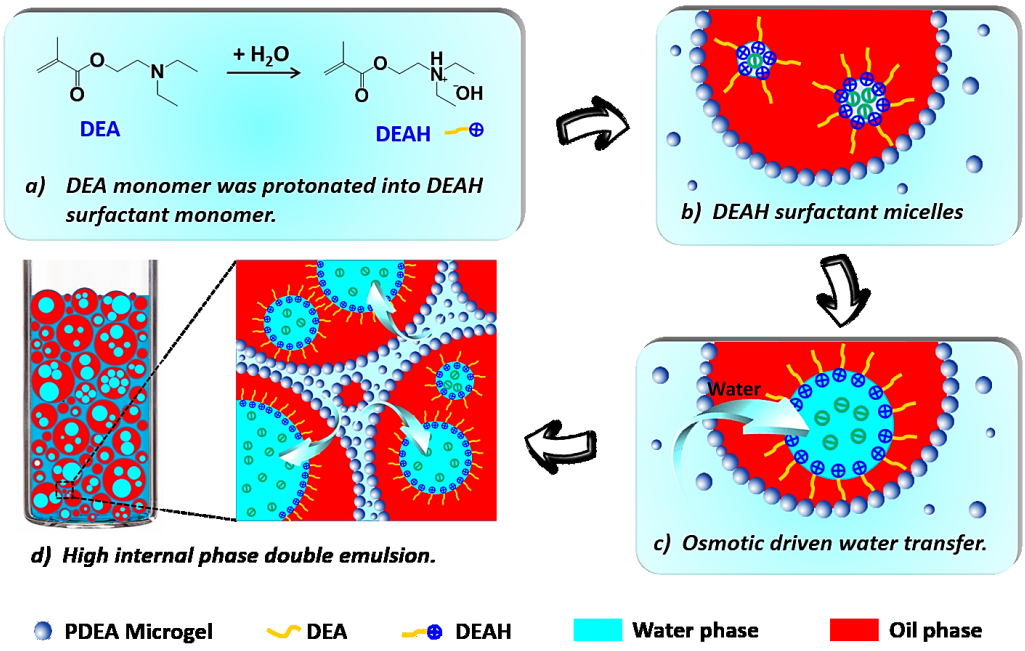

Figure A4. Schematic illustration of HIPE-DE formation. (a) DEA monomer was protonated into DEAH surfactant monomer. (b) DEAH surfactant micelles were formed inside the microgel-stabilized primary oil emulsion droplets. (c) Water molecules were osmotically transferred from the continuous aqueous phase into the DEAH surfactant micelles. (d) Small water droplets were generated in the primary oil emulsion droplets, forming the W/O/W double emulsion.

DEA monomer has an intermolecular amphiphilic structure with a relatively high pKa_{DEA} = 9.5. Depending on pH, it can be partially protonated in an aqueous phase.[32, 33] Before purification, the PDEA microgel dispersion of 50 mg/mL had pH = 9.45 and a conductivity of 3684 μs/cm. After 5 days of dialysis, the pH and conductivity values

decreased to 8.51 and 259.8 us/cm, respectively. Most unreacted DEA molecules were removed from the PDEA microgel dispersion. Figure A4 illustrates the molecular processes involved in the HIPE-DE formation. About 50% DEA molecules are protonated and act as DEAH surfactant at pH=9.45 (a), forming micelles inside the microgel-stabilized primary oil emulsion droplets (b). Water molecules are transferred from the continuous aqueous phase into the micelles driven by an osmotic force (c),[20] resulting in the inner small water droplets (d). This explains why the presence of DEA monomer was critical for the formation of the prepared W/O/W double emulsions. The PDEA microgel particles as Pickering surfactant stabilize the large oil emulsion droplets, while the DEA monomers as molecular surfactant stabilized the small aqueous droplets inside the oil emulsion droplets.

High internal phase emulsion-double emulsion morphology vs. oil phase fraction

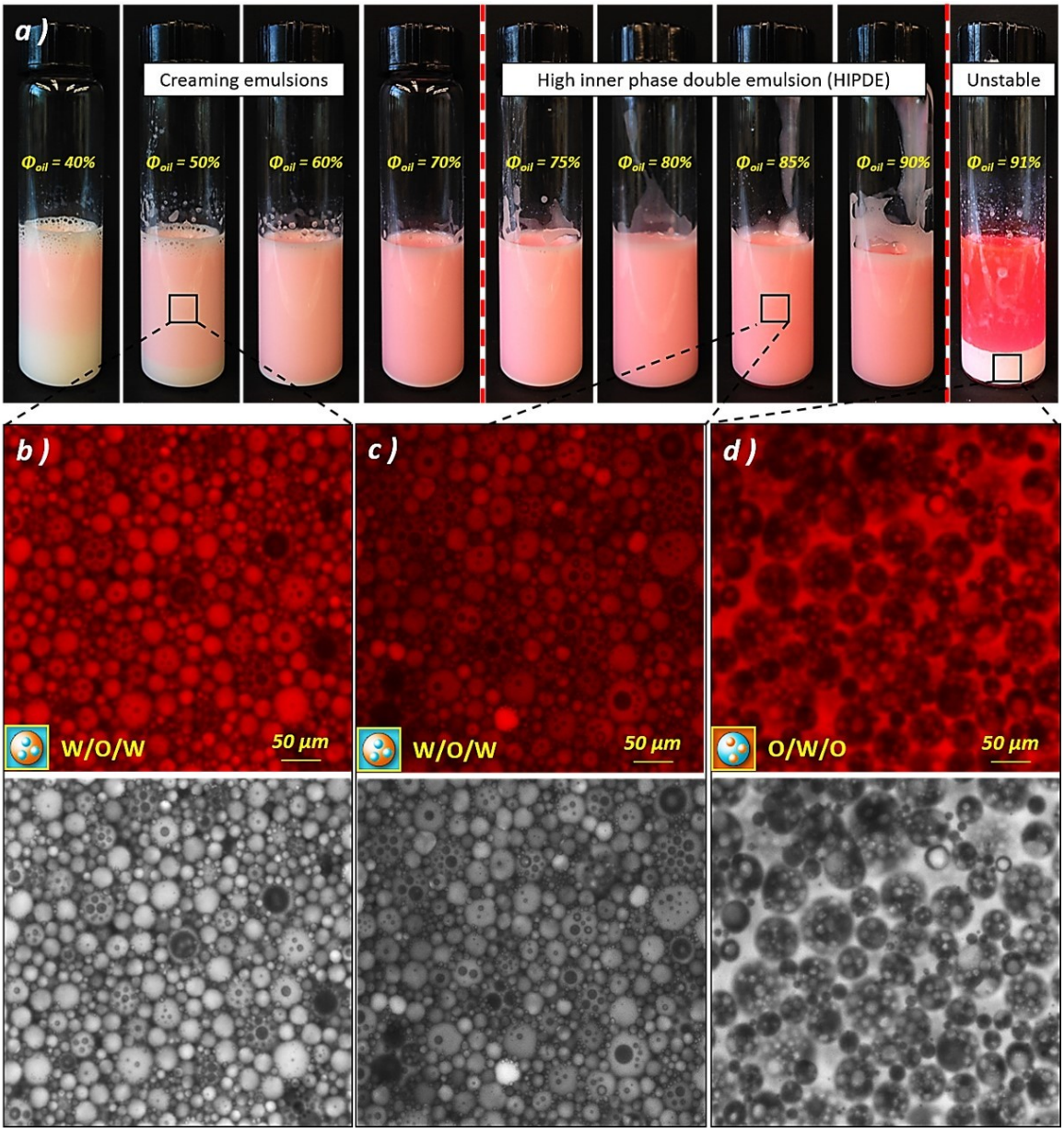

Figure A5. (a) Photographs of Pickering emulsions of styrene stabilized by an aqueous dispersion of 50 mg/mL PDEA microgel particles. The styrene monomer was stained by 0.01 wt% Nile red. The oil phase volume fraction was increased from 40 to 91 vol %. (b), (c) and (d) Confocal fluorescence images of the emulsions having 50, 85 and 91 vol % oil phase fraction, respectively.

Based on the result of 85 vol% styrene HIPE-DE, we investigated the emulsion morphology as a function of oil phase fraction. Figure A5 shows the digital photos (a) and confocal fluorescence microscope (CFM) images (b, c, d) of the Pickering emulsions standing for 2 hours after homogenization. The aqueous phase of all the emulsions contained 50 mg/mL PDEA microgels (94 wt% PDEA and 6 wt% DEA) as stabilizer. The oil phase volume fraction increased from 40 to 91%. When the oil phase fraction was in the range of 40-70 vol%, the emulsion was stable but underwent creaming after standing for a while. The dispersed red emulsion droplets migrated upwards due to buoyancy (styrene is lighter than water). The CFM image in Figure A5 (b) certified the W/O/W double emulsion morphology, instead of the commonly observed O/W emulsion. As the oil phase increased to 75-90 vol %, the emulsions became super viscous, which prevented the emulsion droplets from creaming. These emulsions exhibited remarkable stability with shelf life over months. Unlike the commonly obtained W/O and O/W HIPEs,[16, 21] a large number of W/O/W double emulsion droplets could still be retained and clearly observed in the CFM characterization. All the Pickering emulsions contained W/O/W double emulsions (Figure A5 (b) and (c)). An exception was the sample with 91 vol% oil phase fraction, which exhibited an oil-in-water-in-oil (O/W/O) morphology (Figure A5 (d)). The oil phase fraction of the stable HIPE-DE systems prepared in this work reached an amazing level of 90 vol%. Because some water content was encapsulated in the dispersed oil droplets, the exact volume fraction of the continuous aqueous phase for dispersion of the oil droplets must be less than 10 vol%. It was also of great interest

to discover that further increase in the oil phase fraction by only 1 vol% (from 90 to 91 vol%) would cause a catastrophic phase inversion in the emulsification. A phase separation occurred, with the oil phase (red) floating atop and the O/W/O double emulsion droplets (white) in the bottom (Figure A5 (a), Φ_{oil} = 91 vol%). It was evident in Figure A5 (d) that almost all the water droplets (black) dispersed in the continuous oil phase (red) encapsulated several small oil droplets (red).

It should be pointed out that both W/O/W and O/W/O double emulsions can be prepared through the one-step emulsification, which is much easier than the traditional two-step methods reported in literature. Furthermore, the reported CFM imaging only provided the single cross-section slices of emulsion droplets.[34] In Figure A5 (b) and (c), most double emulsion droplets can be clearly seen in their cross sections, while other droplets are seen in their top views. In this work, we also employed a three-dimensional (3D) CFM scanning in the analysis. The W/O/W morphology of the double emulsion droplets was further elucidated in a great detail. With a distance of 107 micrometers, 12 CFM slices from z-stack were applied. It was found that almost every oil droplets dispersed in water phase encapsulated many small internal water droplets. The appearance and fading of te small inner water droplets (black) within the large oil droplets (red) can be clearly watched in Video AS1, demonstrating the encapsulation of water droplets in almost all the emulsion droplets.

High internal phase emulsion-double emulsion morphology vs. microgel concentration in aqueous phase

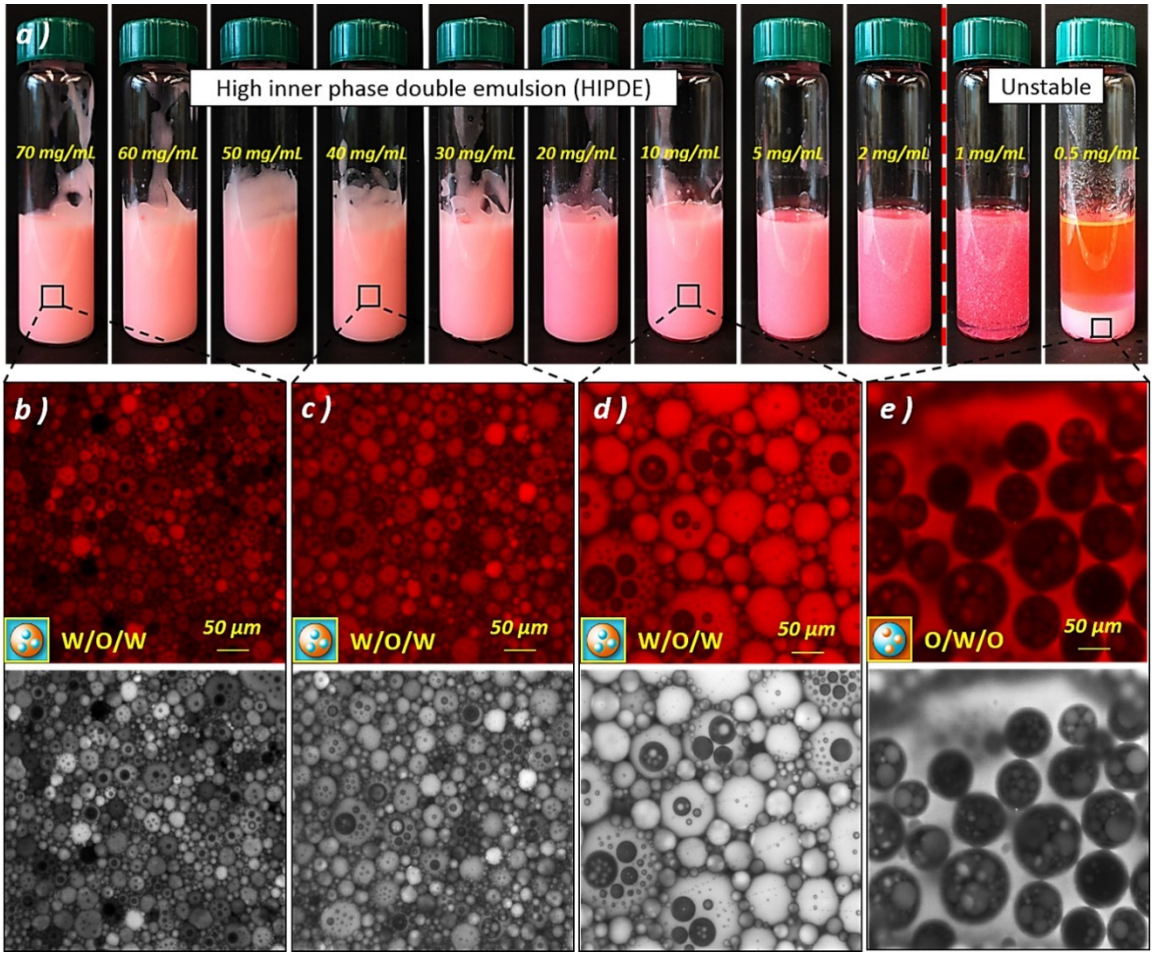

Figure A6. (a) Photograph of Pickering emulsions of 85 vol% styrene phase fraction prepared with microgel concentration from 0.5 to 70 mg/mL. (b)-(e) Confocal fluorescence images of the Pickering emulsion stabilized by 70, 40, 10 and 0.5 mg/mL PDEA microgel aqueous dispersion.

The emulsion morphology as a function of the microgel concentration in aqueous phase has also been examined. A master microgel-in-water dispersion of 100 mg/mL was prepared and diluted to various concentrations (from 0.5 to 70 mg/mL) for the preparation of Pickering emulsions. Figure A6 shows HIPE-DEs having 85 vol% oil

phase, standing for 2 hours after homogenization. It was found that the microgel concentration as low as 2 mg/mL (from 70 to 2 mg/mL) was able to stabilize the HIPE-DE system. There was no apparently visible difference observed after 24 hours standing (Figure 6-S1). A HIPE-DE could also be generated even with 1 mg/mL microgel concentration, but it went creaming after 2 hours of standing still. The stability of the emulsion system against creaming increased dramatically with an increase in the microgel concentration, as shown in Figure A6 (a) and Figure AS1. However, when the microgel concentration was further reduced to 0.5 mg/mL, no HIPE was formed and the whole system underwent a phase separation. It became an O/W/O double emulsion system, as seen from Figure A6 (e). The stability of microgel-stabilized Pickering HIPE-DE systems can be attributed two factors.[16] The microgel particles absorbed at oil-water interface prevent emulsion droplets from coalescence, and the excess microgel particles form a gel matrix in continuous aqueous phase, trapping and preventing the oil droplets from creaming out. In this work, only 2 mg/mL microgel was needed to stabilize HIPE-DE from creaming in 24 hours of standing still. The microgel particles were densely packed in the continuous phase and acted as gel matrix for trapping oil droplets. The denser the gel network was, the more viscous and stable the HIPE-DE became. This could also been seen from appearance of the photographs in Figure A6 (a). The oil phase was stained by Nile red and the microgel particles formed gel matrix and made the emulsion look lighter. The HIPE-DE stabilized by lower amount microgel particles became more red in appearance, because of less gel networks between oil droplets to reflect the light.

HIPE-DEs having different morphologies could be obtained by varying the microgel concentration in aqueous phase. As shown in Figure A6, all the emulsions with 85 vol% oil phase fraction exhibited the W/O/W double emulsion morphology, when the aqueous phase microgel concentration was higher than 0.5 mg/mL (based on water). The double emulsions were readily fabricated. However, the HIPE-DEs with lower microgel concentrations were not as stable and they became creamy after a certain period of standing still. For preparation of highly stable HIPE-DEs, a minimum microgel concentration of 2 mg/mL was required. Moreover, with the microgel concentration increased from 2 to 70 mg/mL, the oil droplets became smaller and more uniform. Increasing the microgel concentration did not affect the double emulsion morphology, but only reduced the emulsion droplet size. However, for the emulsions with <10 mg/mL microgel concentration (Figure A6 (d)), the droplets were very large, with some shape deformation and coalescence. Decreasing the microgel concentration to 0.5 mg/mL caused a catastrophic phase inversion, resulting in an O/W/O double emulsion (Figure A6 (e)).

Porous PS particles and PAM matrix prepared from HIPE-DE templates

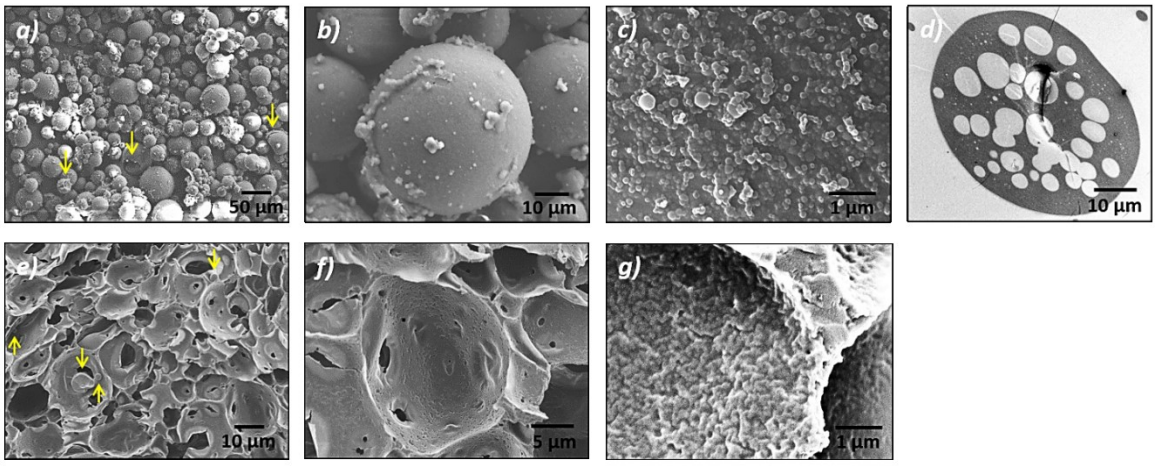

Figure A7. SEM images of porous polystyrene particles (a, b), microgel particles coated on PS particle surface (c) and TEM of the cross-section view of the porous PS particles cutting slice (d). The porous PS particles were templated and polymerized from the styrene phase (with 5 wt% AIBN initiator based on styrene) of the W/O/W HIPE-DE with 85 vol% dispersed styrene phase stabilized by 50 mg/mL PDEA microgel aqueous dispersion. Porous polyacrylamide matrix (e) and its magnification image (f, g) prepared from acrylamide polymerization of the W/O/W HIPE-DE with 85 vol% toluene as the oil phase, and a continuous aqueous phase consisted of water-soluble acrylamide (AM) monomer (20 wt% based on water) and water-soluble initiator V-50 (5 wt% based on AM monomer).

There have been several reports in literature on using HIPE (not DE) and DE (not HIPE) as templates for fabrication of polymeric devices and structures.[24, 35] The HIPE-DEs prepared in this work could also be used as templates for preparation of porous particles and matrixes. The HIPE-DE with 85 vol% dispersed styrene phase stabilized by 50 mg/mL PDEA microgel dispersion was employed for preparation of multi-pore polystyrene (PS) particles. AIBN 5 wt% (based on styrene) was added as a thermal initiator. The system was polymerized at 90 ^{o}C for 24 hours. It was found that this type of Pickering HIPE-DE was very stable at the elevated temperature required for polymerization. The morphology of the HIPE-DE-templated polymer products was

analyzed by SEM and TEM. Figures A7 (a) and (b) show that the W/O/W morphology of the emulsion template was precisely retained in the porous PS particles through the oil-phase polymerization of styrene. A small number of the particles were ruptured and cracked, as highlighted in Figure A7 (a). It was found that the densely packed PS particles were coated and separated by microgel particles, which could be easily rubbed off, suggesting that the microgels successfully stabilized styrene droplets at the primary oil-water interface, and that there was no polymerization occurred in the continuous aqueous phase or in the microgel matrix. The PS particles had similar sizes as the droplets of Pickering emulsion prior to polymerization. The microgels did not change their sizes either. (Figure A7 (c)) The multi-pore structures (white) of PS particles (black) were clearly seen in the cross-section TEM imaging of the cut PS particle slices (Figure A7 (d)).

Highly porous polymer matrixes could also be prepared by polymerizing a monomer in the continuous aqueous phase of W/O/W HIPE-DE. For example, 85 vol% toluene as the oil phase was dispersed into 50 mg/mL PDEA microgel aqueous dispersion, which consisted of water-soluble acrylamide (AM) monomer (20 wt% based on water) and water-soluble initiator V-50 (5 wt% based on AM monomer). The system was polymerized at 90 ^{o}C for 24 hours. Highly porous polyacrylamide (PAM) structures were obtained upon evaporation of the internal phase toluene, as shown in Figure A7 (e, f and g). Different from the polyHIPE prepared via a conventional HIPE, some small PAM particles were found to be trapped in the porous PAM matrix,

as highlighted in Figure A7 (e). This type of particle-in-matrix morphologies was resulted from the polymerization of acrylamide dissolved in internal water droplets of the W/O/W HIPE-DE. The addition of acrylamide and V-50, as well as heating the system for polymerization, did not affect the HIPE-DE stabilization and the W/O/W double emulsion morphology (as supported in Figure AS2).

Conclusion

In conclusion, high internal phase emulsions having water-in-oil-in-water (W/O/W) double emulsion morphology (HIPE-DE) have been prepared with poly(2-(diethylamino)ethyl methacrylate) (PDEA) microgel particles as Pickering stabilizer using a one-step emulsification method. It was discovered that a small amount of unreacted DEA monomer in the PDEA microgel aqueous dispersion played a critical role in the formation of W/O/W double emulsions. The PDEA microgel particles as Pickering surfactant stabilized the oil droplets in the HIPE. The protonated DEA monomer molecules acted as molecular surfactant and formed inversed micelles residing inside the dispersed oil droplets. The micelles contained water and formed the inner water droplets of the W/O/W double emulsion (DE). The oil phase fraction of the HIPE-DE could reach to a level as high as 90 vol% by optimizing the microgel concentration in aqueous phase. A microgel concentration as low as 2 mg/mL was adequate to stabilize the HIPE-DE of 85 vol% oil phase fraction. The HIPE-DE systems having the W/O/W morphology were used as templates for the fabrication of porous polymer structures. The polymerization of styrene in the dispersed oil phase resulted

in multi-pore porous polystyrene particles. The polymerization of water-soluble acrylamide monomer in the continuous aqueous phase, with toluene as the oil phase, converted the W/O/W HIPE-DE's into porous polyacrylamide matrixes. This approach provides a versatile platform for fabrication of a variety of porous polymer products.

References

[1] N.R. Cameron, D.C. Sherrington, *Advances in Polymer Science* **1996**, 126, 162-214.

[2] B.P. Binks, B.P. Binks ed., *The Royal Society of Chemistry*, **1998**, Cambridge.

[3] B. Binks, S. Lumsdon, *Langmuir* **2001**, 17(15), 4540-4547.

[4] G. Caldero, M. Llinas, M.J. Garcia-Celma, C. Solans, *Journal of pharmaceutical sciences* **2010**, 99(2), 701-711.

[5] K. Lissant, Emulsions and Emulsion Technology, New York, **1974**.

[6] M. Bokhari, R.J. Carnachan, S.A. Przyborski, N.R. Cameron, *Journal of Materials Chemistry* **2007**, 17(38), 4088-4094.

[7] H. Zhang, A.I. Cooper, *Soft Matter* **2005**, 1(2), 107-113.

[8] Z. Bhumgara, *Filtralion & Separation* **1995**, 32, 245-251.

[9] B.P. Binks, *Current Opinion in Colloid & Interface Science* **2002**, 7, 21-41.

[10] R. Pelton, T. Hoare, Microgels and Their Synthesis: An introduction, in: A. Femandez-Nieves, Hans M. Wyss, J. Mattsson, D.A. Weitz (Eds.), *Microgel Suspensions: Fundamental and Applications*, **2011**, WILEY-VCH.

[11] P. Liu, W. Lu, W.-J. Wang, B.-G. Li, S. Zhu, *Langmuir* **2014**, 30(34), 10248-10255.

[12] A.J. Morse, D. Dupin, K.L. Thompson, S.P. Armes, K. Ouzineb, P. Mills, R. Swart, *Langmuir* 2012, 28(32) 11733-11744.

[13] A.J. Morse, S.P. Armes, K.L. Thompson, D. Dupin, L.A. Fielding, P. Mills, R. Swart, *Langmuir* **2013**, 29(18), 5466-5475.

[14] L. Lei, Q. Zhang, S. Shi, S. Zhu, *Langmuir* **2015**, 31(7), 2196-2201.

[15] B.P. Binks, R. Murakami, *Nat. Mater*. **2006**, 5(11), 865-869.

[16] Z. Li, T. Ming, J. Wang, T. Ngai, *Angew Chem Int Ed* **2009**, 48(45), 8490-8493.

[17] A. Menner, V. Ikem, M. Salgueiro, M.S.P. Shaffer, A. Bismarck, *Chemical Communications* 2007, (41), 4274-4276.

[18] V.O. Ikem, A. Menner, A. Bismarck, *Angew Chem Int. Ed.* **2008**, 47(43), 8277-8279.

[19] F. Tu, D. Lee, *Chemical Communication* **2014**, 50, 15549-15552.

[20] J. Bae, T.P. Russell, R.C. Hayward, *Angewandte Chem.* **2014**, 53(31), 8240-8245.

[21] T.S. Dunstan, P.D. Fletcher, *Langmuir* **2011**,27(7), 3409-3415.

[22] N. Vilanova, C. Solans, C. Rodriguez-Abreu, *Langmuir* **2013**, 29(49), 15414-15422.

[23] J.M. Morais, O.D.H. Santos, S.E. Friberg, *Journal of Dispersion Science and Technology* **2010**, 31(8), 1019-1026.

[24] Q. Qian, X. Huang, X. Zhang, Z. Xie, Y. Wang, *Angew Chem Int. Ed.* **2013**, 52(40), 10625-10629.

[25] X. Huang, Q. Qian, Y. Wang, *Small* **2014**, 10(7), 1412-1420.

[26] X. Huang, R. Fang, D. Wang, J. Wang, H. Xu, Y. Wang, X. Zhang, *Small* **2014**, 11(13), 1537-1541.

[27] Z. Li, H. Liu, L. Zeng, H. Liu, S. Yang, Y. Wang, *Langmuir* **2014**, 30(41), 12154-12163.

[28] D. Štefanec, P. Krajnc, *Polymer International* **2007**, 56(10), 1313-1319.

[29] Z. Li, X. Wei, T. Ngai, *Chem Commun* **2011**, 47(1), 331-333.

[30] Z. Li, T. Ngai, *Nanoscale* **2013**, 5(4), 1399-1410.

[31] Z. Li, T. Ngai, *Colloid and Polymer Science* **2010**, 289(5-6), 489-496.

[32] J. Xu, G. Chen, R. Yan, D. Wang, M. Zhang, W. Zhang, P. Sun, *Macromolecules* **2011**, 44(10), 3730-3738.

[33] J.-S. Park, Y.-B. Lim, Y.-M. Kwon, B. Jeong, Y.H. Choi, S.W. Kim, *Journal of Polymer Science: Part A: Polymer Chemistry* **1999**, 37, 2305-2309.

[34] L. Hong, G. Sun, J. Cai, T. Ngai, *Langmuir* **2012**, 28(5), 2332-2336.

[35] I. Pulko, P. Krajnc, *Macromolecular rapid communications* **2012**, 33(20), 1731-1746.

Supporting Information

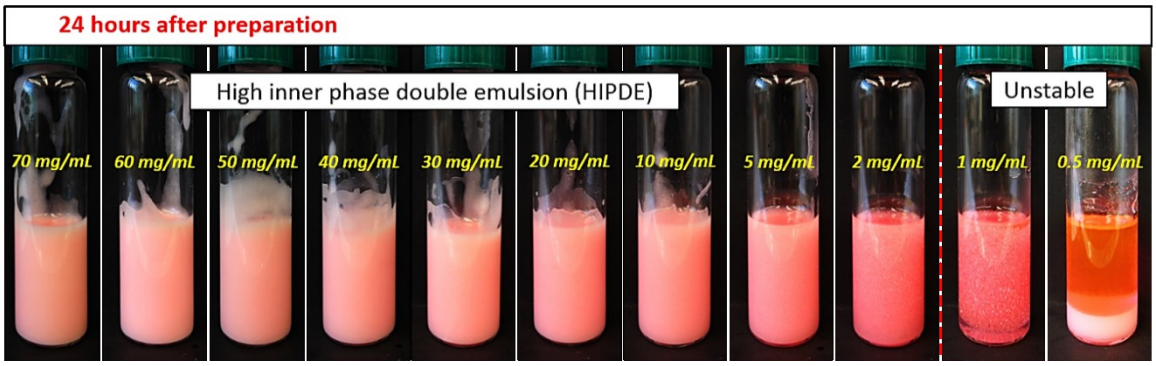

Figure AS1. Photographs of HIPE-DEs prepared with different microgel concentrations at 85 vol% oil phase fraction, taken after standing still for 24 hours after preparation.

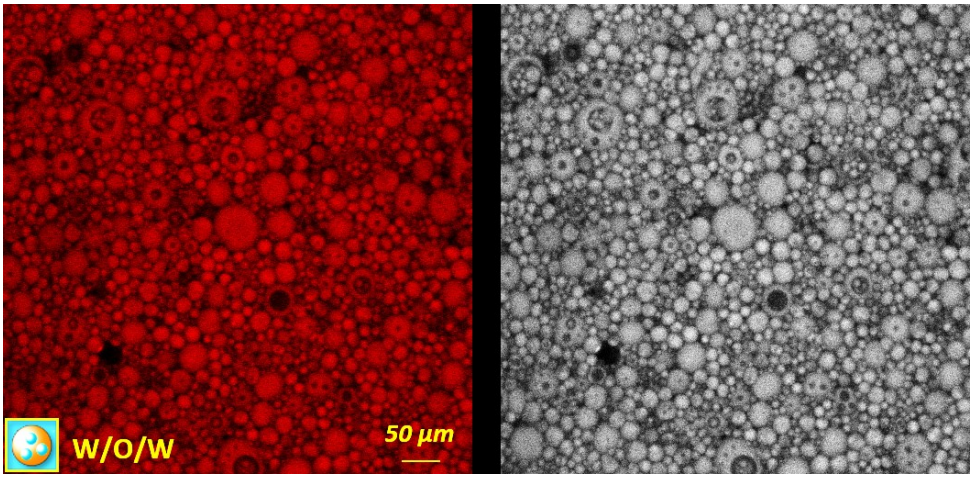

Figure AS2. Confocal fluorescence images of HIPE-DEs prepared by adding acrylamide monomer to the aqueous phase and using toluene as the oil phase